

Collective motion

Tamás Vicsek*

*Department of Biological Physics,
Eötvös University - Pázmány Péter stny. 1A, Budapest,
Hungary H-1117*

*Statistical and Biological Physics Research Group of HAS - Pázmány Péter stny. 1A, Budapest,
Hungary H-1117*

Anna Zafiris†

*Department of Biological Physics,
Eötvös University - Pázmány Péter stny. 1A, Budapest,
Hungary H-1117*

*Department of Mathematics,
National University of Athens - Panepistimioupolis 15784 Athens,
Greece*

We review the observations and the basic laws describing the essential aspects of collective motion – being one of the most common and spectacular manifestation of coordinated behavior. Our aim is to provide a balanced discussion of the various facets of this highly multidisciplinary field, including experiments, mathematical methods and models for simulations, so that readers with a variety of background could get both the basics and a broader, more detailed picture of the field. The observations we report on include systems consisting of units ranging from macromolecules through metallic rods and robots to groups of animals and people. Some emphasis is put on models that are simple and realistic enough to reproduce the numerous related observations and are useful for developing concepts for a better understanding of the complexity of systems consisting of many simultaneously moving entities. As such, these models allow the establishing of a few fundamental principles of flocking. In particular, it is demonstrated, that in spite of considerable differences, a number of deep analogies exist between equilibrium statistical physics systems and those made of self-propelled (in most cases living) units. In both cases only a few well defined macroscopic/collective states occur and the transitions between these states follow a similar scenario, involving discontinuity and algebraic divergences.

CONTENTS

| | | | |
|---|----|---|----|
| I. Introduction | 2 | IV. Basic models | 22 |
| A. The basic questions we address | 2 | A. Simplest self-propelled particles (SPP) models | 22 |
| B. Collective behavior | 2 | 1. The order of the phase transition | 23 |
| C. The main difference between equilibrium and self-propelled systems | 2 | 2. Finite size scaling | 24 |
| D. Goals to be achieved | 3 | B. Variants of the original SPP model | 24 |
| II. Observations and experiments | 3 | 1. Models without alignment rule | 24 |
| A. Physical, chemical and biomolecular systems | 4 | 2. Models with alignment rule | 26 |
| B. Bacterial colonies | 6 | C. Continuous media and mean-field approaches | 27 |
| C. Cells | 9 | D. Exact results | 29 |
| D. Insects | 11 | 1. The Cucker-Smale model | 29 |
| E. Fish schools and shoals | 12 | 2. Network and control theoretical aspects | 31 |
| F. Bird flocks | 13 | E. Relation to collective robotics | 32 |
| G. Leadership in groups of mammals and crowds | 16 | V. Modeling actual systems | 34 |
| H. Lessons from the observations | 18 | A. Systems involving physical and chemical interactions | 34 |
| III. Definitions and techniques for collecting and evaluating data | 18 | 1. The effects of the medium | 34 |
| A. Basic notions and expressions | 18 | 2. The role of adhesion | 35 |
| B. Correlation functions | 19 | 3. Swarming bacteria | 37 |
| C. Data collection techniques | 21 | B. Models with segregating units | 40 |
| | | C. Models inspired by animal behavioral patterns | 41 |
| | | 1. Insects | 41 |
| | | 2. Moving in three dimensions – fish and birds | 42 |
| | | D. The role of leadership in consensus finding | 44 |
| | | VI. Summary and conclusions | 46 |
| | | Acknowledgments | 47 |
| | | References | 47 |

* vicsek@hal.elte.hu

† lanna@hal.elte.hu

I. INTRODUCTION

Most of us must have been fascinated by the eye catching displays of collectively moving animals. Schools of fish can move in a rather orderly fashion or change direction amazingly abruptly. Under the pressure from a nearby predator the same fish can swirl like a vehemently stirred fluid. Flocks of hundreds of starlings can fly to the fields as a uniformly moving group, but then, after returning to their roosting site, produce turbulent, puzzling aerial displays. There are a huge number of further examples both from the living and the non-living world for the rich behavior in systems consisting of interacting, permanently moving units.

Although persistent motion is one of the conspicuous features of life, recently several physical and chemical systems have also been shown to possess interacting, “self-propelled” units. Examples include rods or disks of various kinds on a vibrating table (Blair *et al.*, 2003; Designe *et al.*, 2010; Ibele *et al.*, 2009; Kudrolli *et al.*, 2008; Narayan *et al.*, 2006, 2007; Yamada *et al.*, 2003).

The concept of the present review is to on one hand introduce the readers to the field of flocking by discussing the most influential “classic” works on collective motion as well as providing an overview of the state of the art for those who consider doing research in this thriving multidisciplinary area. We have put a special stress on coherence and aimed at presenting a balanced account of the various experimental and theoretical approaches.

In addition to presenting the most appealing results from the quickly growing related literature we also deliver a critical discussion of the emerging picture and summarize our present understanding of flocking phenomena in the form of a systematic phenomenological description of the results obtained so far. In turn, such a description may become a good starting point for developing a unified theoretical treatment of the main laws of collective motion.

A. The basic questions we address

Are these observed motion patterns system specific? Such a conclusion would be quite common in biology. Or, alternatively, are there only a few typical classes which all of the collective motion patterns belong to? This would be a familiar thought for a statistical physicist dealing with systems of an enormous number of molecules in equilibrium. In fact, collective motion is one of the manifestations of a more general class of phenomena called collective behavior (Vicsek, 2001a). The studies of the latter have identified a few general laws related to how new, more complex qualitative features emerge as many simpler units are interacting.

There is an amazing variety of systems made of such units bridging over many orders of magnitude in size and

purely physical or chemical to and biological systems. Will they still exhibit the same motion patterns? If yes, what are these patterns and are there any underlying universal principles predicting that this has to be so (e.g., non-conservation of moments during interactions)?

In Fig. 1, we show a gallery of pictures representing a few of the many possible examples visualizing the variety of collective motion patterns occurring in a highly diverse selection of biological systems.

B. Collective behavior

In a system consisting of many similar units (such as, e.g., many molecules, but also, flocks of birds) the interactions between the units can be simple (attraction/repulsion) or more complex (combinations of simple interactions) and can occur between neighbors in space or in an underlying network. Under some conditions, transitions can occur during which the objects adopt a pattern of behavior almost completely determined by the collective effects due to the other units in the system. The main feature of collective behavior is that an individual unit’s action is dominated by the influence of the “others” – the unit behaves entirely differently from the way it would behave on its own. Such systems show interesting ordering phenomena as the units simultaneously change their behavior to a common pattern (see, e.g., Vicsek (2001b)). For example, a group of feeding pigeons randomly oriented on the ground will order themselves into an orderly flying flock when leaving the scene after a big disturbance.

Understanding new phenomena (in our case, the transitions in systems of collectively moving units) is usually achieved by relating them to known ones: a more complex system is understood by analyzing its simpler variants. In the 1970s, there was a breakthrough in statistical physics in the form of the ‘renormalization group method’ (Wilson, 1975b) which gave physicists a deep theoretical understanding of a general type of phase transition. The theory showed that the main features of transitions in equilibrium systems are insensitive to the details of the interactions between the objects in a system. Pushing the analogy further, we have reasons to suppose that the orientational forces between atoms can result in ordering phenomena similar to those seen in groups of much more complex units, such as collectively moving organisms.

C. The main difference between equilibrium and self-propelled systems

The essential difference between collective phenomena in standard statistical physics and biology is that the “collision rule” is principally altering in the two kinds of systems: in the latter ones it does not preserve the

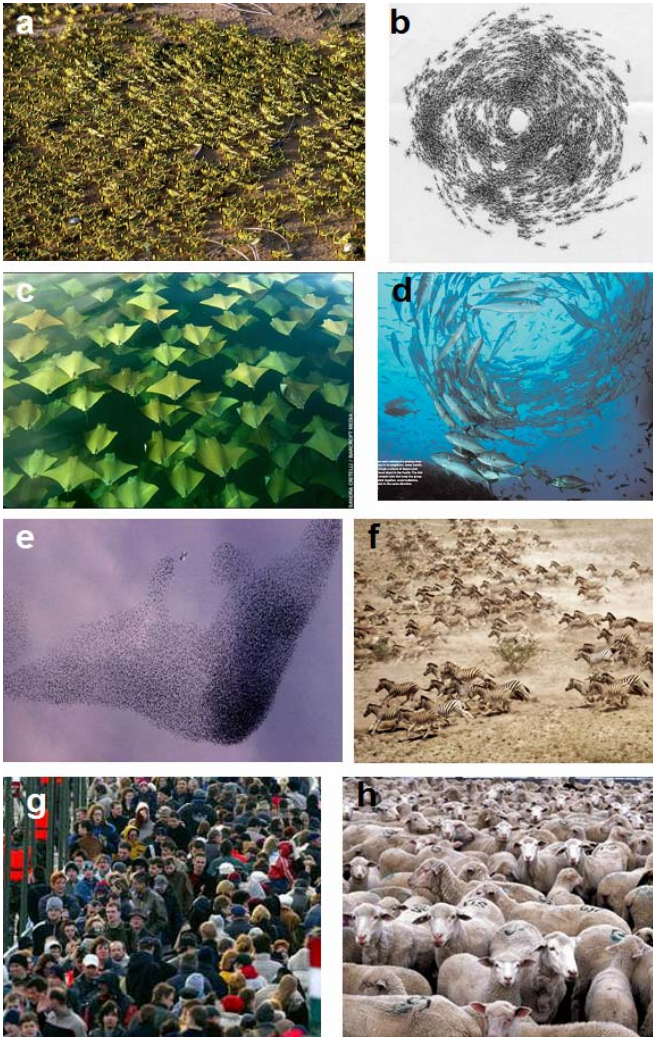


FIG. 1 (Color) A gallery of images related to collective behavior. Among others, it illustrates the possible existence of very general behavioral patterns. (a) Wingless Locusts are marching in the field. (b) A rotating colony of South American fire ants. (c) A nice three-dimensional array of golden rays. (d) Fish are known to produce such vortices. (e) Before roosting, thousands of starlings are producing a fascinating aerial display. They are also trying to avoid a predator bird close to the central finger-like structure. (f) A herd of zebra. (g) People spontaneously ordered into “traffic lanes” as they cross a pedestrian bridge in large numbers. (h) Although sheep are known to move very coherently, just as the corresponding theory predicts, when simply hanging around (no motion), well developed orientational patterns cannot emerge.

momentum. Here the expression collision rule stands for specifying how the states (velocities) of two individual units change during their interaction. In equilibrium systems, according to standard Newtonian mechanics the total momentum is preserved and that is how the well known Maxwellian velocity distribution is being built up from arbitrary initial conditions in a closed Galilean system. The mere condition of the units maintaining an

approximate absolute velocity can be realized in an open system only and drives away the driven particles from any kind of equilibrium behavior. Currents are bound to be generated and the overall momentum is gradually increasing if the initial state is random (in this case the initial momentum is very small because the moments of the oppositely moving particles cancel out). However, for this overall ordering to occur the random perturbations (acting against ordering) have to be small enough.

Most remarkably, however, in spite of this principal difference, a number of deep analogies can still be observed between equilibrium statistical physics systems and those made of self-propelled (living) units. In both only a few well defined macroscopic/collective states occur and the transitions between these states follow a similar scenario as well (discontinuity, algebraic divergences, etc).

D. Goals to be achieved

The approach of treating flocks, or even crowds, as systems of particles naturally leads to the idea of applying the successful methods of statistical physics, such as computer simulations or theories on scaling, to the detailed description of the collective behavior of organisms. Naturally, for better progress, observations/experiments and modeling have to be intimately related. Indeed, over the past few decades, an increasingly growing number of significant attempts have been made to both observe and describe flocking as well as modeling (simulate) the most conspicuous features of the observed natural systems ranging from molecules to groups of mammals.

It would be quite an achievement if we could establish a systematic chart of the types of collective motion since many times understanding is achieved through classification. There are reasons and arguments to think that the same patterns of collective motion apply to the collection of molecules up to groups of humans. There must be some – still to be discovered – laws of such systems from which the above observation follows.

II. OBSERVATIONS AND EXPERIMENTS

It seems that collective motion (or flocking; these two notions will be used as synonyms in this review although in principle there are some subtle differences in their meanings) is displayed by almost every living system consisting of at least dozens of units. One of the main points in this review is that the kinds of systems and the types of collective motion patterns have a greater variety than originally thought of. Below we give a – naturally incomplete – list of systems in which collective motion has been observed (with only some of the representative references included):

- Non-living systems: nematic fluids, shaken metallic rods, nano swimmers, simple robots, boats, etc. (Ibele *et al.*, 2009; Kudrolli, 2010; Narayan *et al.*, 2007; Suematsu *et al.*, 2010)
- Macromolecules (Butt *et al.*, 2010; Schaller *et al.*, 2010)
- Bacteria colonies (Cisneros *et al.*, 2007; Cziráková *et al.*, 1996, 2001; Sokolov *et al.*, 2007)
- Amoeba (Kessler and Levine, 1993; Nagano, 1998; Rappel *et al.*, 1999)
- Cells (Arboleda-Estudillo *et al.*, 2010; Belmonte *et al.*, 2008; Friedl and Gilmour, 2009; Szabó *et al.*, 2006)
- Insects (Buhl *et al.*, 2006; Couzin and Franks, 2003)
- Fish (Becco *et al.*, 2006; Hemelrijk and Kunz, 2005; Parrish *et al.*, 2002; Ward *et al.*, 2008)
- Birds (Bajec and Heppner, 2009; Ballerini *et al.*, 2008; Hayakawa, 2010; Heppner, 1997)
- Mammals (Fischhoff *et al.*, 2007; King *et al.*, 2008; Sueur and Petit, 2008)
- Humans (Faria *et al.*, 2010b; Helbing *et al.*, 2000, 1997)

A. Physical, chemical and biomolecular systems

Along with the accumulating observations and experiments clarified the recognition, that flocking – collective motion – emerges not only in systems consisting of living beings, but also among interacting physical objects, based on mere physical interactions without communication.

Up to now, the simplest physical system has been described by Ibele *et al.* (2009) who reported about simple autonomous micromotors, which are micrometer-sized silver chloride (AgCl) particles exhibiting collective motion in deionized water under UV illumination. The autonomous motion these particles exhibit under the above circumstances (deionized water and UV light) is due to their asymmetric photo-decomposition, and the spatial self-organization is due to the ions which are secreted by the AgCl particles as they move.

Various experiments on non-living self propelled particles (SPPs) possessing diverse features advocate that the shape and symmetry of the SPPs play an important role in their collective dynamics, and that large-scale inhomogeneity and coherent motion can appear in a system in which particles do not communicate except by contact. Symmetric (or “apolar”) rods on vibrating surfaces have been observed to form nematic order and under certain

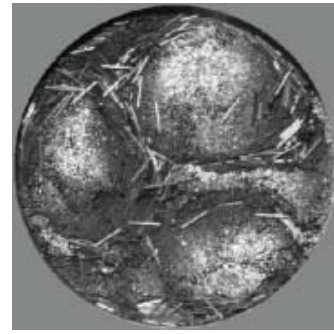


FIG. 2 Periodically, vertically vibrated granular rods spontaneously form vortices which grow with time. From Blair *et al.* (2003)

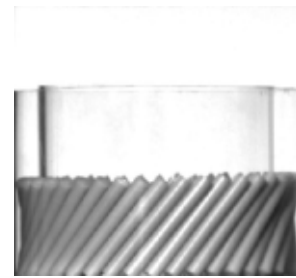


FIG. 3 Experiments performed in an annulus with a single row of rods reveal that the rod motion is generated when these objects are inclined from the vertical, and is always in the direction of the inclination. From Blair *et al.* (2003)

conditions found to exhibit persistent swirling as well (Galanis *et al.*, 2006; Narayan *et al.*, 2006). Narayan *et al.* (2007) have also investigated symmetric macroscopic rods and have found giant number fluctuations lasting long, decaying only as a logarithmic function of time (see Fig. 4).

Periodically, vertically vibrated granular rods form vortex patterns (Blair *et al.*, 2003). Above a critical packing fraction, the ordered domains – consisting of nearly vertical rods – spontaneously form and coexist with horizontal rods (see Fig. 2). The vortices nucleate and grow as a function of time. Experiments performed in an annulus with a single row of rods revealed that the rod motion was generated when these objects were inclined from the vertical, and was always in the direction of the inclination (see Fig. 3). The relationship between the covered area fraction and the diffusion properties in the case of self-propelled rods was also studied (Kudrolli, 2010).

Kudrolli *et al.* (2008) have made experiments with polar (non-symmetric) rods on a vibrating surface. Their rods had a symmetric shape, but a non-symmetrical mass distribution which caused them to move toward their lighter end. They have observed local ordering, aggregation at the side walls, and – in contrast with round-shaped self-propelled particles – clustering behavior.

Tinsley *et al.* (2008) presented an experimental study

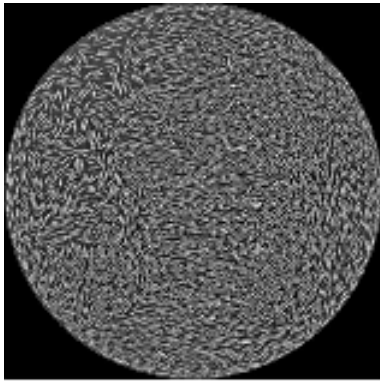


FIG. 4 A snapshot of the nematic order assumed by 2820 rods which are sinusoidally vibrated perpendicularly to the plane of the image. The large density fluctuations take several minutes to relax and to form elsewhere. From Narayan *et al.* (2007).

on interacting particle-like *waves* (see more about the design of wave propagation in Sakurai *et al.* (2002)) and suggested this method as an opportunity to investigate small groups of SPPs in laboratory environment. The stabilized wave-segments they have used were those appearing in the light-sensitive Belousov-Zhabotinsky reaction (Zaikin and Zhabotinsky, 1970). These constant-velocity chemical waves can be interpreted as self-propelled particles which are linked to each other via appropriate interaction potentials.

Along with the accumulation of the experimental results, the assumption that only a few parameters and factors play a crucial role in the emergence of the ubiquitous phenomena of collective motion has been increasingly supported. *Particle-density* turns out to be one of these parameters, or more precisely, the density of the objects or living beings that exhibit collective motion.

The essential role of the density has been demonstrated in a set of elegant experiments on persistently moving biomolecules. In these investigations – involving the smallest, experimentally realized self-propelled particles so far – the so called *in vitro* motility assay is utilized to study the emergence of collective motion on a molecular level. In such an assay actin filaments and fluorescently labeled reporter filaments are propelled by immobilized molecular motors (myosin molecules) attached to a planar surface, as depicted on Fig. 5. In a very recent study, Butt *et al.* (2010) were the first to observe the bulk alignment of the actin filaments sliding movement for high concentration values even though they were powered by randomly oriented myosin molecules (Fig. 6). According to their observations, domains of oriented filaments formed spontaneously and were separated by distinct boundaries. The authors suggested that the self-alignment of actin filaments might make an important contribution to cell polarity and provide a mechanism by which cell migration direction might respond to chemical

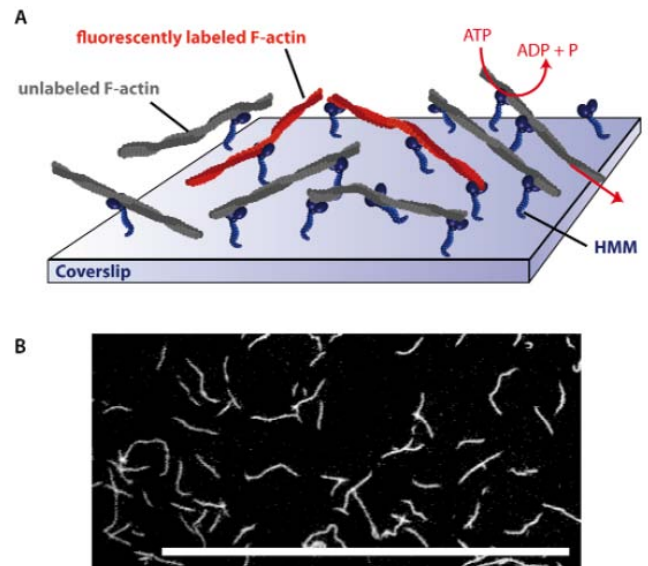


FIG. 5 (Color online) The setup of the experiment designed to investigate the effect of density on the collective motion of actin filaments. (a) Filament-motion is visualized by the usage of fluorescently labeled reporter filaments. The ratio of labeled to unlabeled molecules is around 1:200. (b) For low filament densities a disordered structure is found, where the bio-molecules perform persistent random walk without directional preference. Scale bar represents $50 \mu\text{m}$. From Schaller *et al.* (2010).

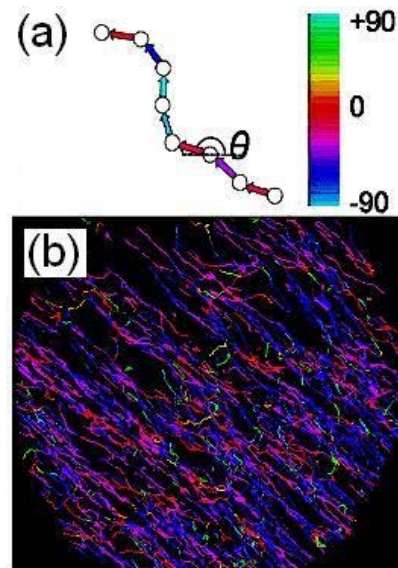


FIG. 6 (Color online) Motion of actin filaments in a motility assay. (a) The individual filaments were tracked automatically and the positions (denoted by circles) were used to estimate their (color coded) direction of motion. (b) The color coded (as above) paths plotted as a continuous track to highlight the trajectory of each filament. The tracks shown are from a 100-frame video sequence recorded at 25 frames/s. After Butt *et al.* (2010).

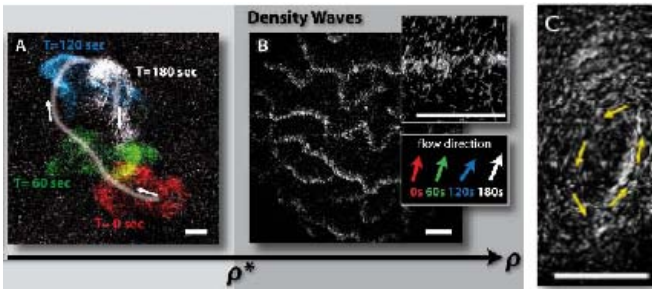


FIG. 7 (Color online) The typical behavior of the bio-molecule actin filament in the function of density. The disordered structure (a) becomes ordered (b) above a certain density ρ^* , which is around 0.8 filaments per μm^2 . In this high density regime, wave-like structures can be observed. Above 0.2 filaments per μm^2 , spirals or swirls can be observed as well (c), which are characterized by huge angular velocity gradients destabilizing the swirl. This limited stability is visible near to the central region of the pattern, where crushing events of the filament current are likely to develop. Scale bar is 50 μm . Adapted from Schaller *et al.* (2010).

cues. At almost the same time, Schaller *et al.* (2010) undertook a very similar study, but in a somewhat different context of active matter and using extensive evaluation and computational techniques to characterize the phenomenon. They also found that the onset of collective motion was a result of increased filament density. In particular, for low filament densities a disordered phase has been discerned, in which individual filaments performed random walk without any directional preference. Above a certain density, which was around 0.2 filaments per μm^2 , in an intermediate regime, the disordered phase became unstable and small clusters of coherently moving filaments emerged. Further concentration-increase caused growth in the cluster-sizes, but the bunches remained homogeneous. Then, above 0.8 filaments per μm^2 (signed with ρ^* on Fig. 7), persistent density fluctuations occurred, leading to the formation of wave-like structures. The authors also identified the weak and local alignment-interactions to be essential for the formation of the patterns and their dynamics. A simulation model was used to interpret the interplay between the underlying microscopic dynamics and the emergence of global patterns in a good agreement with the observations.

B. Bacterial colonies

Since microorganism colonies (such as bacteria colonies) are one of the simplest systems consisting of many interacting organisms, yet exhibiting a non-trivial macroscopic behavior, a number of studies have focused on the experimental and theoretical aspects of colony formation and on the related collective behavior (Alt *et al.*, 1997; Shapiro and Dworkin, 1997; Vicsek, 2001a). The quantitative investigations of how bacterial colonies of

various complex spatial patterns emerge go back to the early 1990-es (Ben-Jacob *et al.*, 1994; Fujikawa and Matsushita, 1989; Vicsek *et al.*, 1990). During these investigations it has become evident that the bacteria within the colonies growing on wet agar surfaces produce an exciting variety of collective motion patterns: among others, motions similar to super-diffusing particles, highly correlated turbulent as well as rotating states have been observed, and colony formations exhibiting various patterns including those reminiscent of fractals. A special category are those studies which contain not only an observation or a theoretical model, but a matching pair of them: detailed description of an observation together with a computational or mathematical model that accounts for the observations (Czirók *et al.*, 1996, 2001; Wu *et al.*, 2007, 2009).

Czirók *et al.* (1996) were the first to interpret an experimentally observed complex behavior through a many-particle-type simulation, incorporating realistic rules. They have investigated the intricate colony formation and collective motion (formation of rotating dense aggregates, migration of bacteria in clusters, etc.) of a morphotype of *Bacillus subtilis* using control parameters, such as the concentration of agar and peptone, which was the source of nutrient. Under standard (favorable) conditions bacterium colonies do not exhibit a high level of organization. However, under certain hostile environmental conditions (like limited nutrient source or hard agar surface) the complexity of the colony as a whole increases, characterized by the appearance of *cell-differentiation* and *long-range information transmission* (Shapiro, 1988). For describing the observed hydrodynamics (vortex-formation, migration of clusters) of the bacteria in an intermediate level, Czirók *et al.* (1996) proposed a simpler model of self-propelled particles, and more complex ones – taking into account further biological details – to capture the more elaborated collective behaviors, like the vortex and colony formation (see Sec. V.A.3). Figure 8 depicts a typical bacterium colony formed by the *vortex* morphotype.

This kind of bacterium, *Bacillus subtilis*, when the cells are very concentrated (nearly close-packed), form a special kind of collective *phase* called “Zooming BioNematics” (ZBN) (Cisneros *et al.*, 2007). This phase is characterized by large scale orientational coherence – analogous to the molecular alignment of nematic liquid crystals – in which the cells assemble together into co-directionally swimming clusters, which often move at speeds larger than the average speed of single bacteria. Figure 9 shows a snapshot of swimming *Bacillus subtilis* cells exhibiting collective dynamics, and Fig. 10 depicts the corresponding vorticity field.

The collective behavior of motile aerobic bacteria (“aerobic” are those bacteria which need the presence of oxygen for their survival), primarily in high cell-concentration, is governed by the interplay between buoy-

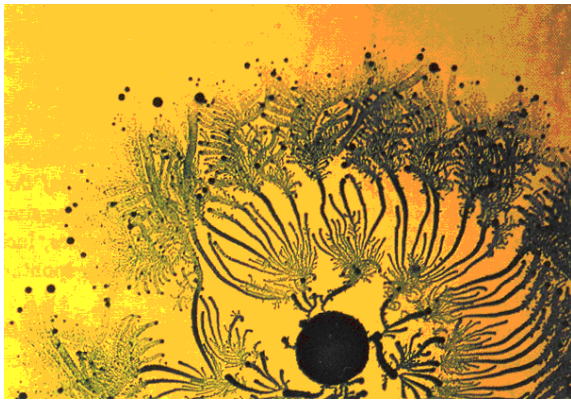


FIG. 8 (Color online) A typical colony of the *vortex* morphotype of *Bacillus subtilis*. The black discs contain thousands of bacteria circling together as the discs themselves glide outward on the surface during colony growth. Courtesy of E. Ben-Jacob.



FIG. 9 Swimming *Bacillus subtilis* cells exhibiting collective dynamics. On a large scale, response to chemical gradients (oxygen, in this case) can initiate behavior that results in striking hydrodynamic flows. From Cisneros *et al.* (2007).

ancy, oxygen consumption, mixing and hydrodynamic interactions. The patter-formation of these bacteria is often governed by another physical mechanism as well, called *bioconvection* (Pedley and Kessler, 1992), which appears on fluid medium having a surface open to the air. The authors argued that the patterns appear because bacteria, which are denser than the fluid they swim in, gather at the surface creating a heavy layer on the top of a lighter medium. When the density of the bacteria-cells exceed a certain threshold, this arrangement becomes unstable resulting in a large-scale cell circulation (or convection).

Sokolov *et al.* (2009) have investigated the onset of large-scale collective motion of aerobic bacteria swimming in a thin fluid, a ‘film’, which had adjustable thickness. They have demonstrated the existence of a clear transition between a quasi-two-dimensional collective motion state and a three-dimensional turbulent state

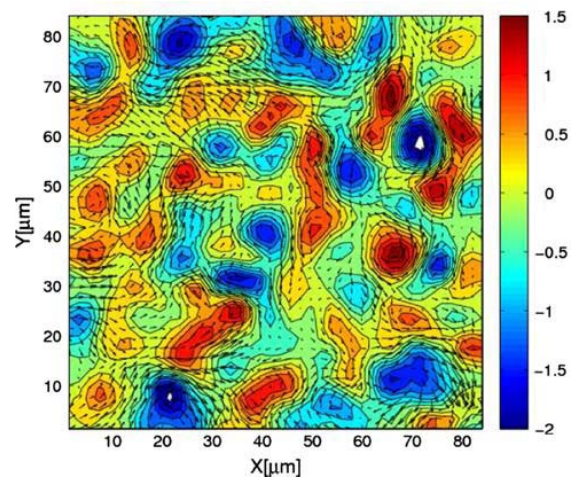


FIG. 10 (Color) A snapshot of the vorticity field of the swimming bacteria *Bacillus subtilis* (depicted on Fig. 9). The small arrows indicate the corresponding velocity field. The color bar indicates vorticity in seconds^{-1} . The turbulent motion of the suspension is well-observable. The regions of aligned motility are hundreds of times larger than the size of the bacteria, remaining coherent for the order of magnitude of a second. From Cisneros *et al.* (2007).

that occurs at a certain fluid-thickness. In the turbulent state – which is qualitatively different from bioconvection – an enhanced diffusivity of bacteria and oxygen can be observed, which – supposedly – serves the better survival of bacteria colonies under harsh conditions.

In another remarkable recent paper, while seeking to understand how certain bacteria colonies are able to spread so efficiently, Wu *et al.* (2009) reported on a completely unexpected phenomenon: they found that members of a certain kind of bacteria (*Myxococcus xanthus*) regularly *reverse their direction*, heading back to the colony which they have just come from, which is – seemingly – only a waste of time and energy. Motivated by these observations, the authors constructed a detailed computational model that took into account both the behavior and the cell biology of the bacteria *M. xanthus*. The model revealed that these reversals generate a more orderly swarm with more cells oriented in parallel, making the cells less likely to collide with each other. Without these turn-backs the cells would become disordered and as a whole, would move at a slower rate while finally coming to a standstill. The model predicts that the swarm expands at the greatest rate when cells reverse their direction approximately every eight minutes – which is in exact match with the observations. Figure 11 shows a snapshot of the expanding colony of bacteria *M. xanthus*.

Wild-type (“normal”) *Myxococcus xanthus* has two different kinds of engines to move itself: a *pilus* at its’ front end which *pulls* the cell, and a slime secretion engine at its’ rear that *pushes* the bacterium forward. Wu *et al.*

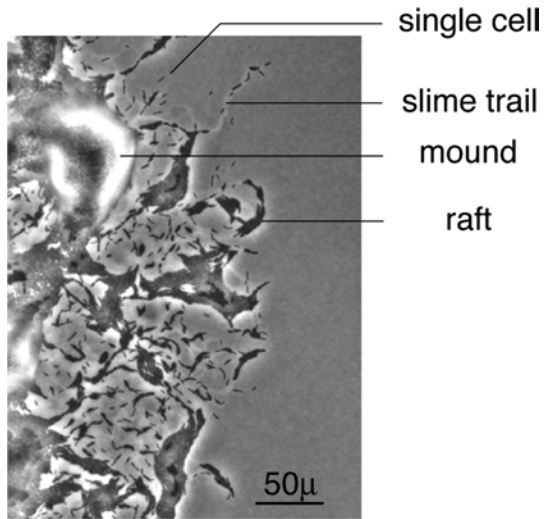


FIG. 11 The edge of the expanding colony of bacteria *M. xanthus*. Some individual cells and slime trails are labeled, along with some multicellular “rafts” and mounds. The colony is expanding in the radial direction, which is to the right in this image. From Wu *et al.* (2009).

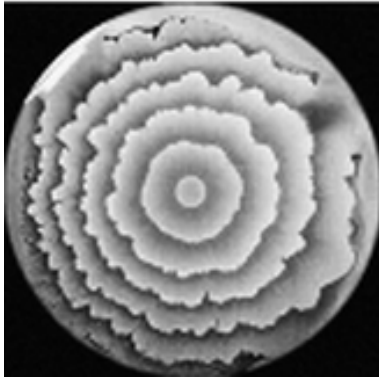


FIG. 12 The colony of *Bacillus subtilis* which – similarly to *P. mirabilis* – grow in a peculiar concentric ring-like pattern, which is the result of a special swarming cycle reported by Czirók *et al.* (2001) and Yamazaki *et al.* (2005). From Yamazaki *et al.* (2005).

(2007) have investigated the coordinated motion and social interactions of this bacteria by using mutants: bacteria that were void of either one or the other type of engine. Based on their observations they have introduced a cell-based model to study the role of the two different kinds of engines and to show how the interactions between neighboring cells facilitate swarming.

Czirók *et al.* (2001) reported on swarming cycles (exhibited by many bacterial species) resulting in a colony with concentric rings (see Fig. 12). (Although the phenomenon had been known for some time, in their study both the quantitative measurements and the theoretical interpretation have been the subject of research.) These zones develop as the bacteria (*Proteus mirabilis* in their

experiments) multiply and swarm following a periodically repeating scenario: when the bacteria cells are applied to the surface of a suitable hard agar medium, they grow as short, immotile “vegetative” rods. Then, after a certain time, cells start to differentiate at the colony margin into long motile “swarmer” cells which then migrate rapidly away from the colony until they stop and revert by a series of cell fissions into the vegetative cell form again. These cells then grow normally for a time, until the swarmer cell differentiation is initiated in the outermost zone again, and the process continues in periodic cycles resulting into the concentric ring-structure. For this process – every step of which has been observed and described in detail – a model has been developed as well, which is in excellent agreement with the observations. Yamazaki *et al.* (2005) investigated the above described periodic change between the motile and the immotile cell states experimentally, and they concluded that the change between the two states was determined neither by biological nor by chemical factors, but by the local cell density.

Many papers deal with the effects of cell-density on the collective behavior of a bacterium colony. Dombrowski *et al.* (2004) artificially created regions in which a given type of bacteria-cells are strongly concentrated. In these regions the authors found striking collective effects with transient, reconstituting, high-speed jets straddled by vortices, and suggested a corresponding modification for the Keller-Segel model which takes into account the hydrodynamic interactions as well. (The Keller-Segel model is probably the most prevalent model for chemical control of cell movements, which has been originally introduced by Keller and Segel (1971).) The relevance of the hydrodynamic effects was highlighted by Sokolov *et al.* (2007) as well, who presented experimental results on collective bacterial swimming in thin, two-dimensional fluid films by introducing a novel technique that made it possible to keep bacterium-cells in condensed populations exhibiting adjustable concentration.

Zhang *et al.* (2009) related the characteristic velocity, time and length scales of the collective motion of a given type of swarming bacteria colonies.

The effects of the biomechanical interactions (arising from the growth and division of the bacteria cells) on the colony formation – although being ubiquitous – have received little attention so far. In a recent paper Volfson *et al.* (2008) addressed this issue by observing and simulating the structure and dynamics of a growing two-dimensional colony of non-motile bacteria, *Escherichia coli*. They found that growth and division in a dense colony led to a dynamic transition from a disordered phase to a highly ordered one, characterized by orientational alignment of the rod-shaped cells (see Fig. 13). The authors highlighted, that this mechanism differed fundamentally from the one arranging the particles of liquid crystals, polymers or vibrated rods, since this lat-

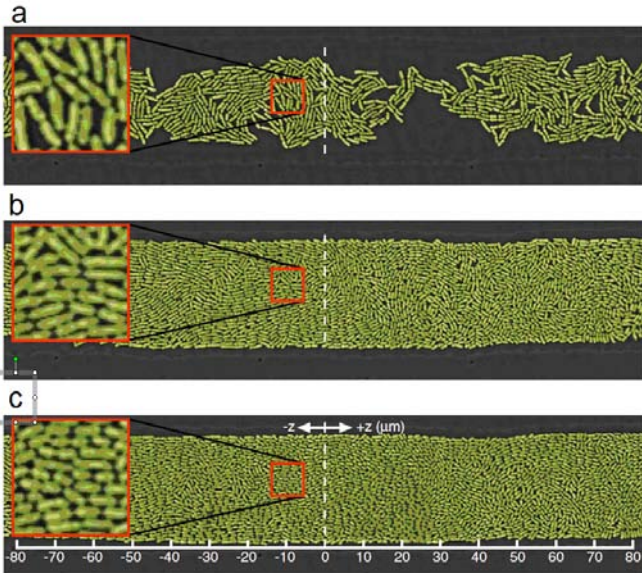


FIG. 13 (Color online) The growth and ordering of the bacteria *E. coli* in a quasi 2D open microfluidic cavity. Originally, at the beginning of the test, the cells are distributed evenly and sparsely. The three snapshots are taken at (a) 60, (b) 90 and (c) 138 minutes from the beginning of the experiment, respectively. Growth and division in a dense colony leads to a dynamic transition from a disordered phase to a highly ordered one, characterized by orientational alignment of the rod-shaped cells. Adapted from Volfson *et al.* (2008).

ter one was due to the combination of fluctuation and steric exclusion.

Using the same bacteria, Tokita *et al.* (2009) studied the *morphological diversity* of bacterial colonies, as a function of the agar and nutrient concentration. Various colony patterns were observed, classified into four basic types after their pattern characteristics.

C. Cells

The basic observations and experiments regarding *unicellular* organisms (which are also: cells) have been discussed in the previous section (II.B) since many kinds of bacteria-stems proved to be good subject for various experiments. However, some interesting experiment regarding the collective motion of unicellular beings, have not been made on bacteria, but other kind of cells.

Here we mention only one experiment which, for describing the dynamics of the cells *Dictyostelium discoideum* (commonly referred to as *slime mold*) took into account their shape and plasticity as well. Based on the observations regarding how these amoeba-cells aggregate into rotating “pancake”-form structures, Rappel *et al.* (1999) built a model of the dynamics of self-propelled deformable objects (see also in Sec. V.A.2). According to the experiments, these cells liked to form round struc-

tures which rotated around the center clockwise or anticlockwise (depending on some initial conditions) often persisting for tens of hours.

Next we discuss the collective motion of cells in highly structured, *multi-cellular* organisms, in which cell migration plays a major role in both embryonic development (e.g. gastrulation, neural crest migration) and the normal physiological or patho-physiological responses of adults (e.g. wound healing, immune response or cancer metastasis). In these organisms, different strategies exist for cell movement, including both individual cell migration and the coordinated movement of groups of cells (Rorth, 2007). Figure 14 summarizes the basic types of collective cell migrations with respect to the strength of the contact among the cells moving together.

i) Groups can be associated loosely with occasional contact and much of the apparent cohesion might come from essentially solitary cells following the same tracks and cues. Examples are germ cells in many organisms; the rostral migratory stream supplying neurons to the olfactory bulb (RMS) and neural crest (NC) cells migrating from the developing neural tube to many distant locations in the embryos of mammals; sperm cells. Although the collective motion of these cells are often guided by chemical signals, in some cases they can also form patterns based on mere hydrodynamic effects (Riedel *et al.*, 2005).

ii) Other migrating groups are more tightly associated and the cells normally never dissociate. Examples are the fish lateral line, structures performing branching and sprouting morphogenesis such as trachea or the vasculature and finally moving sheets of cells in morphogenesis or wound healing. These groups have an additional feature, in that the moving structure has an inherent polarity, a free ‘front’ and an attached ‘back’.

iii) *Drosophila* border cells are a group or cluster of cells performing a directional movement during oogenesis. These migrating cells are associated tightly but the cluster is free, without an inherent ‘back’. A particularly nice visualization of the collectively moving cells during the development of zebra fish (by three dimensional tracing of live-stained cell nuclei) very well demonstrates the relevance of collective motion during morphogenesis (Schoetz, 2008). Zamir *et al.* (2006) have developed a technique in order to distinguish individual, cell-autonomous displacements from convective displacements caused by large-scale morphogenetic tissue movements. Using this methodology, they have separated the active and passive components of cell displacement directly, during the gastrulation process in a warm-blooded embryo. Czirók *et al.* (2008) provided an excellent review on cell-movements and tissue-formation during vasculogenesis in warm blooded vertebrates. As the key mechanism for this process, the authors identified the formation and rapid expansion of multicellular sprouts, by which the originally disconnected endothelial cell clusters join

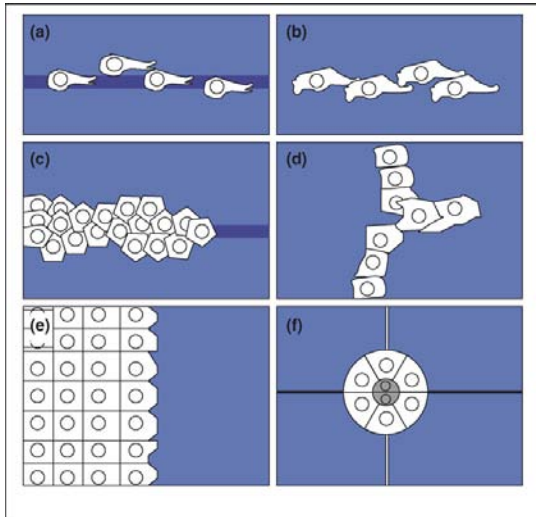


FIG. 14 (Color online) The basic types of collective cell migrations with respect to the strength of the contact among the cells moving together. The schematic draw of the cells are white with gray circles within them, which are the nuclei. The dark lines on (a) and (c) are migration-permissive tracks in the substrate. The movement is from left to right. (a) and (b) depicts loosely associated cells which contact rarely (a) or more frequently (b). Although these kind of motions are sometimes restricted by tracks, the cells mostly contact the substrate with a high degree of freedom. Neural-crest cells and germ-line cells belong to these categories. The cell-structure depicted in (c) has a well-defined front and back part. Example is the neuromast cells of the fish lateral line. (d) shows an example of tracheal or vascular-type branch outgrowth, during which the cells remain associated through the central bud growing out from the existing epithelium cells. (e) shows an epithelial sheet moving to close a gap. These cells most probably have only a small degree of freedom. (f) A border-cell-cluster moves among giant nurse cells which are depicted by the surrounding squares. From Rorth (2007).

and form an interconnected network.

A quantitative analysis of the experimentally obtained collective motion and the associated ordering transition of co-moving fish keratocytes was carried out by Szabó *et al.* (2006). They have determined the phase transition as a function of the cell density and, motivated by their experimental results, have constructed the corresponding model as well (see Sec. V.A.2). Figure 15 shows the typical collective behavior of the keratocyte cells for three different densities.

Further interesting examples for the collective motion of tissue cells are related to the following two processes:

Tissue repair and wound healing. In tissue repair collective migration is seen in vascular sprouts penetrating the wound or the horizontal migration of epithelial cell-sheets across 2d substrates upon self-renewal of keratinocytes migrating across the wound (Friedl, 2004). In epithelial tissue, the opening of a gap induces the proliferation and movement of the surrounding intact

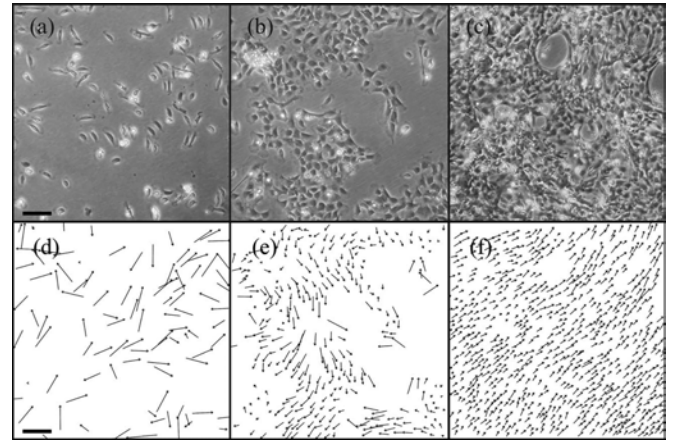


FIG. 15 Phase contrast images showing the collective behavior of fish keratocytes for three different densities. (a) 1.8, (b) 5.3 and (c) 14.7 cells/ $100 \times 100 \mu\text{m}^2$. The scale bar indicates $200 \mu\text{m}$. As cell density increases cell motility undergoes to collective ordering. The speed of coherently moving cells is smaller than that of solitary cells. (d)-(f) on the bottom panel depicts the corresponding velocities of the cells. From Szabó *et al.* (2006).

cells, which eventually closes the gap. Környei *et al.* (2000) studied the responses of artificially mechanically injured astrocytes (a characteristic star-shaped glial cell in the central nervous system) in vitro. In particular, the changes in the cell-motility, proliferation and morphology were analyzed. Their data suggested that the mechanical injury (basically a “scratch”) was not sufficient to indicate changes in the motility of the astroglia cell, but did result in a local enhancement in the cell proliferation. In a recent paper Trepát *et al.* (2009) argued that traction-forces driving collective cell migration did not arise only (or primarily) in the “leader cells” which were at the front of the traveling cell-sheet (Friedl, 2004; Gov, 2007; Vaughan and Trinkaus, 1966), but, as it can be seen on on Fig. 16, in many cell-rows behind the leading front-edge cells as well. Although – like some kind of “tag of war” – the cell-sheet as a whole moved in one direction, many cells within the cluster pulled the sheet in other directions .

Cancer metastasis. Two morphological and functional variants of collective migration have been described in tumors in vivo. The first results from protruding sheets and strands that maintain contact with the primary site, yet generate local invasion. The second shows detached cell clusters or cell files, histologically seen as ‘nests’, which detach from their origin and frequently extend along interstitial tissue gaps and paths of least resistance, as seen in epithelial cancer and melanoma (Friedl, 2004). Collective migration represents the predominant mode of tissue invasion in most epithelial cancers.

Furthermore, recently it has been argued, that malignant tumor cells may be capable of developing collective

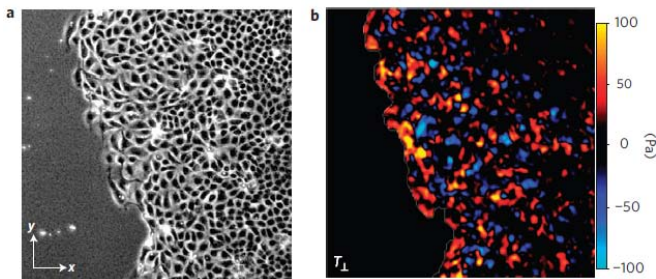


FIG. 16 (Color) Traction forces generated by a sheet of collectively moving cells. (a) is the phase contrast image and (b) depicts the tractions normal to the edge. Adapted from Trepat *et al.* (2009).

patterns that resemble to evolved adaptive behaviors like collective decision-making or collective sensing of the environmental conditions. Deisboeck and Couzin (2009) presented a concept as to how these abilities could arise in tumors and why the emergence of such sophisticated swarm-like behavior would endow advantageous properties to the spatio-temporal expansion of tumors.

D. Insects

Many insect-species exhibit remarkable collective motion. Furthermore, social insects (like termites, ants and several bees) exhibit various kinds of social and spatial organizations as well, but those ones which are characterized by other sophisticated principles (for example production of members with different roles carrying out specialized tasks) are beyond the scope of the present paper. Readers interested in this topic can find more information for example in (Holldobler and Wilson, 2008; Wilson, 1971).

Many species of butterflies (e.g. *Red Admiral*, *Painted Lady*) and moths (*Humming-bird Hawk-moth*, *Silver-Y moth*) migrate twice a year between the two hemispheres: when it is autumn on the Northern hemisphere they form huge “clouds” and fly to south and come back only when spring arrives. Other insects being famous of exhibiting collective motion are *ants*. Many of them create tracks between the nest and the food sources very efficiently, using pheromone trails. For example New World army ant *Eciton Burvehelli* – whose colonies may consist of million or more workers – stage huge swarm raids with up to 200 thousand individuals forming trail systems that are in length up to 100 m or even more, and 20 m wide (Franks *et al.*, 1991; Gotwald, 1995). Based on the observations Couzin and Franks (2003) have investigated the formation of these elaborated traffic lanes, and created a corresponding model exploring the influences of turning rates and local perception on traffic flow. Furthermore, Beekman *et al.* (2001) have investigated another fundamental question regarding these formations,

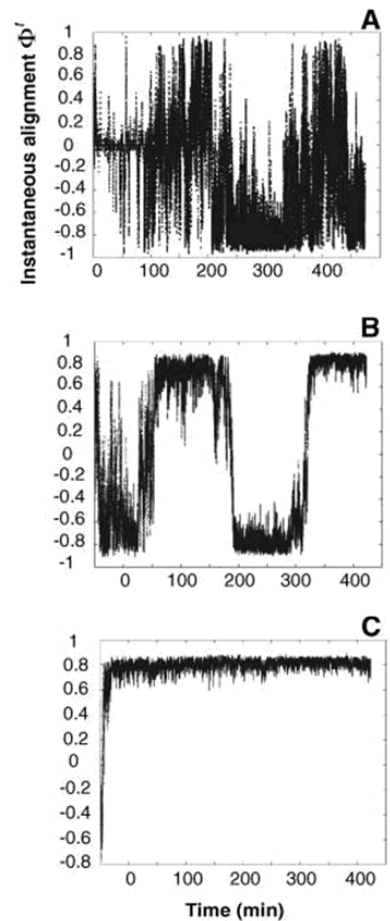


FIG. 17 The alignment of the motion of locusts in the function of animal density. The alignment is defined as the normalized average of the orientation for all moving animals, which means that values close to -1 and 1 indicate strong alignment (all locusts move in the same direction) whereas values close to zero indicate uncoordinated motion. At low densities (a), the alignment among individuals - if occurs - is sparse and sporadic, following a long initial period of disordered motion (5.3–17.2 locusts/ m^2 , equating to 2–7 moving locusts). (b) Intermediate densities (24.6–61.5 locusts/ m^2 , equating to 10–25 moving locusts) are characterized by sharp and abrupt changes in direction, separating long periods of correlated motion. (c) At densities above 73.8 locusts/ m^2 (equating to 30 or more moving locusts) the alignment of the motion is strong and persistent, individual locusts quickly adopt their motion to the others, and spontaneous changes in the direction do not occur. Adapted from Buhl *et al.* (2006).

namely what is the minimum number of workers that are required for this kind of self organization to occur. They have observed Pharaoh ants and they actually discovered that small groups forage in a disorganized way while larger ones are organized. Thus – for the first time – they have provided experimental evidence on a behavioral first-order phase-transition exhibiting hysteresis between organized and disorganized states.

Traditionally, an aggregate is considered to be an evo-



FIG. 18 Locust swarm. From Physorg.com

lutionarily advantageous state for its' members: it provides protection, information and choice of mates on the cost of limited resources and increased probability for various infections (Wilson, 1975a). However, according to some recent studies, in the case of some insect-species the depletion of nutritional resources may easily lead to cannibalism among group-members. Simpson *et al.* (2006) reported how the local availability of protein and salt influenced the extent to which Mormon cricket bands marched, both through the direct effect of nutrient state on locomotion and indirectly through the threat of cannibalism by resource-deprived specimens. Similarly, Bazazi *et al.* (2008) demonstrated that coordinated mass migration in juvenile desert locusts (see Fig. 18) was influenced strongly by cannibalistic interactions: Individuals in marching bands tended to bite each other but risk being bitten themselves. Surgical reduction of individuals' capacity to detect the approach of others from behind decreased their probability to start moving, dramatically reduced the mean proportion of moving individuals in the group and significantly increased cannibalism as well, but it did not influence the behavior of isolated locusts. They also showed, that while abdominal biting and the sight of others approaching from behind triggered movement, the occlusion of the rear visual field inhibited individuals' propensity to march.

Other characteristics of the collective motion of locusts have also been studied: Yates *et al.* (2009) investigated the sudden coherent switches in direction, and Buhl *et al.* (2006) their behavior with respect to the effect of the animal-density on the transition between disordered and ordered states. The experimental results are depicted on Fig. 17, which shows the alignment of the motion in the function of locust density, for three different cases: (a) low density, (b) intermediate density and (c) high density. As it can be seen, coordinated marching behavior strongly depends on the animal-density. With these experiments they also confirmed that the transition fol-

lowed the theoretical predictions of the SPP-model (Vicsek *et al.*, 1995), and identified the critical density for the onset of coordinated marching as well.

Although zooplanktons are not insects, here we briefly mention an interesting study in which *Daphnia*-swarms were artificially induced to carry out vortex motion by using vertical shaft of light, to which *Daphnia* are attracted. When the density of these tiny animals were under a certain threshold they exhibited a circular motion around the optical stimulus, whereas above this density-threshold they formed whirling swarms (Ordemann *et al.*, 2003). The authors suggested a corresponding model as well.

E. Fish schools and shoals

The largest groups of vertebrates exhibiting a rich set of collective motion patterns are certainly fish shoals and schools. Although these two terms cover very similar behaviors – and thus are often mixed – their meaning slightly differs: in a *shoal* fish relate to each other in a more loose way than in a school, and they might include fish of various species as well (Pitcher, 1983). Shoals are more vulnerable to predator attack. In contrast, in a *school* fish swim in a more tightly organized way considering their speed and direction, thus a school can be considered as a special case of shoal (Helfman *et al.*, 1997). At the same time, from one second to the other a shoal can organize itself into a disciplined school and vice versa, according to the changes in the momentary activity: avoiding a predator, resting, feeding or traveling (Hoare *et al.*, 2004; Moyle and Cech, 2003).

Schooling is a very basic feature of aquatic species and may have appeared in a very early stage of vertebrate evolution (Shaw, 1978). Over 50 percent of bony fish species school and the same behavior has been reported in a number of cartilaginous fish species as well (Benoit-Bird and Au, 2003; Shaw, 1978). Since the large scale coherent motion of fish is also very important from the practical point of view (fishing industry), the observational and simulational aspects of fish schools have played a central role in the studies of coherent motion.

Becco *et al.* (2006) recorded the trajectories of young fish in a school (see Fig. 19). Both the individual and the collective behavior were studied as a function of “fish-density”, and a transition from disordered to correlated motion was found. Using a novel technique called “Ocean Acoustic Waveguide Remote Sensing”, OAWRS (Makris *et al.*, 2006), which enables instantaneous imaging and continuous monitoring of oceanic fish shoals over tens of thousands of square kilometers, Makris *et al.* (2009) observed vast herring populations during spawning (see Fig. 20). The team observed a rapid transition from disordered to highly synchronized behavior at a critical density, followed by an organized group migration (see

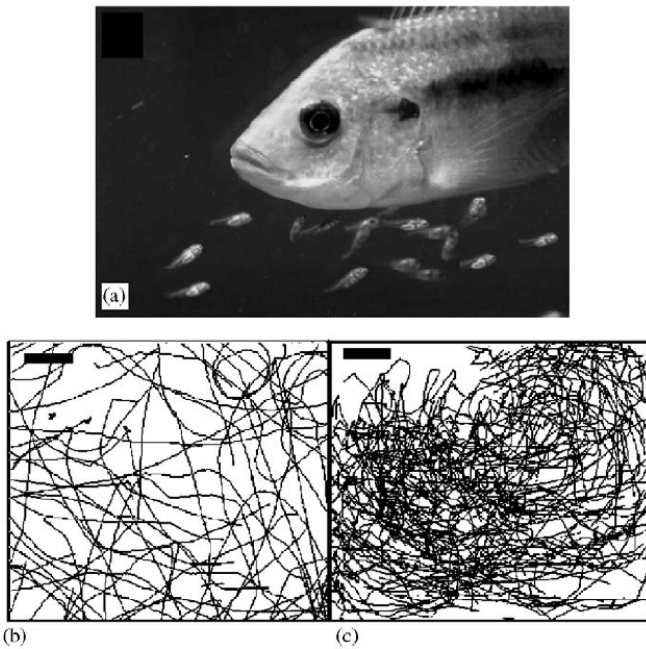


FIG. 19 Becco *et al.* (2006) recorded the trajectories of young Tilapia fish in a school. (a) The photo of a Tilapia together with her offsprings. (b) The trajectory of 20 fish (equating to 350 fish/m²) recorded for 41 seconds. (c) Same as the previous one, but with 905 fish/m². The bar scale on sub-pictures (b) and (c) represents 1cm×5cm. From Becco *et al.* (2006).

Fig. 21). Furthermore, in agreement with other studies (see Sec. II.G), they also found that a small set of leaders can significantly influence the actions of a much larger group.

One of the most fundamental question regarding gregarious animals – thus fishes as well – is how the *common decision* is reached: if they are to stay together, they constantly have to face questions like: which direction to swim, where to stop and forage, how to guard against predators, etc. Is it governed by a leader or by some kind of consensus? (Biro *et al.*, 2006; Reeb, 2000; Sumpter *et al.*, 2008) How does the size of the school influence decision making? (Grunbaum, 1998)

Regarding the connotation of “consensus *decision*”, most scholars follow the definition proposed by Conradt and Roper (2005), who interpreted it as the process in which ‘the members of a group chose between two or more mutually exclusive actions with the aim of reaching a consensus’, and “*leadership*” was ‘the initiation of new directions of locomotion by one or more individuals, which were then readily followed by other group members’ (Krause *et al.*, 2000).

In a recent experiment Ward *et al.* (2008) discovered that individual fish responded only when they saw a threshold number of conspecifics to perform a particular behavior (“quorum responses”). They experimentally investigated (and also modeled) the decision making pro-

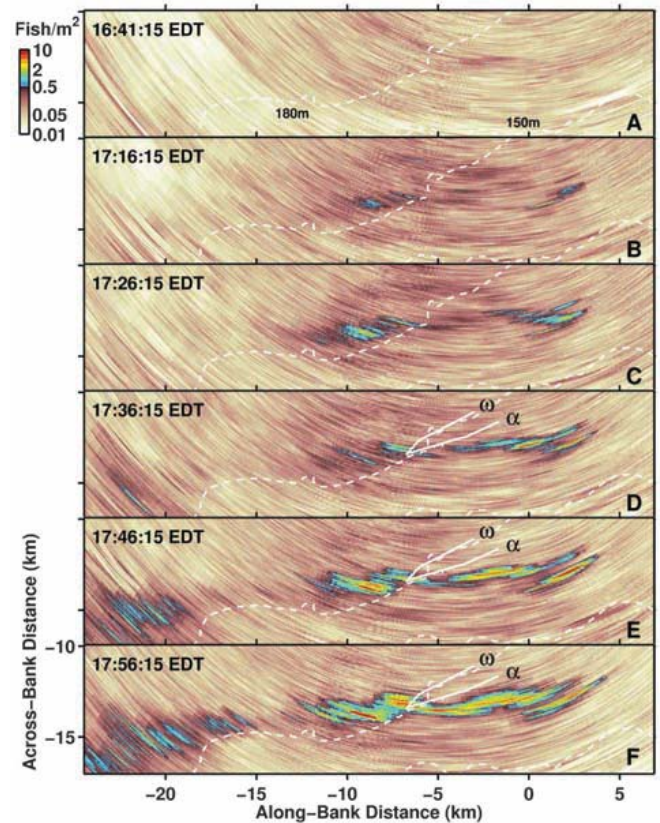


FIG. 20 (Color) OAWRS snapshots showing the formation of vast herring shoals consisting of millions of Atlantic herring on the northern flank of Georges Bank (situated between the USA and Canada) on 3 October 2006. Adapted from Makris *et al.* (2009).

cess about movements of a school in the case of a specific kind of fish. Reeb (2000) trained twelve golden shiners to expect food around midday in one of the brightly lit corners of their tank and investigated whether these informed individuals were able to lead their shoal-mates to the site of the food source later or not. He has indeed found that a minority of informed individuals (even one) can lead a shoal to the food-site. He also observed that the shoals never split up and were always led by the same fish.

Some of the experiments suggesting these results utilized “replica fish” or fish robots in order to study the decision-making behavior (Faria *et al.*, 2010a; Sumpter *et al.*, 2008)

F. Bird flocks

Flocking of birds has been the subject of speculations and investigations for many years. Some of the nearly paradoxical aspects of the extremely highly coordinated motion patterns were pointed out already in the mid 1980-es (Potts, 1984). In this paper Potts discussed

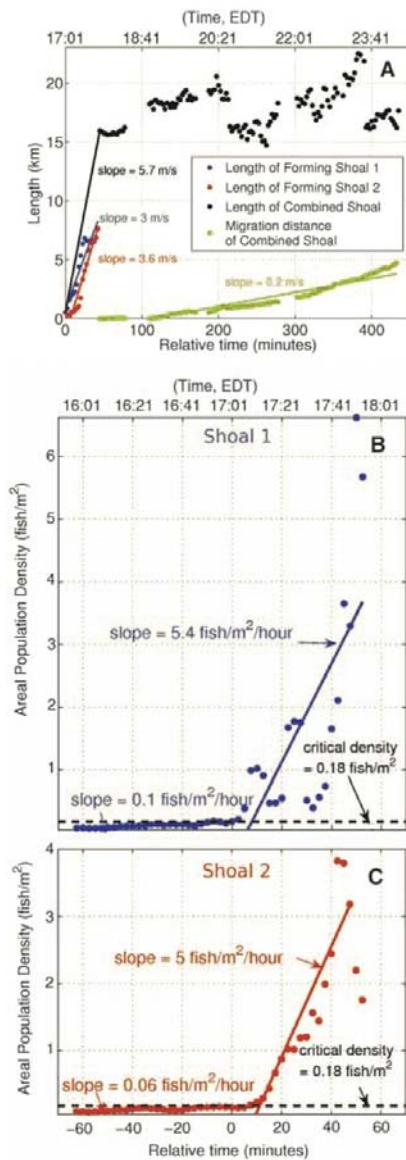


FIG. 21 (Color online) The results obtained from evaluating the data recorded by the technique called “Ocean Acoustic Waveguide Remote Sensing” (OAWRS), see Fig. 20. (a) The length of the three forming shoals (on the left, depicted by red, blue and black colors online) and the migration distance (bottom of the picture, green online) in the function of time. The solid lines are the best-fit slopes to the recorded data. (b) and (c) population density versus time for shoal 1 (blue data online) and shoal 2 (red data online). A slow growth in population density is followed by a rapid increase, immediately after the critical fish-density is reached (0.18 fish/m^2). Adapted from Makris *et al.* (2009).

how the flock movements were initiated and coordinated, through a frame-by-frame analysis of high-speed film of sandpiper flocks. He argued that any individual can initiate a flock movement, which then propagates through the flock in a wave-like form radiating out from the initiation site.

Research investigated various features of the group flight of birds, including positional effects on vigilance (mainly anti-predatory) (Beauchamp, 2003; Elgar, 1989), flock size, positional effects and intra-specific aggression in European starlings (Keys and Dugatkin, 1990), landing mechanisms (Bhattacharya and Vicsek, 2010). Skeins of wild geese are famous for their characteristic V-shaped formations, which was spatio-temporally analyzed by Hayakawa (2010). By performing field measures, he observed long-term fluctuations with single-sided propagation through the string, and proposed a corresponding model as well. Parrish and Hamner (1997) published a remarkable collection of papers about the state of the art of the research on animal congregations in three dimensions. The most recent and impressive experimental observational study was carried out within the framework of a EU FP6 NEST project (Starflag, 2005-07). In this project the team measured the 3D positions of individual birds (European Starlings, *Sturnus vulgaris*) within flocks containing up to 2,600 individuals, using stereometric and computer vision techniques (see Fig. 22). They characterized the structure of the flock by the spatial distribution of the nearest neighbors of each bird. Given a reference bird, they measured the angular orientation of its nearest neighbor with respect to the flock’s direction of motion, and repeated this process for all individuals within a flock as reference bird. Figure 23 depicts the average angular position of the nearest neighbors. The important main observation of the research team in Rome was that starlings in huge flocks interact with their 6-7 closest neighbors instead of those being within a given distance. Thus, they argued, the effect of density was quantitatively different in these (and probably most) flocks from that one would expect from models assuming a spatially limited interaction range (Ballerini *et al.*, 2008).

On the other hand, other experiments – concerning various other species – rendered the opposite version also probable, namely that the range of interaction did not change with density (Buhl *et al.*, 2006). This question is still the subject of investigations, and it may easily lead to the conclusion that this mechanism differs from species to species. An other, not yet investigated possibility is that the qualitative nature of the global behavior is not effected by this difference of the local interactions.

Cavagna *et al.* (2010) obtained high resolution spatial data of thousands of starlings using stereo imaging in order to calculate the response of a large flock to external perturbation. They were aiming at understanding the origin of collective response, namely the way the group as a whole reacts to its environment. The authors argued that collective response in animal groups may be achieved through scale-free behavioral correlations. This suggestion was based on measuring to what extent the velocity fluctuations of different birds are correlated to each other. They found that behavioral correlations are

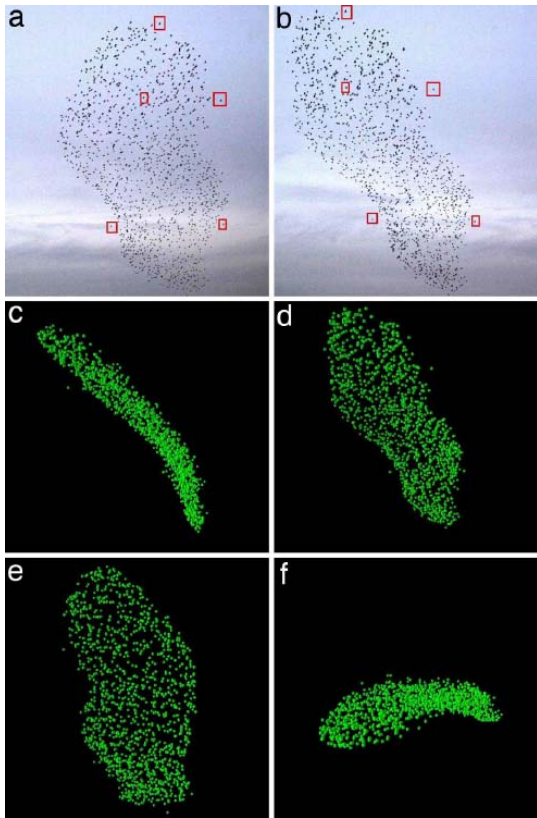


FIG. 22 (Color online) A typical starling flock and its 3D reconstruction. (a) and (b) is the photograph of one of the analyzed flocks. The pictures have been made at the same moment by two different cameras being 25 m far from each other. For reconstructing the flocks in 3D, each bird's image on the left photograph had to be matched to its corresponding image on the right photo. The small red squares indicate five of these matched pairs. (c-f) The 3D reconstructions of the analyzed flock from four different perspectives. (d) The reconstructed flock from the same view-point as (b). From Ballerini *et al.* (2008).

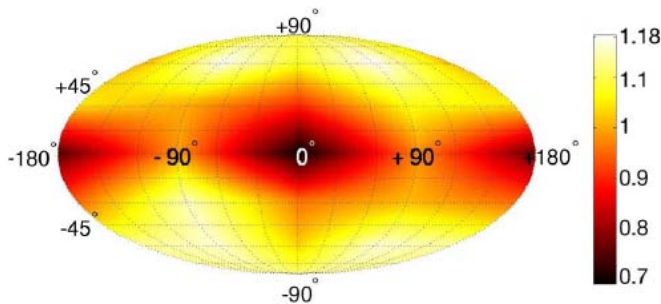


FIG. 23 (Color online) The average angular density of the birds' nearest neighbors. The map shows a striking lack of nearest neighbors along the direction of motion, thus the structure is strongly anisotropic. (A possible explanation for this phenomenon might lie in the anatomical structure of this genera's visual apparatus.) According to the authors, the observed anisotropy is the effect of the interaction among the individuals. Adapted from Ballerini *et al.* (2008).



FIG. 24 (Color online) A highly pre-trained homing pigeon with a small GPS device on his back. A recent technology to obtain information about the position of the individual birds. From Nagy *et al.* (2010).

scale free providing each animal with an effective perception range much larger than the direct interindividual interaction range. Such a scale free behavior is commonly observed for systems being at their critical state.

A very recent direction (made possible by technological advances) is to obtain information about the position of the individual birds during the observations using ultra light GPS devices (see Fig. 24). Although the present technology is still not suitable for large scale, high precision studies (only a couple of birds per experiment and a resolution of the order of meters have been achieved yet), this method has already called to forth important results (Ákos *et al.*, 2008; Roberts *et al.*, 2004).

Applying GPS data-loggers in six highly pre-trained pigeons, the efficiency of a flock was investigated by Dell'Arciccia *et al.* (2008). They found that the homing performance of the birds flying as a flock was significantly better than that of the birds released individually. Employing high-precision GPS tracking of pairs of pigeons Biro *et al.* (2006) found that if conflict between two birds' directional preferences was small, individuals averaged their routes, whereas if conflict rose over a critical threshold, either the pair split or one of the birds became the leader.

Using similar method, track-logs obtained from high-precision lightweight GPS devices, Nagy *et al.* (2010) found a well-defined hierarchy among pigeons belonging to the same flock by analyzing data concerning leading roles in pairwise interactions (see Fig. 25). They showed that the average spatial position of a pigeon within the flock strongly correlates with its place in the hierarchy.

One of the long standing questions about the collective behavior of organisms is the measurement and interpretation of their positions relative to each other during flocking. Precise data of this sort would make the reconstruction of the rules of interaction between the individual organisms possible. In a very recent paper Lukeman *et al.* (2010) carried out an investigation with this specific goal. They analysed a high-quality dataset of flocking

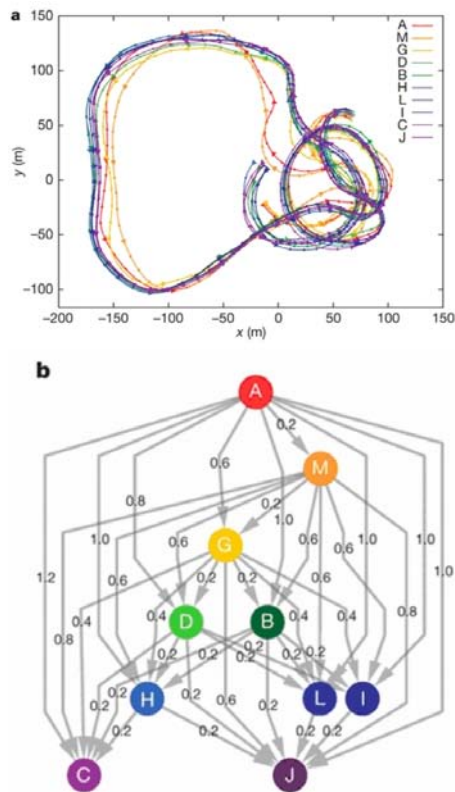


FIG. 25 (Color online) The route of a flight and the corresponding leadership-network of a pigeon flock. (a) A two-minute segment of the trajectory of ten pigeons recorded by small GPS devices (as depicted on Fig. 24). The different letters (and colors online) refer to the different individuals. The small dots on the lines indicate 1 second, the triangles indicate 5, and they point in the direction of the flight. (b) The leadership-network for the flight depicted on sub-figure (a). Each node (letter) represent a bird, among which the directed edges point from the leader to the follower. The numbers on the edges indicate the time delay (in seconds) in the two birds' motion. For those bird-pairs which are not connected directly with each other with an edge, directionality could not be resolved by means of the applied threshold. Adapted from Nagy *et al.* (2010).

surf scoters, forming well spaced groups of hundreds of individuals on the water surface. Lukeman *et al.* (2010) were able to fit the data to zonal interaction models (see, e.g., Couzin *et al.* (2002)) and characterize which individual interaction forces suffice to explain observed spatial patterns. The main finding is that important features of observed flocking surf scoters can be accounted for by zonal models with specific, well-defined rules of interaction.

G. Leadership in groups of mammals and crowds

Many insect, fish and bird species live in large groups in which members are considered to be identical (from

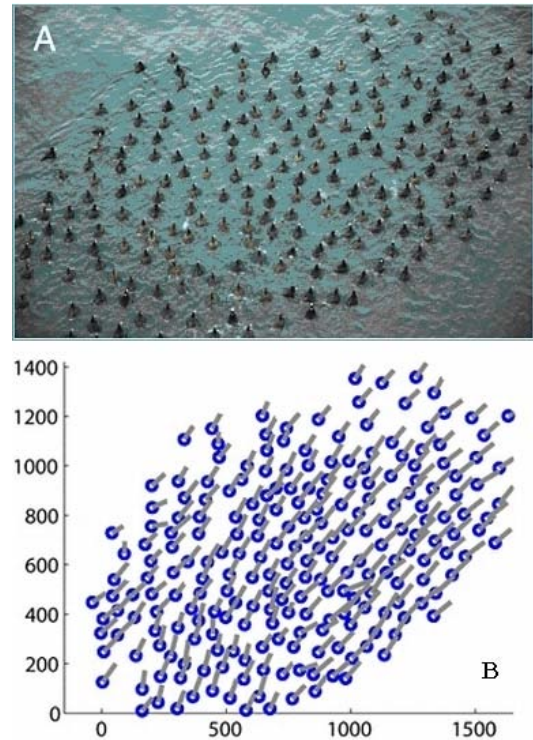


FIG. 26 (Color online) A flock of surf scoter (*M. perspicillata*) swimming on the water surface (A). The actual coordinates and velocities after correction for perspective and drift currents effects. After Lukeman *et al.* (2010).

the viewpoint of collective motion), unable the recognize each other on the individual level (although not all, (Nagy *et al.*, 2010)). Such groups might reach a consensus either without leader (by quorum response, mean value, etc.) or with a leader, but even in this latter case leadership is temporal since it is based on temporal differences, such as pertinent information of food location or differences in some inner states (hunger, spawning inducement, etc). As an important difference, most mammals do have the capacity for individual recognition enabling the emergence of hierarchical group structures. Although the assumption that the dominant individuals are at the same time the ones that lead the herd seems quite plausible, in fact, recent biological studies reveal that in many cases there is *no* direct relationship between dominance and leadership. Most probably it is an interaction among kinship, dominance, inner state and some outer conditions.

Zebras, like many other mammals, need significantly more water and energy during the lactation period, than they need otherwise. Fischhoff *et al.* (2007) investigated the effect of two factors, *identity* and *inner state*, on leadership in herds of zebras, *Equus burchellii*. “Identity” covers both dominance and kinship, while the inner state was interpreted as the reproductive state (if the individual is in its lactation period or not). Zebra harems consist

of tightly knit individuals in which females were observed to have habitual roles (“personal differences”) in the initiation of group movements. The authors also found that lactating females initiate movements more often than non-lactating ones, thus lactation, as inner state, plays an important role in leadership. Others find more direct relationship to hierarchy. Sárová *et al.* (2010) recorded the motion of a herd of 15 beef cows, *Bos taurus*, for a three-week period using GPS devices. They found that short-distance travels and foraging movements are not lead by particular individual, instead, they are rather influenced in a *graded* manner, i.e., the higher an individual was in the group hierarchy, the bigger influence it exerted on the motion of the herd. According to the observations, Rhesus macaques (*Macaca mulatta*) preferred to join related or high-ranking individuals too, whereas Tonkean macaques (*Macaca tonkeana*) exhibited no specific order at departure (Sueur and Petit, 2008). In a recent review article Petit and Bon (2010) interpreted the process of collective decision making (regarding group movements) as a combination of two kinds of rules: ‘individual-based’ and ‘self-organized’. The first one covers the differences of the (mostly inner) states of the animals, that is, differences in social status, physiology, energetic state, etc. The second one, self-organization, corresponds to the interactions, simple responses among individuals.

Regarding the case when leadership emerges solely from differences in the inner states of the group members (those ones lead who have pertinent information), Couzin *et al.* (2005) suggested a simple model to show how a few informed individuals can lead a whole group. In this model (which is detailed in Sec. V.D) group members do not signal and do not know which of them (if any) has information regarding the desired direction. This model predicts that even if the portion of the informed individuals within the group is very small, the group as a whole can achieve great accuracy in its movement. In fact, the larger the group size, the smaller the portion of informed members are needed to lead the group. Dyer *et al.* (2008) tested these predictions on *human* groups in which the experimental subjects were naïve and they did not use verbal communication or any other active signaling. The experiments indeed supported the predictions. Other experiments investigated the relationship between the spatial position of informed individuals and the speed and accuracy of the group motion (Dyer *et al.*, 2009). The results proved to remain valid in larger crowds as well (100 and 200 people) which can have important implications on plans aiming to guide human groups for example in case of emergency.

Faria *et al.* (2010b) studied the effect of the knowledge regarding the presence and identity of a leader in small human groups, and also investigated those inadvertent social cues by which group members might identify leaders. With this object they conducted 3 treatments: in the *first* one, participants did not know that there was

a leader, in the *second* treatment they were instructed to follow the leader but they did not know who it was, while in the *third* one they knew who the leader was. The experiments took place in a circular area with 10m diameter labeled by numbers from 1 to 16. These marks were spaced equally around the perimeter, as shown in Fig. 27. In all the trials, participants were instructed (i) not to talk or to make any gesture (ii) to walk continuously, and (iii) to remain together as a group. Further instructions were provided on a piece of paper: a (randomly chosen) person was asked to move to a (randomly chosen) target but stay with the group. She/he was the “informed individual”, the “leader”. The rest of the group was uninformed, whose instructions differed from treatment to treatment: In the first one, they were only asked to stay with the group. In the second treatment they were told to follow the leader, but they did not know who it was. In the third one, they were asked to follow the leader whose identity was provided (by the color of his/her sash). Although the accuracy of the group movement significantly differed from treatment to treatment, the leader always succeeded to guide the group to the target. The least accurate group motions were measured during the first treatment, while the second and third ones resulted group motions whose accuracy were close to the possible maximum value. Three main factors were exposed as inadvertent social cues that might help uninformed group members to identify the leader(s): (i) time to start walking – informed individuals usually started walking sooner, (ii) distance from the group center – leaders were farther from the center than others, and (iii) proportion of time spent following – informed people spent significantly less time following.

Many authors study animal groups from the viewpoint of a cost-benefit interpretation. They highlight that for an individual, living in a group brings more benefit than disadvantage, which is after all the ultimate reason for group-formation. However, during reaching a consensus, if individuals differ in state and experience – which is reasonable to assume – then some individuals will have to pay bigger “consensus costs” than others (which is the cost that an individual pays by foregoing its optimal behavior to defer to the common decision (King *et al.*, 2008)). Theoretical models estimate “democratic decisions” less costly (in terms of average consensus cost) than “despotic decisions” (Conradt and Roper, 2003) which estimation is supported by a number of observations as well (Conradt and Roper, 2005). However, many animal groups (including primates and humans) often follow despotic decisions. Field experiments (for example on wild baboons (King *et al.*, 2008)) highlight the role of social relationships and leader incentives in such cases. From a more theoretical viewpoint, Conradt and Roper (2010) discussed the cost/benefit ratio during group movements, separately for timing and spatial decisions.

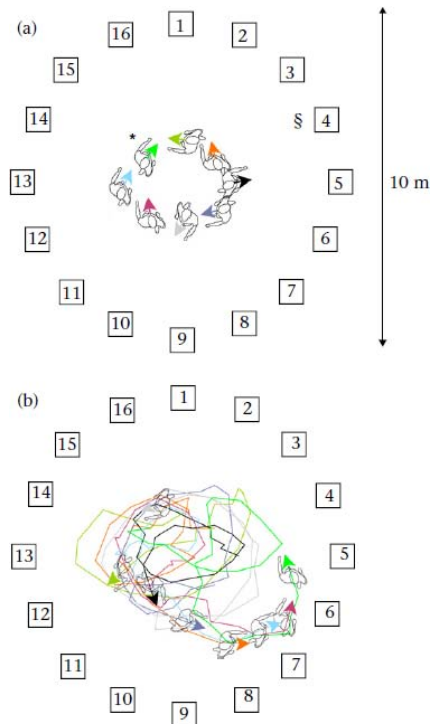


FIG. 27 (Color online) Orientations (arrows) and walking trajectories (lines) of the eight participants during the second treatment. The colors identify the participants. The leader – marked by a '*' on subpicture (a) – was instructed to reach the randomly selected target which is marked by a '§'. (a) depicts the situation at the beginning of the trial and (b) 25 s later. Adapted from Faria *et al.* (2010b).

H. Lessons from the observations

The main, commonly assumed advantages of flocking are:

1. Defense against predators,
2. More efficient exploration for resources or hunting,
3. Improved decision making in larger groups (e.g., where to land)

In general, it can be argued that with the increasing size of a group the process of decision making is likely to become more efficient (Camazine *et al.*, 2001; Conradt and List, 2009; Krause *et al.*, 2010). In addition, based on the numerous observations the following hypotheses can be made about the nature of the patterns of motion arising:

1. Motion and a tendency to adopt the direction of motion of the neighbors is the main reason for ordered motion,
2. Apparently the same, or very similar behaviors occur in systems of very different origin. This suggests the possibility of the existence of universal classes of collective motion patterns,

3. Boundary conditions may significantly affect the essential features of flocking,
4. Collective decision making is usually made in a critical, turbulent state of the flocks.

III. DEFINITIONS AND TECHNIQUES FOR COLLECTING AND EVALUATING DATA

Throughout this overview the notion of flocking is used as a synonym of any kind of *coherent motion* of individual units. However, the notion of coherent motion needs some further elaboration since, as it turns out, it can be manifested in a number of specific ways. In any case, coherent or ordered motion is assumed to be a counterpart of disordered, random motion. In the various models of flocking it emerges through a kind of phase transition (from disorder to order) as a function of the relevant parameter(s) of the models. To demonstrate more clearly this aspect of collective motion the best approach is to adopt a few related definitions motivated mainly by statistical physics (the physics of many interacting molecules).

In this section we overview the relevant physical quantities used in the later chapters. Physicists and other readers who are familiar with the basic concepts and laws of statistical physics might skip this section. Before that, however, we would like to point out that according to the numerous related results obtained so far, there seems to be a surprisingly close analogy between the fundamental features of phase transitions in equilibrium systems and the corresponding behavior in systems of self-propelled particles.

A. Basic notions and expressions

In a general sense, *phase transition* is a process, during which the elements of a system consisting of many interacting particles collectively change their behavior as a function of an external parameter. A well known example is the freezing of a fluid when the temperature drops. In this case the temperature is the external parameter. Phase transitions are typical examples for collective phenomena.

The *level of order* in a system is usually described by a parameter called *order parameter*, which is 0 in one phase (usually in the disordered), and non-zero in the other. Its value characterizes the onset of order during phase transition. In the case of collective motion the most naturally (but not necessarily) chosen *order parameter* is the average normalized velocity φ ,

$$\varphi = \frac{1}{Nv_0} \left| \sum_{i=1}^N \vec{v}_i \right|, \quad (1)$$

where N is the total number of the units and v_0 is the average absolute velocity of the units in the system. If the motion is disordered, the velocities of the individual units point in random directions and average out to be a small vector, while for ordered motion the velocities all add up to a vector of absolute velocity close to Nv_0 (thus the order parameter for large N can vary from about zero to about 1).

Phase transitions (in case of flocking systems as well) can be of *first order* (or *discontinuous*), during which the order parameter jumps from one value to another. In contrast, during *continuous* (mostly *second order*) phase transitions the change in the level of order is usually sharp (e.g., very quickly increasing), but not discontinuous at the transition point. Second order phase transitions are always accompanied by large fluctuations of some of the relevant quantities.

Phenomena associated with a continuous phase transition are often referred to as *critical phenomena* because of their connection to a *critical point* at which the phase transition occurs. (“Critical”, because here the system is extremely sensitive to small changes or perturbations.) Near to the critical point, the behavior of the quantities describing the system (e.g., pressure, density, heat capacity, etc.) are characterized by the so called *critical exponents*. For example the (isothermal) compressibility κ_T of a liquid substance, near to its critical point, can be expressed by

$$\kappa_T \sim |T - T_c|^{-\gamma}, \quad (2)$$

where T is the temperature, T_c is the critical temperature (at which the phase transition occurs), \sim denotes proportionality and γ is the critical exponent. In systems of self-propelled particles, noise (η) plays the role of temperature (T): an external parameter that endeavors to destroy order. Correspondingly, the fluctuation of the order parameter, $\sigma^2 = \langle \varphi^2 \rangle - \langle \varphi \rangle^2$, is described as

$$\sigma \sim |1 - \eta/\eta_c|^{-\gamma}, \quad (3)$$

where η is the noise, η_c is the critical noise that separates the ordered and disordered phases, and γ is again the ‘susceptibility’ critical exponent. By introducing $\chi = \sigma^2 L^2$, where L is the linear size of the system, we get

$$\chi \sim (\eta - \eta_c)^{-\gamma} \quad (4)$$

κ_T in Eq. (2) corresponds to χ in Eq. (4).

Another descriptive expressing the change in the density between the liquid and the gas phases, $\rho_l - \rho_g$, obeys to

$$\rho_l - \rho_g \sim (T_c - T)^\beta, \quad (5)$$

where β is the critical exponent. For systems of self-propelled particles, when $L \rightarrow \infty$, the corresponding equation is

$$\varphi \sim \begin{cases} (1 - \eta/\eta_c)^\beta & \text{for } \eta < \eta_c \\ 0 & \text{for } \eta > \eta_c \end{cases} \quad (6)$$

Regarding the relation between the order parameter φ and the external bias field h (“wind”), φ scales as a function of h according to the power law

$$\varphi \sim h^{1/\delta} \quad (7)$$

for $\eta > \eta_c$, where δ is the relevant critical exponent.

Various similar expressions can be formulated involving further quantities as well as critical exponents. Interestingly, very different physical systems exhibiting seemingly different kind of phase transitions follow similar laws. For example the magnetization M of a ferromagnetic material subject to a phase transition near to a critical temperature called Curie point, obeys $M \sim (T_c - T)^\beta$.

Another surprising observation is that these critical exponents are related to each other, that is, expressions like $\alpha + 2\beta + \gamma = 2$ or $\delta = 1 + \frac{\gamma}{\beta}$ can be formulated, which hold independently of the physical system the critical exponents ($\alpha, \beta, \gamma, \delta$) belong to. Note, that this is a far from trivial observation! For more details on this topic see (Cardy, 1996; Isihara, 1971; Pathria, 1996), and for further analogies and differences between ferromagnetic models and systems of self propelled particles see (Czirók *et al.*, 1997).

Another phenomenon accompanying phase transitions is the formation of clusters of units behaving (e.g., being directed or moving) in the same way. Units which can be reached through neighboring units belong to the same cluster, where neighboring stands for a predefined proximity criterion. Thus, the behavior of units in the same cluster is usually highly correlated. In general, *correlation functions* represent a very useful tool to characterize the level of order in a system.

B. Correlation functions

Generally speaking, two series of data (X and Y) are *correlated* if there is some kind of relationship between their elements. A *correlation function* measures the similarity between the data-sequences, or, in the continuous case, the similarity between two signals or functions. *Auto-correlation* is the correlation of a signal with itself, typically as a function of time. This is often used to reveal repeating patterns, such as the presence of a periodic signal covered by noise. If the two signals compared are different, we consider *cross-correlation*.

For example, let us consider two real-valued data-series f_1 and f_2 , which differ only by a shift in the element-numbers, e.g., the 5th element in the first series is the

same than the 12th in the second, the 6th corresponds to the 13th, etc. In this case the shift is $s = 7$, that is, the first series has to be shifted with 7 elements in order to be congruous with the second one. The corresponding (cross) correlation function will show a maximum at 7.

Formally, for discrete data-sequences f_1 and f_2 , the correlation function is defined as:

$$c(s) = \sum_{n=-\infty}^{\infty} f_1^*[n] f_2[n+s], \quad (8)$$

where ‘*’ refers to the complex conjugate operation¹.

Accordingly, in continuous case, when f_1 and f_2 are continuous functions (or “signals”), the cross-correlation function will reveal how much one of the functions must be shifted (along the horizontal axis) to become congruous with the other one. Formally,

$$c(\tau) = \int_{n=-\infty}^{\infty} f_1^*(t) f_2(t+\tau) dt \quad (9)$$

Equation (9) shifts f_2 along the horizontal axis (which is in this example the time-axis), and calculates the product at each time-step of the two functions. This value is maximal when f_1 and f_2 are congruous, because when lumps (positives areas) are aligned, they contribute to making the integral larger, and similarly, when the troughs (negative areas) align, they also make a positive contribution to the expression, since the product of two negative values is positive.

With this introduction we can now formulate some specific correlation functions that are often used in the field of collective motion.

The *velocity-velocity correlation function*, c_{vv} , is an auto-correlation function that shows how closely the velocity of a particle (unit, individual, etc.) at time t is correlated with the velocity at a reference time. It is defined as follows:

$$c_{vv}(t) = \frac{1}{N} \sum_{i=1}^N \frac{\langle \vec{v}_i(t) \cdot \vec{v}_i(0) \rangle}{\langle \vec{v}_i(0) \cdot \vec{v}_i(0) \rangle}, \quad (10)$$

where $\vec{v}_i(0)$ is the starting (reference) time and N is the number of particles within the system and $\langle \dots \rangle$ denotes taking an average over a set of starting times. The way $c_{vv}(t)$ decays to zero shows how the velocities at later times become independent of the initial ones.

¹ A pair of complex numbers are said to be *complex conjugates*, if their real part is the same, but their imaginary parts are of opposite signs. For example, $2 + 3i$ and $2 - 3i$ are complex conjugates. It also follows, that the complex conjugate of a real number is itself.

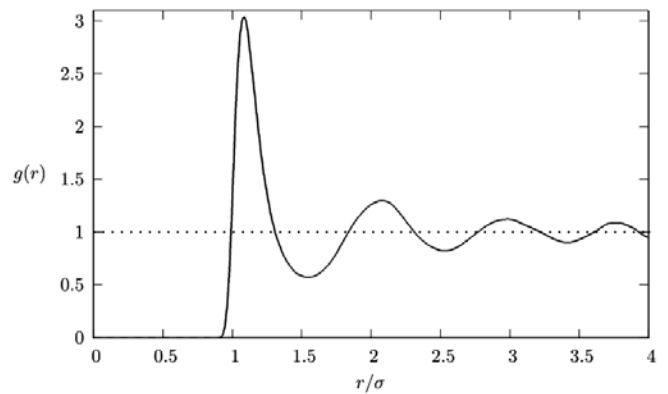


FIG. 28 Radial distribution function for the so called Lennard-Jones model. It describes how the unit density varies as a function of the distance from one particular element in the case of an interaction potential having both a shorter range, strong repulsive and a longer range attractive part.

The *pair correlation function*, $c_p(r)$, (or radial distribution function, $g(r)$), depicted on Fig. 28, describes how the unit density varies as a function of the distance from one particular element. More precisely, if there is a unit at the origin, and if $n = N/V$ is the average number density (N is the number of units in a system with volume V), then the local density at distance r from the origin is $ng(r)$. It can be interpreted as a measure of local spatial ordering. Equation 11 gives the exact formula.

$$c_p(r) = \frac{V}{4\pi r^2 N^2} \left\langle \sum_i \sum_{j \neq i} \delta(r - r_{ij}) \right\rangle \quad (11)$$

The *directional correlation function*,

$$c_{ij}(\tau) = \langle \vec{v}_i(t) \cdot \vec{v}_j(t+\tau) \rangle, \quad (12)$$

tells to what degree the velocity of the i th particle at time t is correlated with that of particle j at time $t + \tau$. $\langle \dots \rangle$ denotes averaging over time, and $\vec{v}_i(t)$ is the normalized velocity of the i th SPP. (Note that $c_{ij}(\tau) = c_{ji}(-\tau)$.) The directional correlation *delay* is primarily used to determine the leader-follower relationship within a flock of birds, fish, or more general, in a swarm of self-propelled particles (SPPs), as illustrated on Fig. 29 (Nagy *et al.*, 2010). The directional correlation delay *for a pair* of SPPs (i and j , where $i, j = 1, 2, \dots, N$ and N is the number of SPPs within the flock) is calculated according to Eq. 12. Then the maximum value of the $c_{ij}(\tau)$ correlation function is allocated, τ_{ij}^* . Negative value means that the direction of motion of the i th SPP is falling behind that of the j th one, so this can be interpreted as j is leading. The directional correlation function for an SPP with respect to the rest of a given flock or swarm, is $c_i(\tau) = \langle \vec{v}_i(t) \cdot \vec{v}_j(t+\tau) \rangle_{i,j}$.

Further useful correlation functions were suggested in Cavagna *et al.* (2010) in order to characterize the

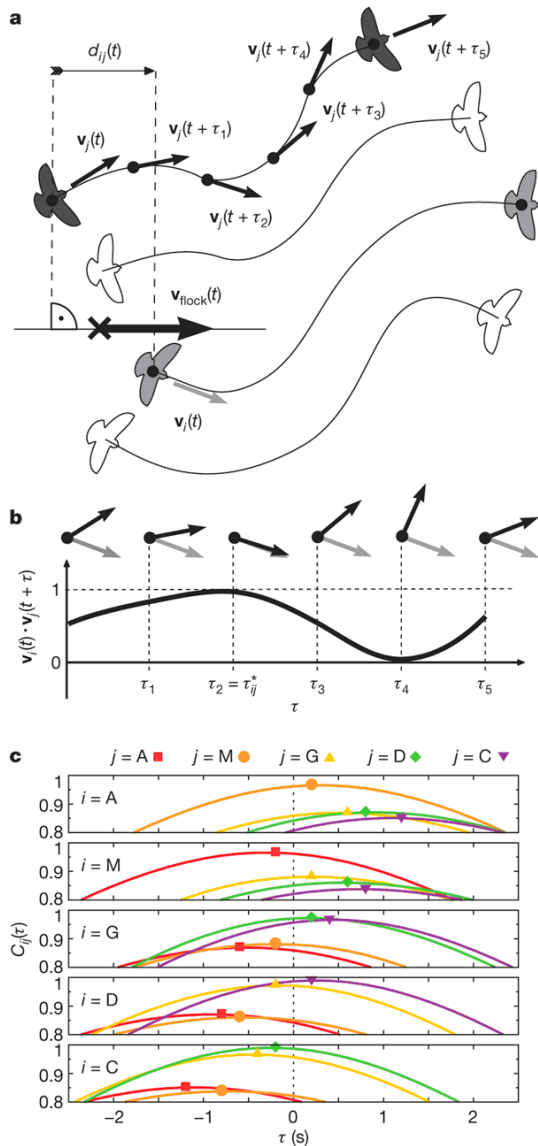


FIG. 29 (Color online) Illustration for the directional correlation function, which is a tool for determining the leader-follower relationships within a flock or swarm. This example shows the case of a bird-flock. (a) Determining the projected distance $d_{ij}(t)$ of birds i and j onto the direction of motion of the whole flock at time step t . Bird i is light gray on the draw, and bird j is dark. The $\vec{v}_j(t)$ arrows indicate the direction of bird j at each time step t . The center of mass of the flock is denoted with a cross, which moves with $v_{flock}(t)$, the average velocity of the flock. The relative position of the birds i and j is projected onto $v_{flock}(t)$. The directional correlation function for each $i \neq j$ pair is defined by Eq. (12). (b) Scalar products $\vec{v}_i(t) \cdot \vec{v}_j(t + \tau)$ of the normalized velocity vectors of bird i at time t , and that of bird j at time $t + \tau$. On this example bird j follows bird i with correlation time τ_{ij}^* . (c) The directional correlation functions $c_{ij}(\tau)$ during the flock flight depicted on Fig. 25. For better transparency only five of the items are shown, the data belonging to birds A, M, G, D and C. The solid symbols indicate the maximum value of the correlation functions, which have been used to determine the leader-follower network, depicted on 25 b. From Nagy *et al.* (2010).

response of a flock to external perturbation.

C. Data collection techniques

Collective motion of cells has been followed by computer controlled phase contrast video microscope system (Czirók *et al.*, 1998). Cell's trajectories have been recorded for several days to determine the velocities of several cell types. Particle Image Velocimetry (PIV) (Raffel *et al.*, 2002) techniques have been used to evaluate the velocity field of thousands of swimming bacteria (Cisneros *et al.*, 2007). Originally, PIV is an optical method used to produce the two dimensional instantaneous velocity vector field of fluids, by seeding the media with 'tracer particles'. These particles are assumed to follow the flow dynamics accurately, and it is their motion that is then used to calculate velocity information. The movement of vertebrate flocks has been tracked mainly by camera based techniques. (Sinclair, 1977) used aerial photos to investigate the individual's spatial positions within grazing African buffalo herds in two dimensions. Because of the difficulties of analyzing three dimensional group motions, fish schools also have been studied in shallow water. The camera in these studies followed the flock from above (Becco *et al.*, 2006). To reconstruct the three-dimensional positions and orientations of the fish Cullen *et al.* (1965) used the so called shadow method. With the shadow method Partridge *et al.* (1980) were investigating positioning behavior in fish groups of up to 30 individuals. Three dimensional trajectories of fish group have been recorded with three orthogonally positioned video cameras by Parrish and Turchin (1997). Major and Dill. (1978) applied the stereo photography technique first for recording the three dimensional positions of birds within flocks of European starlings and dunlins. Ballerini *et al.* (2008) have recently reconstructed with high precision the three-dimensional positions of hundreds of starlings in airborne flocks with the same technique. The stereo photography method allowed the detailed and accurate analysis of nearest neighbor distances in large flocks, but still did not make the trajectory reconstruction of the individual flock members possible. Exploiting acoustic waves, a new technology called "Acoustic Waveguide Remote Sensing" makes the monitoring and imaging of vast oceanic fish population possible, over tens of thousands of square kilometers (Makris *et al.*, 2009, 2006).

The development of GPS technology makes it possible to equip individual flock members with GPS device. With this method the trajectory of flock members can be collected with high temporal resolution in their natural environment. The limits of this method at this moment are on the one hand the growing cost of the research with the growing number of tracked flock members, and on the other hand the limited accuracy of the devices. GPS

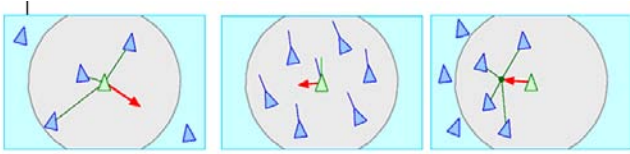


FIG. 30 (Color online) The three basic steering behaviors determining the motion of the objects (called “boids”). (a) *Separation*, in order to avoid crowding local flock-mates. (Each boid reacts only to flock-mates within a certain neighborhood around itself, they are the “local flock-mates”.) (b) *Alignment*: objects steer towards the average heading direction of their local flock-mates. (c) *Cohesion*: objects move toward the average position of their neighboring boids. From <http://www.red3d.com/cwr/boids/>.

logged flight tracks of homing pigeon pairs have been analyzed by Biro *et al.* (2006) and Nagy *et al.* (2010) to investigate hierarchical leadership relations inside the group. Dell’Ariccia *et al.* (2008) also used the GPS method to study the homing efficiency of a pigeon group consist of 6 birds.

IV. BASIC MODELS

A. Simplest self-propelled particles (SPP) models

Modeling of flocks has simultaneously been considered by the – initially – relatively separated communities of computer graphics specialists, biologists and physicists. Perhaps the first widely known flocking simulation was published by Reynolds (1987) who was mainly motivated by the visual appearance of a few dozens of coherently flying objects, among them imaginary birds and space-ships. His bird-like objects, which he called “boids”, were moving along trajectories determined by differential equations taking into account three types of interactions: avoidance of collisions, heading in the direction of the neighbors and finally, trying to stay close to the center of mass of the flock, as illustrated on Fig. 30. The model was deterministic and had a number of relatively easily adjustable parameters. The website <http://www.red3d.com/cwr/boids/> created and maintained until 2001 by Reynolds is a unique source of links to all sorts of information (programs, demos, articles, visualizations, essays, etc.) related to group motion.

In order to establish a quantitative interpretation of the behavior of huge flocks in the presence of perturbations, a statistical physics type of approach to flocking was introduced in 1995 by Vicsek *et al.* (1995), which nowadays is widely referred to as “Vicsek Model” (VM) e.g., (Baglietto and Albano, 2008, 2009b; Chaté *et al.*, 2008a; Ginelli *et al.*, 2010; Jadbabaie *et al.*, 2003; Kulinskii and Chepizhko, 2009; ZhiXin and Lei, 2008). In the present paper we will refer to this approach as the “SVM”, corresponding to Standard Vicsek Model as sug-

gested in (Bertin *et al.*, 2009; Huepe and Aldana, 2008). In this model the perturbations, which are considered to be a natural consequence of the many stochastic and deterministic factors affecting the motion of the flocking organisms, are taken into account by adding a random angle to the average direction (Eq. 15). In this cellular-automaton-like approach of self-propelled particles (SPPs) the units move with a fixed absolute velocity v_0 and assume the average direction of others within a given distance R . Thus, the equations of motion for the velocity (\vec{v}_i) and position (\vec{x}_i) of particle i having neighbors labeled with j are

$$\vec{v}_i(t+1) = v_0 \frac{\langle \vec{v}_j(t) \rangle_R}{|\langle \vec{v}_j(t) \rangle_R|} + \text{perturbation} \quad (13)$$

$$\vec{x}_i(t+1) = \vec{x}_i(t) + \vec{v}_i(t+1) \quad (14)$$

Here $\langle \dots \rangle_R$ denotes averaging (or summation) of the velocities within a circle of radius R surrounding particle i . The expression $\frac{\langle \vec{v}_j(t) \rangle_R}{|\langle \vec{v}_j(t) \rangle_R|}$ provides a unit vector pointing in the average direction of motion (characterized by its angle $\vartheta_i(t)$) within this circle. It should be pointed out that the processes accounted for by such an alignment rule can be of very different origin (stickiness, hydrodynamics, pre-programmed, information processing, etc). Perturbations can be taken into account in various ways. In the standard version they are represented by adding a random angle to the angle corresponding to the average direction of motion in the neighborhood of particle i . The angle of the direction of motion $\vartheta_i(t+1)$ at time $t+1$, is obtained from $\vartheta_i(t) = \arctan \left[\frac{\langle v_{j,x} \rangle_R}{\langle v_{j,y} \rangle_R} \right]$, as

$$\vartheta_i(t+1) = \vartheta_i(t) + \Delta_i(t), \quad (15)$$

where $v_{j,x}$ and $v_{j,y}$ are the x and y coordinates of the velocity of the j th particle in the neighborhood of particle i , and the perturbations are represented by $\Delta_i(t)$ which is a random number taken from a uniform distribution in the interval $[-\eta\pi, \eta\pi]$ (i.e., the final direction of particle i is obtained after rotating the average direction of the neighbors with a random angle). The only parameters of the model are the density ρ (number of particles in a volume R^d , where d is the dimension), the velocity v_0 and the level of perturbations $\eta < 1$. For order parameter φ , the normalized average velocity is suitable, $\varphi \equiv \frac{1}{Nv_0} \left| \sum_{i=1}^N \vec{v}_i \right|$, as defined by Eq. (1).

This extremely simple model allows the simulation of many thousands of flocking particles and displays a second order type phase transition from disordered to an ordered (particles moving in parallel) state as the level of perturbations is decreased (see Fig. 31). At the point of the transition features of both order and disorder are simultaneously present leading to flocks of all sizes (and an algebraically decaying velocity correlation function).

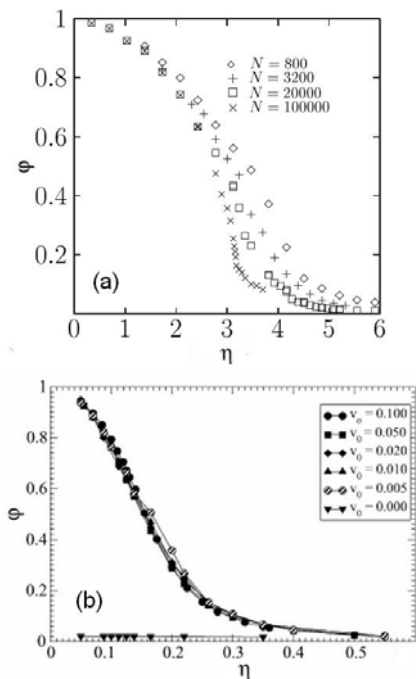


FIG. 31 Order parameter (φ) versus noise (η) in the SVM. (a) The different kind of points belong to different system sizes. (b) The different curves belong to different v_0 velocities, with which each particles move. As it can be seen, the concrete value of v_0 does not effect the nature of the transition (except when $v_0 = 0$, that is, when the units do not move at all). (a) is adapted from Cziráok *et al.* (1997) and (b) is from Baglietto and Albano (2009a).

Shimoyama *et al.* (1996) proposed a mathematical model (neglecting noise) from which they obtained a categorization of the different types of collective motion patterns and determined the corresponding phase diagrams as well.

1. The order of the phase transition

In the paper introducing the original variant (OVM) of the SVM (Vicsek *et al.*, 1995), a second order phase transition from disordered to ordered motion was shown to exist. In particular, in the thermodynamic limit, the model was argued to exhibit a kinetic phase transition analogous to the continuous ones in equilibrium systems, that is,

$$\begin{aligned} \varphi &\sim [\eta_c(\rho) - \eta]^\beta \\ \varphi &\sim [\rho - \rho_c(\eta)]^\delta \end{aligned} \quad (16)$$

which defines the behavior of the order parameter at criticality, in the case of a standard second order transition. β and δ are critical exponents, η is the noise (in the form of random perturbations), ρ is the particle density, and $\eta_c(\rho)$ and $\rho_c(\eta)$ are the critical noise and critical den-

sity, respectively, for $L \rightarrow \infty$. (L is the linear size of the system.)

However, the continuous nature of this transition has been questioned (Grégoire and Chaté, 2004) resulting in a number of studies investigating this fundamental aspect of collective motion. Chaté and coauthors (Chaté *et al.*, 2008b), in their extensive, follow up study presented numerical results indicating that there exists a “crossover” system size which they call L^* beyond which the discontinuous character of the transition appears independent of the magnitude of the velocity. They claim that this discontinuous character is the “true” asymptotic behavior in the infinite-size limit. Importantly, Chaté *et al.* (2008b) argued and presented results in favor of their picture that L^* diverges in various limits: both the low and high density limits, as well as in the small velocity limit. In particular, an extrapolation of their estimates towards the small velocity regimes considered in prior works, gives values of L^* so large that do not make the corresponding simulations feasible.

Further recent works presented results in support of the original findings. It seems that in spite of its simplicity, the SPP model proposed in 1995 exhibits an unusually rich behavior as a function of its few parameters. In particular, according to the simulations for relatively large velocities ($v_0 > 0.5$), the transition is discontinuous, while Baglietto and Albano (2009a) showed that for smaller velocities, even in the limit when the velocity goes to zero (except when it is exactly equal to zero), the transition to ordering is continuous (is independent of the actual value of the velocity, as it can be seen in Fig. 31 b). Very recently Ihle (2010) and Mishra *et al.* (2010) were able to see band-like structures in their solutions obtained from a hydrodynamic (continuum theory) approach. Bands usually signal first order phase transition, however, Ihle (2010) found them for a large velocity case, while Mishra *et al.* (2010) assumed throughout their calculation that the transition from disorder to order was continuous. Aldana *et al.* (2007) addressed this question by analyzing two network models that capture some of the main aspects characterizing the interactions in systems of self-propelled particles. They argued that the type of the phase transition (whether it is first or second order) depends on the way in which the noise is introduced into the system.

In the so called “vectorial noise model” the perturbation (in the form of a random vector) is first added to the average of the velocities and only after this the final direction is determined (Grégoire and Chaté, 2004). When the average velocity is small (disordered motion) this seemingly subtle difference in the definition of the final direction leads to a qualitatively different ordering mechanism (sudden – first order-type – transition to the ordered state). Correspondingly, Aldana *et al.* (2009) analyzed the order-disorder phase transitions driven by two different kinds of noises: “intrinsic” (the original form,

perturbing the final angle) and “extrinsic” (the vectorial one, perturbing the direction of the individual particles before averaging). Intrinsic is related to the decision mechanism through which the particles update their positions, while extrinsic affects the signal that the particles receive from the environment. The first one calls continuous phase transitions forth, whereas the second type produces discontinuous phase transitions (Pimentel *et al.*, 2008). Finally, Nagy *et al.* (2007) argued that the vectorial noise results in a behavior which can be associated with an instability.

2. Finite size scaling

So far, the most complete study regarding the scaling behavior of systems of self-propelled particles exhibiting simple alignment plus perturbation, has been carried out by Baglietto and Albano (2008). They performed extensive simulations of the SVM, and analyzed them both by a finite-size scaling method (a method used to determine the values of the critical exponents and of the critical point by observing how the measured quantities vary for different lattice sizes), and by a dynamic scaling approach. They observed the transition to be continuous. In addition they demonstrated the existence of a complete set of critical exponents for the two dimensional case (including those corresponding to finite size scaling²) and numerically determined their values as well. In particular, within the framework of finite-size scaling theory, the scaling ansatz for the order parameter φ of the SVM has been rewritten as

$$\varphi(\eta, L) = L^{-\beta/\nu} \tilde{\varphi}((\eta - \eta_c)L^{1/\nu}), \quad (17)$$

where L is the finite size of the system, $\tilde{\varphi}$ is a suitable scaling function, and finally, β and ν are two of the critical exponents in question: β is the one belonging to the order parameter, and ν is the correlation length critical exponent.

Similarly, the fluctuation of the order parameter, $\chi = \sigma^2 L^2$, takes the form

$$\chi(\eta, L) = L^{\gamma/\nu} \tilde{\chi}((\eta - \eta_c)L^{1/\nu}), \quad (18)$$

where $\tilde{\chi}$ is a suitable scaling function, γ is the susceptibility critical exponent, and $\sigma^2 \equiv \langle \varphi^2 \rangle - \langle \varphi \rangle^2$ is the

variance of the order parameter. In the thermodynamic limit, χ obeys $\chi \sim (\eta - \eta_c)^{-\gamma}$. (See also Eq. (4))

Equations (17) and (18) are convenient to determine the critical exponents within the framework of finite size scaling theory. As a crucial result, the authors found that the exponents they calculated satisfy the so called *hyperscaling relationship*

$$d\nu - 2\beta = \gamma \quad (19)$$

which is, in general, valid for standard (equilibrium) critical phenomena. d denotes the dimension, $d = 2$.

The nature of “intermittency” – intermittent bursts during which the order is temporarily lost in such systems – has also been a subject of investigations recently (Huepe and Aldana, 2004).

B. Variants of the original SPP model

Several variants of the above introduced, simplest SPP model have been proposed over the years. One of the main directions comprises of those studies that investigate systems in which the particles (units) do not follow any kind of alignment rule, only collisions occur between them in the presence of some kind of interaction potential. We shall overview this approach in Sec. IV.B.1. Models assuming some kind of alignment rule for the units, will be dealt with in Sec. IV.B.2.

1. Models without alignment rule

As mentioned in Sec. IV.A, in the most simple SPP models, an alignment term is assumed. However, according to very recent studies (see Sec. II.A), the motion of particles may become ordered even if no explicit alignment rule is applied (Grossman *et al.*, 2008). The simplest (most minimal) model of ordered motion emerging in a system of self-propelled particles looks like this: The particles are trying to maintain a given absolute velocity and the only interaction between them is a repulsive linear force (\vec{F}) within a short distance (i.e., they do not “calculate” the average of the velocity of their neighbors, and the only interaction is through a pair-wise central force). The corresponding equations are:

$$\frac{d\vec{v}_i}{dt} = \vec{v}_i \left(\frac{v_0}{|\vec{v}_i|} - 1 \right) + \vec{F}_i + \vec{\xi}_i \quad (20)$$

where $\vec{\xi}_i$ is noise (random perturbations, typically white noise)

$$\vec{F}_i = \sum_{i \neq j} \vec{F}_{ij} + \vec{F}_i \text{ (wall)} \quad (21)$$

² Numerical simulations carried out on systems having finite size L in at least one space dimension exhibit so called *finite size effects*, most importantly rounding and shifting effects during second-order phase transitions. These artifacts are particularly emphasized near the critical points, but they can be accounted for by means of the so called *finite-size scaling*. See more on this topic in (Brankov *et al.*, 2000; Cardy, 1996).

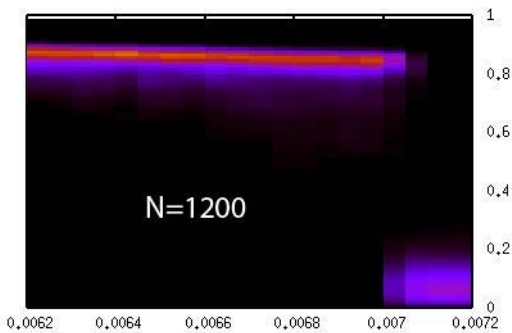


FIG. 32 (Color online) Probability density distribution of the order parameter versus noise for 1200 particles. The first order nature of the transition is indicated by the behavior of the order parameter – depicted on the vertical axis – which abruptly falls, in this case at noise level 0.007. From <http://hal.elte.hu/~vicsek/SPP-minimal/>.

$$\vec{r}_{ij} = \vec{x}_i - \vec{x}_j \quad (22)$$

$$\vec{F}_{ij} = \begin{cases} C\vec{r}_{ij} \left(\frac{r_0}{|\vec{r}_{ij}|} - 1 \right) & , \text{if } |\vec{r}_{ij}| \leq r_0, \text{ and} \\ 0 & , \text{otherwise} \end{cases} \quad (23)$$

Simulations of the above minimal model result in a first order transition from disordered to coherent collective motion (Derzsi *et al.*, 2009), as it can be seen in Fig. 32.

Analogous results were recently obtained for another simple model assuming only a specific form of inelastic collisions between the particles (Grossman *et al.*, 2008). In their numerical experiments, self-propelled isotropic agents move and collide on a two-dimensional frictionless flat surface. Imposing reflecting boundary-conditions produce a number of collective phenomena: ordered migration, the formation of vortices (see Fig. 33) and random chaotic-like motion of subgroups. Changing the particle density and the physical boundary of the system – for example from a circular to an elliptical shape – again results in different types of collective motion; for certain densities and boundary-types the system exhibits non-trivial spatio-temporal behavior of compact subgroups of units. The reason why coherent collective motion appears in such a system is that each of these inelastic collisions between isotropic particles increase the overall velocity correlation (it can be shown that the collisions do not preserve the momentum, but lead to at least a slight increase each time). Such numerical experiments are fundamental in clarifying the question regarding the minimal requirements for a system to exhibit collective motion, based solely on physical interactions.

The first work in which the relevance of the simultaneous presence of volume exclusion and self-propulsion for an effective alignment of the particles was published

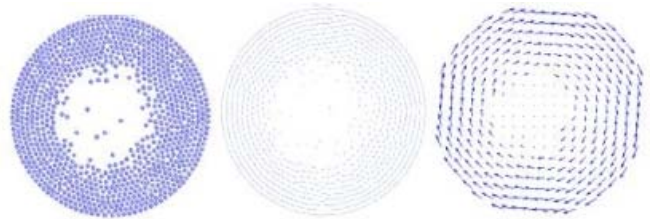


FIG. 33 (Color online) Vortex formation in a reflective round boundary. Reflecting boundaries cause particles to move parallel to them. Both clockwise and anti-clockwise vortices can form according to the randomly chosen initial direction. (a) A snapshot of the particles ($N = 900$). (b) Their movement within a short period of time. (c) Coarse graining average velocity. From Grossman *et al.* (2008).

by Peruani *et al.* (2006). They stressed the importance of the particle shape by showing that self-propelled objects moving in a dissipative medium and interacting by inelastic collision, can self-organize into large coherently moving clusters. Their simulations have direct relevance to the experiments on shaken rods (Kudrolli, 2010) and on the collective motion patterns by mixobacteria (Wu *et al.*, 2009). Furthermore, Peruani *et al.* (2006) showed that self-propelled rods exhibit non-equilibrium phase transition between a monodisperse phase to an aggregation phase that depends on the aspect ratio and density of the self-propelled rods. To see all this, no specific boundary conditions had to be applied due to the elongated shape of the particles.

In a similar spirit, Ginelli *et al.* (2010) investigated in more detail the properties of a collection of elongated, asymmetric (“polar”) units moving in two dimensions with constant speed, interacting only by “nematic collisions”, in the presence of noise. We discuss this work here, although the rule applied can be regarded as resulting from a mixture of volume exclusion and alignment (see also Peruani *et al.* (2008)). Nematic collision, illustrated on Fig. 34, means the following: if the included angle of the two velocity vectors belonging to the colliding rod-like units was smaller than 180° before they impinge on each other, they would continue their motion in the same direction, in parallel, after the collision. If this angle was bigger than 180° , then they would continue their travel in parallel, but in the opposite direction. Four phases were observed, depending on the strength of the noise (labeled I to IV by increasing noise-values). Phase I is spatially homogeneous and ordered, from which phase II differs in low-density disordered regions, which appear in the steady state. The order-disorder transition occurs between phases II and III. Both of these phases (II and III) are characterized by spontaneous segregations into bands, but in phase III these bands are thinner and are more unstable, constantly bending, breaking, reforming and merging, displaying a persistent space-time chaos. Phase IV is spatially homogeneous with global and local

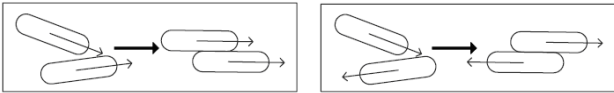


FIG. 34 Nematic collision means that, if the included angle of the two velocity vectors belonging to the colliding rod-like units was smaller than 180° before they impinge on each other, they would continue their motion in the same direction, in parallel, after the collision. If this angle was bigger than 180° , then they would continue their travel in parallel, but in the opposite direction. From Ginelli *et al.* (2010).

disorder on small length- and timescales.

A swarm of identical self-propelled particles interacting via a harmonic attractive pair potential in two dimensions in the presence of noise was also considered. By numerical simulations Erdmann *et al.* (2005) found that, if the noise is increased above a certain limit, a transition occurs during which the translational motion breaks down and instead of it, rotational motion takes shape.

2. Models with alignment rule

Compared to the original SVM, an important additional feature has been introduced by Grégoire *et al.* (2003) who added adhesion between the particles to avoid “evaporation” of isolated clusters in simulations with open boundary conditions. Adding this new feature has changed the universality class (order of transition) and the observed ordering was discontinuous as a function of perturbations.

The most common way to introduce cohesion to a system without resorting to global interactions, is to complement the interaction rules defining the units’ behavior with some kind of pairwise attraction-repulsion mechanism. In this spirit, Chaté *et al.* (2008a) have added a new term to Eq. (13), which determines a pairwise attraction-repulsion force between the particles (See Fig. 35).

Another generalization has recently been considered by Szabó *et al.* (2009). By extending the factors influencing the ordering, the model assumes that the velocity of the particles depends both on the velocity and the acceleration of neighboring particles. (Recall, that in the original model it depends solely on the velocity). Changing the value of a weight parameter determining the relative influence of the velocity and acceleration terms, the system undergoes a kinetic phase transition. Below a critical value the system exhibits disordered motion, while above the critical value the dynamics resembles that of the original SPP model.

One might interpret the particles of the SVM as *polar*



FIG. 35 (Color online) The SVM augmented with cohesive interactions among the particles. A snapshot of a flock consisting of 16,384 particles, moving ‘cohesively’. Adapted from Chaté *et al.* (2008a).

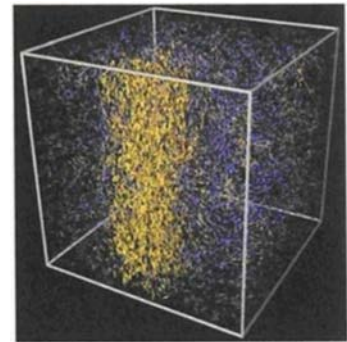


FIG. 36 (Color online) A snapshot of the simulations with point-like particles, but subject to a nematic-type interaction, performed by Chaté *et al.* (2008a). The behavior of the system is qualitatively different from those with isotropic particles and exhibits characteristic density and velocity fluctuations. Color code refers to the local denseness from blue (low density) to yellow (high density). Adapted from Chaté *et al.* (2008a).

units, since they carry a velocity vector. Accordingly, Chaté *et al.* (2006) consider a bipolar version of the SVM, in which after the angle corresponding to the local average velocity is determined, the particles can ‘decide’ whether they move along this direction or in a direction opposite to it. Such a model arises from the consideration of the self-propelled motion of elongated particles preferably moving along their main axis. The authors find a distinctively different disorder-order transition involving huge density fluctuations, compared to the previously considered cases. According to Chaté *et al.* (2008a), the expression $\langle \vec{v}_j(t) \rangle_{S_i}$ appearing in the interaction rule of the SVM (Eq. (13)) – expression which is in close relation to the *local* order parameter around particle i in its neighborhood S – can be replaced by the eigenvector of the largest eigenvalue belonging to the nematic tensor calculated on the same neighborhood. Denoting the angle defining the direction of \vec{v}_j by θ_j , this eigenvalue, which is also directly related to the local order parameter, for

uniaxial nematics in two space dimensions is calculated as $|\langle \exp(2i\theta_j(t)) \rangle_{S_i}|$. j denotes those particles that are within the neighborhood S of particle i , S_i , at time-step t . Since each particle i chooses the direction defined by θ_i or the opposite direction $\theta_i + \pi$ with the same probability $1/2$, Eq. (14) gets the form

$$\vec{x}_i(t+1) = \vec{x}_i(t) \pm \vec{v}_i(t+1)$$

A snapshot of the resulting collective motion pattern can be seen in Fig. 36.

By using a novel set of diagnostic tools related to the particles' spatial distribution Huepe and Aldana (2008) compared three simple models qualitatively reproducing the emergent behavior of various animal swarms. The most important aim of introducing the above measures is to unveil previously unreported qualitative differences and characteristics (which were unclear) among the various models in question. Comparing only the standard order parameters (measuring the degree of alignment), the authors find very similar order-disorder phase transitions in the investigated models, as a function of the noise. They demonstrated that the distribution of cluster sizes is typically exponential at high noise-values, approaches a power-law distribution at reduced noise levels, and interestingly, that this trend is sometimes reversed near to the critical noise value, suggesting a non-trivial critical behavior.

Smith and Martin (2009) used a Lagrangian individual based model with open boundary conditions to show that the Morse and the Lennard-Jones potentials (coupled with an alignment potential) are also capable to describe many aspects of flocking behavior.

C. Continuous media and mean-field approaches

Self-propelled particles, during their motion, consume energy and dissipate it in the media they move in, meanwhile performing rich collective behavior at large scales. Recent studies devoted to deriving hydrodynamic equations for specific microscopic models have led to new ideas and approaches within this field.

The continuous media approaches to collective motion have been carried out, on one hand, in the context of giving a macroscopic description of SPP systems, however, at the same time, also to interpret the so called "active matter" systems associated mainly with applications from physics, such as active nematics.

The first theory describing the full nonlinear higher dimensional dynamics was presented in (Toner and Tu, 1995, 1998). Tu and Toner followed the historical precedent (Forster *et al.*, 1977) of the Navier-Stokes equation by deriving the continuum, long wavelength description *not* by explicitly coarse graining the microscopic dynamics, but, rather, by writing down the most general contin-

uum equations of motion for the velocity field \vec{v} and density ρ consistent with the symmetries and conservation laws of the problem. This approach allows to introduce a few phenomenological parameters, (like the viscosity in the Navier-Stokes equation) whose numerical values will depend on the detailed microscopic behavior of the particles. The terms in the equations describing the large-scale behavior, however, should depend only on symmetries and conservation laws, and *not* on the microscopic rules.

The only symmetry of the system is rotation invariance: since the particles lack a compass, all direction of space are equivalent to other directions. Thus, the "hydrodynamic" equation of motion cannot have built into it any special direction picked "a priori"; all directions must be spontaneously selected. Note that the model does *not* have Galilean invariance: changing the velocities of all the particles by some constant boost \vec{v}_b does *not* leave the model invariant.

To reduce the complexity of the equations of motion still further, a spatial-temporal gradient expansion can be performed keeping only the lowest order terms in gradients and time derivatives of \vec{v} and ρ . This is motivated and justified by the aim to consider *only* the long distance, long time properties of the system. The resulting equations are

$$\begin{aligned} \partial_t \vec{v} + \lambda_1 (\vec{v} \cdot \nabla) \vec{v} + \lambda_2 (\nabla \cdot \vec{v}) \vec{v} + \lambda_3 \nabla (|\vec{v}|^2) = \\ \alpha \vec{v} - \beta |\vec{v}|^2 \vec{v} - \nabla P + D_L \nabla (\nabla \cdot \vec{v}) + D_1 \nabla^2 \vec{v} + D_2 (\vec{v} \cdot \nabla)^2 \vec{v} + \vec{\xi} \end{aligned} \quad (24)$$

and

$$\partial_t \rho + \nabla (\rho \vec{v}) = 0. \quad (25)$$

In Eq. (24), the terms $\alpha, \beta > 0$ make v to have a nonzero magnitude, $D_{L,1,2}$ are diffusion constants and $\vec{\xi}$ is an uncorrelated Gaussian random noise. The λ terms on the left hand side are the analogs of the usual convective derivative of the coarse-grained velocity field \vec{v} in the Navier-Stokes equation. Here the absence of Galilean invariance allows all *three* combinations of one spatial gradient and two velocities that transform like vectors; if Galilean invariance *did* hold, it would force $\lambda_2 = \lambda_3 = 0$ and $\lambda_1 = 1$. However, Galilean invariance does *not* hold, and so all three coefficients can be non-zero phenomenological parameters whose values are determined by the microscopic rules. Eq. (25) reflects the conservation of mass (birds). The pressure P depends on the local density only, as given by the expansion

$$P = P(\rho) = \sum_{n=1}^{\infty} \sigma_n (\rho - \rho_0)^n \quad (26)$$

where ρ_0 is the mean of the local number density and σ_n is a coefficient in the pressure expansion.

It is possible to treat the whole problem analytically using dynamical renormalisation group and show the existence of an ordered phase in 2D, and extract exponents characterizing the velocity-velocity and density-density correlation functions (Toner and Tu, 1998). The most dramatic result is that an intrinsically non-equilibrium and nonlinear feature, namely, convection, suppresses fluctuations of the velocity \vec{v} at long wavelengths, making them much smaller than the analogous fluctuations found in ferromagnets, for all spatial dimensions $d < 4$.

Bertin *et al.* (2006, 2009) made a very important step towards a fundamental theory of collective motion by deriving the hydrodynamic equations for the density and velocity fields of a gas of self-propelled particles with binary interactions from the corresponding microscopic rules. They gave explicit expressions for the transport coefficients as a function of the microscopic parameters. Comparison with numerical simulations on a standard model of self-propelled particles (SVM, see Sec. IV.A) resulted in an agreement as well as in a demonstration of the robustness of the phase diagram they obtained. Ihle (2010) showed how to explicitly coarse grain the microscopic dynamics of the SVM to obtain expressions for all transport coefficients as a function of the three main parameters, noise, density and velocity.

Over the last 4 years, the hydrodynamic equations became increasingly precise by including higher order terms and more precise coefficients. Very recently Mishra *et al.* (2010) solved the equations describing the collective motion of self-propelled polar rods moving on an inert substrate. From their theoretical considerations and numerical analysis, the authors obtained a remarkable phase diagram for this system (Fig. 37). They showed that the same physics that leads to global ordering destabilizes the homogeneous ordered state above a critical value of self-propulsion speed and allows the nonlinear equations to admit a propagating front solution that yields the striped phase identified numerically. The two phases they observed, namely, the striped phase and the fluctuating flocking phase, have been identified earlier in the context of numerical studies of the SVM model, thus, the approach of Mishra *et al.* (2010) identified the origin of these phenomena in the model independent framework of the dynamics of conserved quantities and broken symmetry variable.

It is important to point out that the above mentioned equations (Bertin *et al.*, 2006, 2009; Mishra *et al.*, 2010) obtained as a result of detailed derivations based on microscopic dynamics have an analogous structure and contain the same major terms as the ones (Eqs. 24 and 25) proposed by Toner and Tu inspired by general considerations.

Another important approach involving continuum mechanics is based on considering the hydrodynamic properties of systems consisting of microscopic swimmers. This is a quickly growing field of its own and has recently been

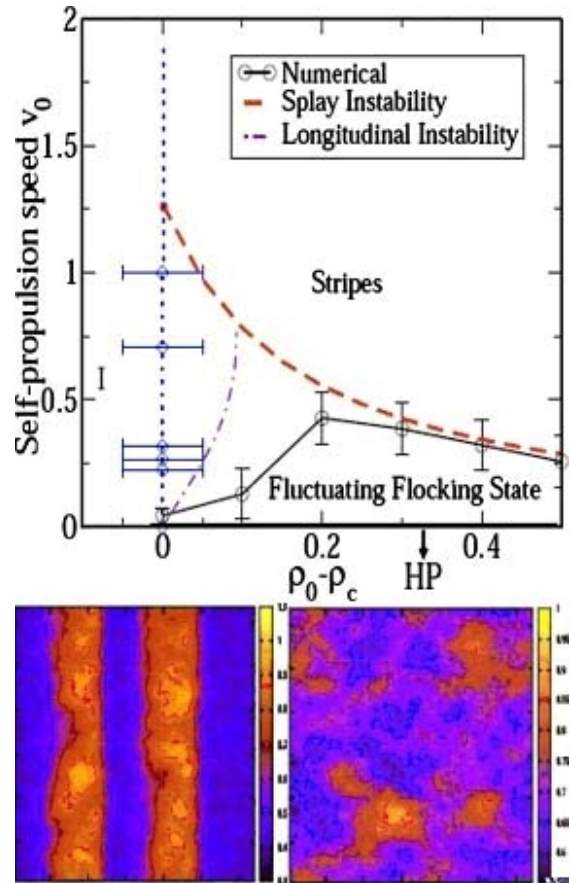


FIG. 37 (Color online) (A) Phase diagram of the solutions of the Eqs. (24) and (25) in the (v_0, ρ_0) plane. At $v_0 = 0$ the system exhibits a continuous mean-field transition at $\rho_0 = \rho_c$ from an isotropic (I) to a homogeneous polarized (HP) state. For $\rho_0 > \rho_c$ there is a critical $v_c(\rho_0)$ separating a polarized moving state with large anomalous fluctuations, named the fluctuating flocking state, at low self-propulsion speed from a high-speed phase of traveling stripes. The circles denote the values of $v_c(\rho_0)$ obtained numerically. The dashed-dotted line (purple online) is the longitudinal instability boundary $v_{c1}^L(\rho_0)$ obtained in the calculations. The dashed line is the splay instability boundary $v_{c1}^S(\rho_0)$. (B) shows a snapshot of the density profile in the striped phase. The stripes travel horizontally. (C) shows a snapshot of the density profile in the coarsening transient leading to the fluctuating flocking state at $v_0 < v_c$. Density values grow from dark to light. After Mishra *et al.* (2010).

reviewed by Lauga and Powers (2009). Here we briefly describe one of the representative examples of interpreting this aspect of collective motion.

Starting with a simple physical model of interacting active particles (swimmers) in a fluid, Baskaran and Marchetti (2009) derived a continuum description of the large-scale behavior of such active suspensions. They differentiated “shakers” from “movers”. Both of them are active, but a mover, in contrast with a shaker, is self propelled. Shakers are also active, but they do not move themselves. Furthermore “pushers” are propelled from

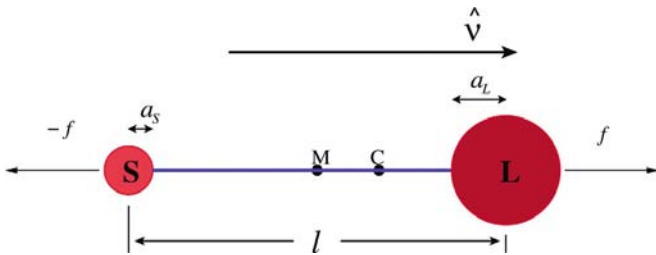


FIG. 38 (Color online) The simplified physical model of the active self-propelled particles in the paper of Baskaran and Marchetti (2009) are basically asymmetric rigid dumbbells. Two different size of spheres (S and L) are connected with an infinitely rigid rod having a length l . The radii of the smaller and larger spheres are a_S and a_L respectively. The geometrical midpoint of the swimmer is depicted by M , while the hydrodynamic center is marked with C , at which the propulsion is centered. The orientation of these asymmetric particles are characterized by a unit vector \hat{v} . $|f|$ denotes the force they exert on the fluid they swim in. With this notation, pullers correspond to $f < 0$ and pushers to $f > 0$. From Baskaran and Marchetti (2009).

the rear (like most bacteria), while “pullers” are propelled by flagella at the head of the organism.

The simplified physical model of a swimmer is basically an asymmetric rigid dumbbell, as depicted in Fig. 38. Each of these units has a length l , and their orientation is characterized by a unit vector \hat{v} , directed along its axis from the small sphere (having radius a_S) to the large sphere (having radius a_L). They exert a force dipole of strength $|f|$ on the fluid they swim in, which has a viscosity $\tilde{\eta}$. The velocity of the particles are $\vec{v}_{SP} = \nu_0 \hat{v}$.

The dynamics of a swimming particle α is given by

$$\begin{aligned} \partial_t \vec{r}_{L\alpha} &= \vec{u}(\vec{r}_{L\alpha}), \\ \partial_t \vec{r}_{S\alpha} &= \vec{u}(\vec{r}_{S\alpha}), \end{aligned} \quad (27)$$

where $\vec{r}_{S\alpha}$ and $\vec{r}_{L\alpha}$ denote the position of the small and large “heads” of swimmer α , respectively, with respects to a fixed pole. $\vec{u}(\vec{r})$ is the flow velocity of the fluid at point \vec{r} which is determined by the solution of the Stokes equation, that is,

$$\tilde{\eta} \nabla^2 \vec{u}(\vec{r}) = \nabla p - \vec{F}_{active} + \vec{F}_{noise}, \quad (28)$$

where \vec{F}_{noise} describes the effect of the fluid-fluctuations, and \vec{F}_{active} is the active force exerted by swimmer α on the fluid.

Closed formulas can be obtained for the translational and rotational motion, and for the hydrodynamical force and the torque between two swimming particles as well. Baskaran and Marchetti (2008) analyzed a simple model that captured two crucial properties of self-propelled systems: the orientable shape of the particles and the self propulsion. Using the tools of non-equilibrium statistical

mechanics they derived a modified Smoluchowski equation for SPP and used it to identify the microscopic origin of several observed or observable large scale phenomena.

Peruani *et al.* (2008) suggested a mean-field theory for self-propelled particles which accounted for ferromagnetic (F) and liquid-crystal (LC) alignment. The approach predicted a continuous phase transition with the order parameter scaling with an exponent of $1/2$ in both cases. The critical noise amplitude below which orientational order emerges found to be smaller for LC-alignment than for F-alignment. Czirók *et al.* (1999) derived a continuum theory that can account for a surprising observation, namely that – in contrast with preceding analytical predictions – a system of self-propelled particles can exhibit spontaneous symmetry breaking and self-organization in one dimension. Csahók and Czirók (1997) presented a hydrodynamic approach to describe the motion of migrating bacteria as a special class of SPP systems.

D. Exact results

By exact results here we mean results obtained with a minimum or completely missing amount of any kind of assumptions or approximations concerning the behavior of the moving units (beyond the rules/definitions they obey). Originally most results in this area were obtained only for systems in which the noise (an otherwise essential aspect of flocking) was completely neglected. Thus, one could consider the related systems as fully deterministic. However, it has recently been shown (see later) that the theorems we review below are in most cases valid for systems with a low level of perturbations as well.

1. The Cucker-Smale model

An exact formulation of the convergence to consensus in a population of autonomous agents was achieved by Cucker and Smale (2007a) and Cucker and Smale (2007b) based on their model (CS). Following their train of thought, let us consider birds, denoted by $i = 1, \dots, k$, moving in 3 dimensional (Euclidean) space, \mathbb{R}^3 , endeavoring to reach a common direction (– which is in this case the topic of “consensus”). The position of the i th bird is given by $x_i \in \mathbb{R}^3$. (Of course, $x_i = x_i(t)$.) Let us define the adjacency matrix $A = (a_{ij})$, where the element a_{ij} measures the ability of birds i and j to communicate with each other, or one could say, the *influence* they exert on each other. Formally,

$$a_{ij} = \frac{1}{(1 + \|x_i - x_j\|^2)^\beta}, \quad (29)$$

where $\beta \geq 0$ (not to be confused with the critical exponent introduced in Sec. III.A). Thus, the closer the

birds i and j are to each other, the bigger the influence is among them. The main advantage of this form of the distance dependence of the interaction is that it is a smooth function allowing analytical treatment. Importantly, this adjacency matrix A changes with time, since the positions of the birds change with time. For the more manifest usage of graphs they introduce the *Laplacian matrix* of A as well, $L = D - A$, where D is a $k \times k$ diagonal matrix whose i th diagonal element is $d_i = \sum_{j=1}^k a_{ij}$.

Denoting the velocity of bird i at time t by $v_i(t)$,

$$\vec{f}_{ij} = -c \left\{ \left(\frac{|\vec{r}_j - \vec{r}_i|}{r_c} \right)^{-3} - \left(\frac{|\vec{r}_j - \vec{r}_i|}{r_c} \right)^{-2} \right\} \cdot \left(\frac{\vec{r}_j - \vec{r}_i}{r_c} \right) \cdot e^{-\frac{|\vec{r}_j - \vec{r}_i|}{r_c}}, \quad (30)$$

$$v_i(t+h) - v_i(t) = h \sum_{j=1}^k a_{ij} (v_j - v_i) \quad (31)$$

Recall, that the a_{ij} value measures the strength of the communication between birds i and j , thus the right hand side of Eq. (31) signifies a *local averaging* around bird i .

The *equations of flocking* are obtained by letting h tend to zero:

$$\begin{aligned} x' &= v \\ v' &= -Lv \end{aligned} \quad (32)$$

on $(\mathbb{R}^3)^k \times (\mathbb{R}^3)^k$. (Note that the matrices A and L are acting on $(\mathbb{R}^3)^k$ by mapping (v_1, \dots, v_k) to $(a_{i1}v_1 + \dots + a_{ik}v_k)_{i \leq k}$.)

After the above preparations, one can ask, *under what conditions do a system (described by the above equations) exhibit flocking behavior?* When do the solutions of $v_i(t)$ converge to a common $v^* (\in \mathbb{R}^3)$? One of the most important results of Cucker and Smale (2007a) is that the emergence of the flocking behavior depends on β , according to the following

Theorem: For the equations of flocking (Eqs. 32) there exists a unique solution for all $t \in \mathbb{R}$.

If $\beta < 1/2$ then the velocities $v_i(t)$ tend to a common limit $v^* (\in \mathbb{R}^3)$ as $t \rightarrow \infty$, where v^* is independent of i , and the vectors $x_i - x_j$ tend to a limit-vector \hat{x}_{ij} for all $i, j \leq k$, as $t \rightarrow \infty$, that is, the relative positions remain bounded.

If $\beta \geq 1/2$ dispersal (the split up of the flock) is possible. But, provided that some certain initial conditions are satisfied, flocking will occur.

To obtain more general results for the conditions of flocking, let us define the so called *Fiedler-number*, which is a crucial descriptive measure of the conditions needed to be satisfied for the emergence of flocking.

Let G denote a graph and A be the corresponding adjacency matrix defined as usually, that is,

$$a_{ij} = \begin{cases} 1 & \text{if } i \text{ and } j \text{ are connected,} \\ 0 & \text{if not} \end{cases} \quad (33)$$

Let D be a diagonal matrix with the same dimensions as A , defined by $d(i, i) = \sum_j a(i, j)$. Then the general form of the Laplacian matrix of G , is given as $L = L(G) = D - A$. The eigenvalues of L can be expressed by

$$0 = \lambda_1 \leq \lambda_2 \leq \lambda_3 \leq \dots \quad (34)$$

Then, the Fiedler-number F is defined as the second eigenvalue of L , λ_2 , that is

$$F = F(G) = \lambda_2 \quad (35)$$

This Fiedler-number F is zero, if the graph G is separated (the flock disintegrates to two or more smaller flocks), and non-zero if and only if G is connected.

Importantly, in the case of flocking, $F = F(t)$ (it is a function of time), because the elements of G depend on the x_i positions of the individual birds. In fact, one obtains flocking, if and only if

$$0 < \text{const} \leq F = F(x(t)). \quad (36)$$

Otherwise the flock disperses.

The above definitions can be extended to weighted, general matrices as well.

In addition, Cucker and Dong (2010) extended the model by adding to it a repelling force between particles. They showed that, for this modified model, convergence to flocking is established along the same lines while, in addition, avoidance of collisions (i.e., the respect of a minimal distance between particles) is ensured.

The main differences between the systems described by Cucker and Smale and by the SVM are, from the one hand, is the definition of the range of interaction, and from the other hand, is the existence (or absence) of noise. The SVM comprises noise, while the original Cucker-Smale model does not. Regarding the range of interaction, in the present model it is a long-range effect decaying with the distance according to β (see Eq. (29)), while in the SVM it has the same intensity for all the neighboring units around a given particle, but only within a well-defined range (see Eq. (13)).

Very recently perturbations have also been considered in the CS model. This has been done with various forms of noise by Cucker and Mordecki (2008) and Shang (2009), modeled with stochastic differential equations by Ha *et al.* (2009), and taking into account random failures between agent's connections by Dalmao and Mordecki (2009).

Other works developing the Cucker-Smale (CS) model in several directions include an extension to fluid-like swarms (Carrillo *et al.*, 2010; Ha and Liu, 2009; Ha and Tadmor, 2008), collision avoiding flocking (Cucker and Dong, 2010), the inclusion of agents with a preferred velocity direction (Cucker and Huepe, 2008), and its proposal as a control law for the spacecrafts of the Darwin mission of the European Space Agency (Perea *et al.*, 2009).

2. Network and control theoretical aspects

Networks have recently been proposed to represent a useful approach to the interpretation of the intricate underlying structure of connections among the elements of complex systems. A number of important features of such networks have been uncovered (Albert and Barabási, 2002; Watts and Strogatz, 1998). It has been shown that in many complex systems ranging from the set of protein interactions to the collaboration of scientists the distribution of the number of connections is described by a power law as opposed to a previously supposed Poissonian. Most of the networks in life and technology are dynamically changing and are highly structured. In particular, such networks are typically made of modules that are relatively more densely connected parts within the entire network (e.g., interacting flocks) (Newman, 2004, 2006; Palla *et al.*, 2005; Scott, 2000). The evolution of these modules plays a central role in the behavior of the system as a whole (Palla *et al.*, 2007).

In these terms, a dynamically changing network can be associated with a flock of collectively moving organisms (or robots, agents, units, dynamic systems, etc.). In such a network two units are connected if they interact. Obviously, if two units are closer in space have a better chance to influence the motion of each other, but their interaction can also be disabled by environment or internal disturbances. Since the units are moving and the environment is also changing, the network of momentarily interacting units is evolving in time in a complex way. Using the conventional terminology of control theory, this kind of topology (that is, when certain number of edges are added or removed from the graph from time to time), is called “switching topology”.

Jadbabaie *et al.* (2003) investigated a theoretical explanation for a fundamental aspect of the SVM, namely, that by applying the nearest neighbor rule, all particles tend to align into the same direction despite the absence of centralized coordination and despite the fact that each agent’s set of nearest neighbors changes in time. By addressing the question of global ordering in models analogous to Eqs. (13) and (15) they presented some rigorous conditions for the graph of interactions needed for arriving at a consensus.

Several further control theory inspired papers dis-

cussed both the question of convergence of the simplest SPP models as well as the close relation of flocking to such alternative problems as consensus finding, synchronization and “gossip algorithms” (Blondel *et al.*, 2005; Boyd *et al.*, 2005).

Ren and Beard (2005) considered the problem of consensus finding under the conditions of limited and unreliable information exchange for both discrete and continuous update schemes. They found that in systems with dynamic interaction-topologies consensus can be reached asymptotically, if the union of the directed communication network across some time intervals has spanning trees frequently enough, as the system evolves. Similarly, Xiao and Wang (2006) found the existence of spanning trees to be crucial in the directed graphs representing the interaction topologies, in systems in which the topology, weighting factors and time-delays are time-invariant. They studied the consensus-problem for dynamic networks with bounded time-varying communication delays under discrete-time updating scheme, based on the properties of non-negative matrices.

An efficient algorithm controlling a flock of unmanned aerial vehicles (UAVs) is considered by Ben-Asher *et al.* (2008). The units are organized into a minimal set of rooted spanning trees (preserving the geographical distances) which can be used for both distributed computing and for communication as well, in addition to computation and propagation of the task assignment commands. The proposed protocol continually attempts to keep the number of trees minimal by fusing separate adjacent trees into single ones: as soon as radio connection between two nodes belonging to separate trees occurs, the corresponding networks fuse. This arrangement overcomes the typical deficiencies of a centralized solution. The motion of the certain UAVs is coordinated by Reynolds’ algorithm (Reynolds, 1987) (see also Sec. IV.A).

Tanner *et al.* (2003a) proposed a control law for flocking in free-space. Dynamically changing topology of the interacting units has also been considered (Tanner *et al.*, 2003b). Lindhe *et al.* (2005) suggested a flocking algorithm providing stable and collision-free flocking in environments with complex obstacles. Holland *et al.* (2005) proposed a flocking scheme for unmanned ground vehicles similar to Reynolds’ algorithm based on avoidance, flock centering and alignment behaviors, where the units receive the range, bearing and velocity information from the base station based on pattern recognition techniques. Very recently, many further papers have appeared both on the original flocking problem as well as on interesting variants including the role of “leaders”, delays in communication, convergence time, etc.

One of the most general theoretical frameworks for design and analysis of distributed flocking algorithms was discussed by Olfati-Saber (2006). Three algorithms were investigated in detail: two for free-flocking (one fragmented and one not) and one for constrained flocking.

The basic driving rules and principles and their relation to specific underlying network structures were discussed.

Formally, from a control theoretical view-point, the problem looks as next: given a set of agents, who want to reach a *consensus*, which, in this terminology, means a common value (an “agreement”) regarding a certain quantity that depends on the state of the agents. (For example, this ‘certain quantity’ can be the direction of motion.) The interaction rule that defines the information exchange between a unit and its neighbors is called the consensus algorithm (or “*protocol*”).

This system can be represented by a graph $G = (V, E)$, in which the agents are the nodes $V = \{1, 2, \dots, n\}$. Two nodes are connected with an edge $e \in E$ if, and only if, they communicate with each other. In this case they are *neighbors*. Accordingly, the neighbors of node i are $N_i = \{j \in V : (i, j) \in E\}$. If the state of the i th agent (regarding the quantity of interest) is denoted by x_i , then the agreement is

$$x_1 = x_2 = x_3 = \dots = x_n. \quad (37)$$

Within this framework, *reaching a consensus* means to converge asymptotically to an agreement (defined by Eq. 37) via local communication.

Let $A = (a_{ij})$ denote the adjacency matrix, which defines the communication pattern among the agents: if i and j interact with each other, then $a_{ij} > 0$, otherwise $a_{ij} = 0$. Notably, in the case of flocks $A = A(t)$ and $G = G(t)$, that is, they vary with time. Such graphs – called *dynamic graphs* – are useful tools for describing the (time-dependent) topology of flocks and mobile sensor networks (Olfati-Saber, 2006).

Assuming a simple protocol, the state of agent i can change according to

$$\dot{x}_i(t) = \sum_{j \in N_i} a_{ij} (x_j(t) - x_i(t)) \quad (38)$$

which linear system always converges to a collective decision, that is, it defines a *distributed consensus algorithm* (Olfati-Saber and Murray, 2004).

In the case of undirected graphs (when $a_{ij} = a_{ji}$ for all $i, j \in V$) the sum of the state-values does not change, that is, $\sum_i \dot{x}_i = 0$. Applying this condition for $t = 0$ and $t = \infty$,

$$\alpha = \frac{1}{n} \sum_i x_i(0), \quad (39)$$

that is, the collective decision (α) is the average of the initial state of the nodes.

In fact, regarding the protocol defined by Eq. (38), a more strict statement can also be formulated (Olfati-Saber *et al.*, 2007):

Lemma: Let G be a connected undirected graph. Then, the algorithm defined by Eq. (38) asymptotically solves an average-consensus problem for all initial states.

E. Relation to collective robotics

The collective robotics literature is on the one hand about mathematical questions concerning the control theoretical aspects of coherently moving devices whereas, on the other hand, it represents important efforts to eventually produce and describe the collective patterns of behavior of a collection (ranging from 5 to a few dozen) of robots moving on a plane surface. Experimental attempts to produce flocking of aerial devices have been very limited.

In one of the earliest attempts towards obtaining flocking in a group of actual robots, Mataric (1994) combined a set of “basic behaviors”; namely safe-wandering, aggregation, dispersion and homing. In this study, the robots were able to sense the obstacles in the environment, localize themselves with respect to a set of stationary beacons and broadcast the position information to the other robots in the group. Kelly and Keating (1996) used a group of ten robots, which were able to sense the obstacles around them through ultrasound sensors, and the relative range and bearing of neighboring robots through the use of a custom-made active infra-red (IR) system. The proximity sensors on most mobile robots (such as ultrasound and IR-based systems) can sense only the range to the closest point of a neighboring robot and multiple range-readings can be returned from a close neighboring robot. Furthermore, as Turgut *et al.* (2008) pointed out, the sensing of bearing, velocity and orientation of neighboring robots is still difficult with off-the-shelf sensors available on robots. Hence, there exist a major gap between the studies that propose flocking behaviors and robotics.

An interesting experiment on flocking in 3D was carried out by Welsby *et al.* (2001) using motorized balloon-like objects. The slow coherent wondering of 3 of the robots was observed. Model (toy) helicopters were also proposed to observe flocking in three dimensions (Nardi and Holland, 2006).

Several major efforts have been documented about the collective exploration of swarms of robots. A variety of algorithms have been published about the optimal strategy to locate a given object or uncover the details of an area (in which the robots could move) having a complex shape. Recent papers have demonstrated that using an appropriate algorithm, such tasks can be achieved effectively. The largest collection of swarming robots has now over 100 miniature devices (<http://www.swarmrobot.org/>).

Turgut *et al.* (2008) examined the spatial self organization properties of robot swarms using mobile units (called “Kobots”, see Fig. 39). Every unit were equipped with a digital compass, an infrared-based short range sensing system (capable of measuring the distance from obstacles and detecting other robots) and an other appliance sensing the relative direction of the neighboring units. The



FIG. 39 (Color online) A photo of seven mobile robots (called “Kobots”) moving in a swarm. According to Turgut *et al.* (2008), the main factor defining the size of the swarm (the number of Kobots flocking together) is the range of communication, and it is highly independent from both the noise (encumbering the sensing systems) and from the number of neighbors each robot had. Adapted from Turgut *et al.* (2008).

group investigated the behavior of the flock in the function of: (1) the amount and nature of the noise encumbering the sensing systems (2) the number of neighbors each unit had, and (3) the range of the communication. They found that the main factor defining the size of the swarm (number of units that can flock together) is the range of communication, and that this size is highly robust against the other two parameters.

The motion of such robot swarms can be influenced by externally guiding some of their members towards a desired direction (Celikkanat and Sahin, 2010).

Only a few examples are known about trying to combine robots and animals into a single system and monitor the joint behavior. In a beautiful paper Halloy *et al.* (2007) investigated whether the behavior of a population of cockroaches can be influenced by micro-robots imitating cockroaches (these micro-robots had about the same size and had the same odor than the cockroaches). It turned out that it was possible to increase the number of cockroaches hiding under a given “shelter” if the mini-robots were moving there upon switching on the light.

In a more theoretical work, Sugawara *et al.* (2007) investigated the formations of motile elements (robots) as a function of various control parameters. Their kinetic model – inspired by living creatures, such as birds, fishes, etc. – is defined by Eqs. (40) and (41).

$$m \frac{d\vec{v}_i}{dt} = -\gamma \vec{v}_i + a \vec{n}_i + \sum_{j \neq i} \alpha_{ij} \vec{f}_{ij} + \vec{g}_i \quad (40)$$

$$\tau \frac{d\theta_i}{dt} = \sin(\phi_i - \theta_i) + \sum_{j \neq i} J_{ij} \sin(\theta_j - \theta_i), \quad (41)$$

where \vec{r}_i is the position, \vec{v}_i is the velocity, and \vec{n}_i is the *heading unit vector* of the i th element of a swarm consisting of N units ($i \in 1, 2, \dots, N$), respectively. The

velocity \vec{v}_i is relative to the medium (air, fluid, etc.) in which the motion occurs. The last quantity, \vec{n}_i is parallel to the axis of unit i , but not necessarily parallel to its velocity \vec{v}_i . For example, bigger birds often glide, during which the heading direction \vec{n}_i and the velocity \vec{v}_i encloses an angle, which is assumed to disappear within a relaxation time τ . In other words, τ is the time needed to \vec{n}_i and \vec{v}_i to relax to parallel. θ_i and ϕ_i are the angles between the x axis and the vectors \vec{n}_i and \vec{v}_i , respectively. m is the mass of the elements (of *all* the elements – apart from the initial conditions, every unit is identical in this model). a is the motile force acting in the direction of \vec{n}_i , and γ is a quantity proportional to the relaxation time in velocity. The term α_{ij} denotes a “direction sensibility factor” which is introduced to account for the possible anisotropy of the interaction. For example, if the robots gather information about the motion of their mates through vision (that is, with camera), than the interaction is strong towards the visual field that is covered by the camera, and zero elsewhere. It is defined as

$$\alpha_{ij} = 1 + d \cos \Phi, \quad (42)$$

where Φ is the angle enclosed by \vec{n}_i and $\vec{r}_j - \vec{r}_i$, and d is the sensitivity control parameter, $0 \leq d \leq 1$.

J_{ij} is introduced to account for the observation that animals tend to align with each other (Hunter, 1966) through an interaction which is supposed to decrease in the linear function of distance between individuals i and j :

$$J_{ij} = k \left(\frac{|\vec{r}_j - \vec{r}_i|}{r_c} \right)^{-1}, \quad (43)$$

where k is the control parameter and r_c is the preferred distance between neighbors. The term g_i is a force directed towards the center of the group, and finally, f_{ij} denotes a mutual attractive/repulsive force between elements i and j , in analogy with the intermolecular forces, as suggested by Breder (1954).

$$\vec{f}_{ij} = -c \left\{ \left(\frac{|\vec{r}_j - \vec{r}_i|}{r_c} \right)^{-3} - \left(\frac{|\vec{r}_j - \vec{r}_i|}{r_c} \right)^{-2} \right\} \cdot \left(\frac{\vec{r}_j - \vec{r}_i}{r_c} \right) \cdot e^{-\frac{|\vec{r}_j - \vec{r}_i|}{r_c}}, \quad (44)$$

where c is the control parameter defining the magnitude of the interaction.

Using numerical simulations and experiments with small mobile robots (called “Khepera”, a popular device for such experiments), the authors observed various formations, depending on the control parameters (see Fig. 40). They classified the observed collective motions

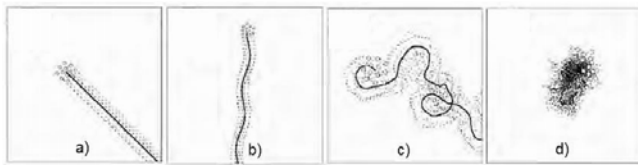


FIG. 40 Trajectories with various control parameters, obtained from numerical simulations. The solid line shows the center of mass. (a) marching, (b) oscillation, (c) wandering, and (d) swarming. Adapted from Sugawara *et al.* (2007).

into four categories: (1) “*Marching*”. Obtained when the value of the anisotropy of mutual attraction is kept small. This state exhibits only small velocity-fluctuations and it is stable against disturbance. (Fig. 40 a) (2) The category called “*Oscillation*” includes motions exhibiting regular oscillations, such as the wavy motion of the swarm, along its linear trajectory, depicted on Fig. 40 b. The stability of this state is weaker than that of the marching, and these two phases (1 and 2) may coexist for some parameters. (3) “*Wandering*”. When $d \neq 0$ (see Eq. (42)), the mutual positions of the units abruptly vary, according to stochastic changes in the direction of motion. Such a phase is often exhibited by – for example – small non-migratory birds. (Fig. 40 c) (4) “*Swarming*”. Irregularly moving units within a persistent cluster. The mobility of the entire cluster is small. For example mosquitoes travel in such swarms. (See Fig. 40 d).

In general, the point in organizing robots into a swarm is to accomplish tasks (preferably without centralized control), that are too challenging for an individual agent. The fields of the possible applications are extremely wide, including practical applications (such as the localization of hazardous emission sources in unknown large-scale areas (Cui *et al.*, 2004), the surveillance in hostile or dangerous places (Marshall, 2005), the optimization of telecommunication networks (Lipperts and Kreller, 1999)) as well as theoretical topics (like discrete optimization (Dorigo *et al.*, 1999) or providing new heuristics for the Traveling Salesman Problem (Dorigo and Gambardella, 1997)).

Furthermore, within these robot swarms, the appearance of the most variable forms of collective behavior (like co-operative, altruistic, selfish, etc.) can be studied as well through various genetic algorithms, conditions and tasks. Many homepages maintained by research groups working on this field contain further information for those who are interested (for example Laboratory of Autonomous Robotics and Artificial Life: <http://laral.istc.cnr.it/>, Laboratory of Intelligent Systems: <http://lis.epfl.ch/>, Distributed Robotics Lab of MIT: <http://groups.csail.mit.edu/drl/wiki/index.php/>, or the web-page of the Swarm-bots Project: <http://www.swarm-bots.org/> and

<http://www.swarm-robotics.org/index.php/>), just to mention a few. For a more engineering viewpoint of the topic, see also (Eberhart *et al.*, 2001).

V. MODELING ACTUAL SYSTEMS

A. Systems involving physical and chemical interactions

1. The effects of the medium

In the case of microorganisms swimming in a medium, the hydrodynamic effects are often significant enough to generate collective motion passively, that is, various coherent structures (e.g., clusters, vortices, etc.) arise merely as a result of hydrodynamic interactions. Getting wise to this fact, Hatwalne *et al.* (2004) and Simha and Ramaswamy (2002) constructed hydrodynamic equations for suspensions of SPPs suitable for making testable predictions for systems consisting of bacteria, cells with motors or artificial machines moving in a fluid. Saintillan and Shelley (2007) studied numerically the dynamics and orientational order of self-propelled slender rods using the so called slender-body theory, a method used to obtain an approximation to the field surrounding a slender object and to get an estimation for the net effect of the field on the body (Batchelor, 1970; Cox, 1970). They found local nematic ordering over short length scales as well having a significant impact on the mean swimming speed. Sankararaman and Ramaswamy (2009) showed that polar self-propelled particles were prone to exhibit various types of instabilities through the interplay of polarity, activity and the existence of a free surface, by using a thin-film hydrodynamic model.

The motion of the fluid generated by the particles swimming in it seems to depend strongly on the way these organisms propel themselves (Lauga and Powers, 2009). Underhill *et al.* (2008) simulated *pushers* (organisms propelled from the rear, like most bacteria) and *pullers* (creatures that are propelled at the head of the organism) separately to capture the differences in the effects of the forces these creatures exert on the fluid while swimming in it. Figure 41 shows the scheme of their self-propelled swimmers. Each of them consists of two beads connected by a rod. They propel themselves by a “phantom flagellum”. (“Phantom”, because its physical appearance is not taken care of, only its effect on the swimmer and on the fluid.) It exerts an F_f force on bead 1, and $-F_f$ force on the fluid. Pushers and pullers are distinguished by the *direction* of F_f : if it points from bead 1 to bead 2, then it is a pusher, and if it points in the opposite direction, then it is a puller. The motion of the particles is calculated by solving the force balance for each bead, as given by Eq. (45):

$$F_f + F_{h1} + F_{c1} + F_{e1} = 0, \quad (45)$$

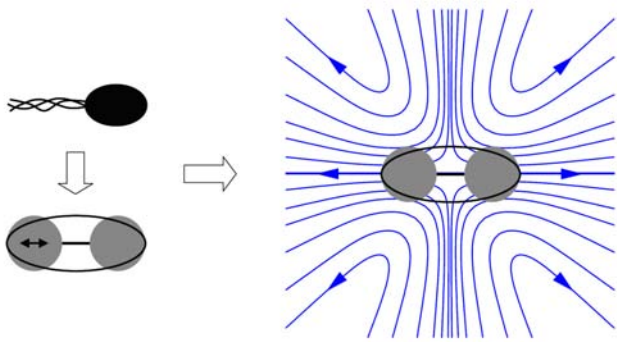


FIG. 41 (Color online) The scheme of a pusher and the fluid disturbance it causes. Each SPP is represented by two spheres connected by a rod. The propulsion is provided by a “phantom flagellum” (“phantom”, because it is not treated explicitly, only through the effect it exerts to the swimming body and to the fluid.) The force exerted by this flagellum acts at the center of the first sphere. A puller produces the same streamlines (dark gray curves) but the arrows point in the opposite direction. From Underhill *et al.* (2008).

where F_{c1} is the force exerted by the rod (connecting the two beads), F_{h1} is the hydrodynamic drag force and F_{e1} is the excluded volume force on the bead. The force balance defining the motion of bead 2 is the same as Eq. (45), but without the F_f flagellum force.

Using this model, Underhill *et al.* (2008) observed qualitative differences between the effects of pushers and pullers, exerted on the fluid they move in: SPPs that are pushed from the behind show greater enhancement than particles that are pulled from the front. This model – supported by Mehandia and Nott (2008) as well – describes the far-field behavior of interacting swimming particles.

The notion of “squirmers” has also been introduced in order to apprehend the most important features of swimming microorganisms (with respect to their motion in a fluid) (Lighthill, 1952). These are neutrally buoyant squirming spheres with a tangential surface velocity and with anisotropic structures, that is, their center of mass and geometric center do not necessarily coincide (Ishikawa and Pedley, 2008). The surface velocity, \vec{u}_S , of such squirmers is analyzed by Blake (1971) in detail and is given in the form of

$$\vec{u}_S = \sum_{n=1}^2 \frac{2}{n(n+1)} B_n \left(\frac{\vec{e} \cdot \vec{r}}{r} \frac{\vec{r}}{r} - \vec{e} \right) P'_n(\vec{e} \cdot \vec{r}/r), \quad (46)$$

where \vec{r} is the position vector, $r = |\vec{r}|$, \vec{e} is the orientation vector of the squirmer, B_n is the n th mode of the surface squirming velocity and P_n is the n th Legendre polynomial.

A solitary squirmer moves with the speed $2B_1/3$. Let β be the ratio of the second mode squirming to the first

mode: $\beta = B_2/B_1$. Positive β denotes *pullers*, and negative β describes *pushers*.

At the same time, the Stokesian dynamics – a technique used for solving the Langevin equation – can also be applied in this case (Brady and Bossis, 1988; Brady *et al.*, 1988). According to Ishikawa *et al.* (2008), the force \vec{F} , the torque \vec{L} and the stresslet \vec{S} balances for the squirmers can be calculated as

$$\begin{pmatrix} \vec{F} \\ \vec{L} \\ \vec{S} \end{pmatrix} = \begin{bmatrix} \vec{R}^{far} - \vec{R}_{2B}^{far} + \vec{R}_{2B}^{near} \end{bmatrix} \begin{pmatrix} \vec{U} - \langle \vec{u} \rangle \\ \vec{\Omega} - \langle \vec{\omega} \rangle \\ -\langle \vec{E} \rangle \end{pmatrix} + \begin{bmatrix} \vec{R}^{far} - \vec{R}_{2B}^{far} \end{bmatrix} \begin{pmatrix} -\frac{2}{3} B_1 \vec{e} + \vec{Q}_{sq} \\ 0 \\ -\frac{1}{5} B_2 (3\vec{e}\vec{e} - \vec{I}) \end{pmatrix} + \begin{pmatrix} \vec{F}_{sq}^{near} \\ \vec{L}_{sq}^{near} \\ \vec{S}_{sq}^{near} \end{pmatrix}, \quad (47)$$

where the indices “far” and “near” denote far- and near-field interaction, respectively, \vec{R} denotes the resistance matrix, \vec{U} is the translational and $\vec{\Omega}$ is the rotational velocity of a squirmer. $\langle \vec{u} \rangle$ and $\langle \vec{\omega} \rangle$ are the bulk suspension’s translational and rotational velocity, and $\langle \vec{E} \rangle$ is the rate of its strain tensor. $2B$ in the index indicates interaction between two inert spheres and *sq* means interaction between two squirmers.

Using Eqs. (46) and (47), Ishikawa and Pedley (2008) simulated the motion of squirmers in a monolayer, and demonstrated that various types of processes resulting in coherent structures (such as aggregation, band formation or mesoscale spatio-temporal motion) can be generated *by pure hydrodynamic interactions*. Accordingly, Fig. 42 shows the velocity correlation function among the particles $I_U = I_U(r)$, as a function of the distance r separating the squirmers. c_a is the areal fraction of the particles in the monolayer, thus it refers to their sizes: bigger c_a denotes larger sphere.

Importantly, similar simulations carried out for three-dimensional suspension (that is, when the particles are not restricted to move on a monolayer) do not show such vigorous coherent structures (Ishikawa *et al.*, 2008).

An interesting example of collective motion is the synchronized beating of flagella on the surface of unicellular, or simple multicellular organisms. It was shown that such a coherent motion of flagella leads to a highly increased exchange rate of the nutrients around such organisms (Short *et al.*, 2006).

2. The role of adhesion

The problem regarding the mechanisms determining tissue movements dates back to the beginning of the 20th century. In 1907 Wilson discovered that sponge cells which have been previously squeezed through a mesh of

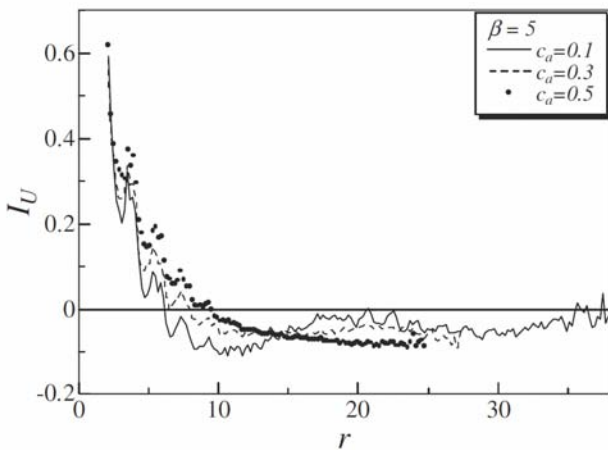


FIG. 42 The velocity correlation function among the particles (I_U) as a function of the distance among the units r for three different sphere-sizes. In the region $r < 6$, I_U is positive, denoting that nearby particles tend to swim together in similar direction. In the region $r > 10$, the correlation turns into anti-correlation, since I_U is negative, meaning that squirmers at least 10 radii apart tend to swim in opposite direction. From Ishikawa and Pedley (2008).

fine bolting-cloth are able to reunite again reconstituting themselves into a functioning sponge (Wilson, 1907). Early studies mainly envisioned cell sorting as a resultant of inhomogeneities (for example of pressure) in the immediate environment. Since then many theoretical and experimental studies have been dedicated to this question supporting the idea that the movements are due to intrinsic properties of the individual tissues themselves (landmarked by, among many others Wilson and Penney (1930), Bronsted (1936), Weiss (1941), Moscana (1952), Trinkaus and Groves (1955), Weiss and Taylor (1960)).

To explain the phenomenon of cell sorting, Steinberg (1963) developed the hypothesis that the local rearrangement behavior (characterizing cells during the process of sorting out and tissue reconstruction) follows directly from their *motility* and quantitative *differences in adhesiveness*. (This theory is often referred to as “differential adhesion hypothesis”, DAH). Based on the basic ideas of DAH, Belmonte *et al.* (2008) introduced a simple self-propelled particle model to study cell sorting (see Sec. V.B).

Regarding the collective motion and phase transition observed in migrating keratocyte cells (cells taken from the scales of goldfish), Szabó *et al.* (2006) constructed a model describing their experimental observations (see also Sec. II.C). Using long-term videomicroscopy they observed kinetic phase transition from disordered to ordered state, taking place as the cell density exceeds a relatively well-defined critical value. Short-range attractive-repulsive inter-cellular forces are suggested to account for the organization of the motile keratocyte cells into coherent groups.

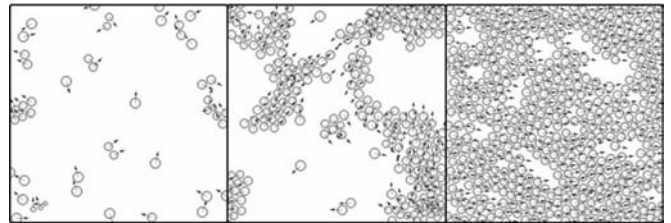


FIG. 43 Computer simulations obtained by solving Eqs. (48) and (49) for different particle densities. In agreement with the observations, the model exhibit a continuous phase transition from disordered to ordered phase. From Szabó *et al.* (2006).

Instead of applying an explicit averaging rule (which would not be realistic), the model-cells (self-propelled particles) adjust their direction toward the direction of the net-force acting on them (see Eq. (48)). In this two-dimensional flocking model, N SPPs move with a constant speed v_0 and mobility μ in the direction of the unit vector $\vec{n}_i(t)$ while the i and j particles experiences the inter-cellular force $\vec{F}(\vec{r}_i\vec{r}_j)$. The motion of cell $i(\in 1, \dots, N)$ in the position $\vec{r}_i(t)$ is described by

$$\frac{d\vec{r}_i(t)}{dt} = v_0\vec{n}_i(t) + \mu \sum_{j=1}^N \vec{F}(\vec{r}_i\vec{r}_j). \quad (48)$$

The direction $\vec{n}_i(t)$ can be described by $\theta_i^n(t)$ as well, which attempts to relax to $\vec{v}_i(t) = d\vec{r}_i(t)/dt$ within a relaxation time τ . Denoting the noise by ξ and the unit vector orthogonal to the plane of motion by \vec{e}_z ,

$$\frac{d\theta_i^n(t)}{dt} = \frac{1}{\tau} \arcsin \left[\left(\vec{n}_i(t) \frac{\vec{v}_i(t)}{|\vec{v}_i(t)|} \right) \cdot \vec{e}_z \right] + \xi \quad (49)$$

Figure 43 shows the typical simulation results obtained by solving Eqs. (48) and (49) with periodic boundary conditions. The model – in good agreement with the observations – exhibit a continuous phase transition from disordered to ordered phase. (For the corresponding observations see also Fig. 15 in Sec. II.C.)

Some authors put big emphasis on the actual *shape* and *plasticity* of the cells as well, since these properties also play an important role in the emergent behavior of the system (Glazier and Graner, 1993; Graner and Glazier, 1992; Maree and Hogeweg, 2001; Savill and Hogeweg, 1997). Following this line, Rappel *et al.* (1999) suggested a model consisting of self-propelled deformable objects to explain their experimental results on the dynamics of *Dictyostelium discoideum* (see also in Sec. II.C). Their model reproduces the observed self-organized vortex states (the “pancake”-structures), as the resultants of the coupling between the self-generated propulsive force and the cell’s configuration, and of the cohesive energy between the cells.

In a nice paper, the dynamics of *sprouting* during vasculogenesis is described by an interacting particle model

(Czirók *et al.*, 2008).

3. Swarming bacteria

By using models and simulations, experimentally observed behaviors which are seemingly unintelligible might also be elucidated. Recently, as described in Sec. II.B, bacteria belonging to *Myxococcus xanthus* swarms were observed to reverse their gliding directions regularly, while the colony itself expanded (Wu *et al.*, 2009). To compass this seemingly energy-wasting behavior, the authors simulated the observed phenomena using a cell-based model, taking into account only the contact-mediated, local interactions (Wu *et al.*, 2007). The individual cells are represented by a flexible string of N nodes, consisting of $N - 1$ segments, as depicted on Fig. 44 (basically a bendable rod, bended in $N - 2$ points, being able to move in 2-D space). Each segment has the same length r . In the simulations N was chosen to be 3, thus each cell had two segments, as the rod was blended in one point, in the middle. The orientations of the cells are defined by the vectors directed from the tail nodes to the head nodes. In order to keep the shapes of the cells within an interval that agrees with the observations, a Hamiltonian function was defined to characterize the certain node-configurations, as given by Eq. (50).

$$H = \sum_{i=0}^{N-1} K_b (r_i - r_0)^2 + \sum_{i=0}^{N-2} K_\theta \theta_i^2, \quad (50)$$

where r_i is the length of the i th segment, r_0 is its “target length” and θ_i is the angle enclosed by the neighboring segments i and $i + 1$. K_b and K_θ are the stretching and the bending coefficients, respectively, defining the extent to which the length of the segments and the angles between them can vary. Both of them are dimensionless values, and are the same for all the segments and angles.

Regarding the active motion of the certain cells, first the head-node moves in a particular direction, followed by the other nodes which take positions so that the Hamiltonian function belonging to the new configuration is minimal. Since according to the observations, *Myxococcus xanthus* cells do not have any kind of long-range communicating systems (Kaiser, 2003), the model takes the interactions only among neighboring cells into account.

The experimentally observed reversals (sudden changes in the direction with 180°) are most probably regulated by an internal biochemical clock, which is independent of the actual interactions of the given cell. Therefore, the model takes into account these reversals by simply switching the roles of the head-nodes and the tail-nodes, according to an internal clock.

Simulations based on the above model did not result in swarming of the non-reversing cells in contrast to the

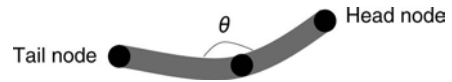


FIG. 44 Each cell is represented by a string of N nodes. In the simulations $N = 3$, thus the cells consist of two segments, enclosing the angle θ . The orientation is defined by the vector directed from the tail node to the head node. From Wu *et al.* (2007).

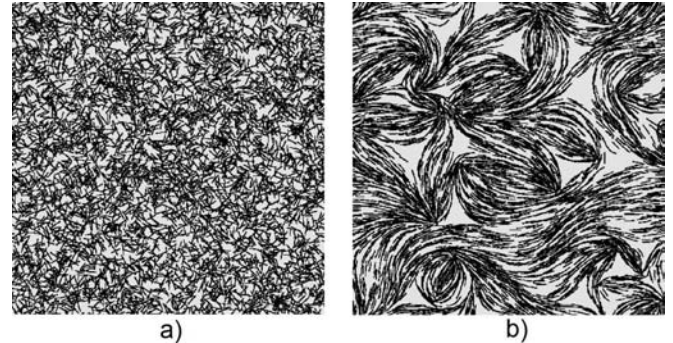


FIG. 45 Simulational results of the bacteria motion and pattern formation deep inside the colony. (a) In the initial setup the cells are randomly distributed. (b) The inner area of the colony after 3 h of evolution. Adapted from Wu *et al.* (2007).

simpler models by Peruani *et al.* (2006) and Ginelli *et al.* (2010). On the other hand, it was found that the expansion rate of the colony depends on the length of the reversal period. Notably, the biggest expansion is obtained within the same time-period that was experimentally observed, that is ≈ 8 min. The cellular motion and the emerged patterns deep inside the colony was also modeled. As it can be seen on Fig. 45, the considered social interactions result an enhanced order regarding the collective cellular motion. It should be noted, that in a very recent preprint Peruani *et al.* (2010) found signs of both ordering and clustering in experiments with a non-reversing, genetically modified mutant of a myxobacteria strain.

One of the earliest works on the collective motion of bacteria pointing out the reason why such models are important, is done by Czirók *et al.* (1996). The authors emphasized that the study of bacterial colonies can lead to interesting insights into the functioning of self-organized biological systems which rest on complex networks of regulation systems, since these are perhaps the simplest living systems exhibiting collective behavior, governed by interactions that are simple enough to be captured by mathematical tools.

In this paper the authors, on the one hand, reported on their experiments with *Bacillus subtilis* (see also Sec. II.B and Fig. 8) and on the other hand introduced a step-by-step elaborated model, which is capable to describe the increasingly elaborated complex collective behavior. The simplest expression describes the *collective migration*

of the cells, which move with a fixed-magnitude velocity v in the direction characterized by ϑ , according to Eq. (51)

$$\frac{d\vartheta_i}{dt} = \frac{1}{\tau} \left[\langle \vartheta(t) \rangle_{i,\epsilon} - \vartheta_i(t) \right] + \zeta \quad (51)$$

where $\vartheta_i(t)$ is the direction of the i th bacterium at time t , τ is the relaxation time, which is related to the bacterial length to width ratio (the interaction is stronger for longer bacteria), and ζ indicates an uncorrelated noise. The term $\langle \vartheta(t) \rangle_{i,\epsilon}$ represents the average direction of the cells in the neighborhood of particle i , in the radius ϵ .

For the simulations, a more simple, time-discretized form of Eq. (51) was used (Eq. 13), which is valid if the rotational relaxation time is fast compared to the change of the locations, that is, if $\tau \ll v^{-1}/\sqrt{\bar{\rho}}$. ($\bar{\rho}$ denotes the average bacterium density.)

Eq. (13) can be interpreted as a “starting-point” which is to be refined according to the specific systems. Here the noise takes values from the interval $[-\eta/2, \eta/2]$ randomly, with uniform distribution. The x_i positions of particle i is updated in each time-step according to Eq. (14).

Modifying the above model to be more system-specific, two changes were introduced: (i) the periodic boundary conditions were replaced with reflective circular walls, and (ii) a short-range “hard-core” repulsion was introduced, in order to prevent the cells to aggregate in a narrow zone. In other words, if the distance among cells decrease under a certain value ϵ^* , then these cells will repel each other, and their direction of motion will be given by

$$\vartheta_i(t + \Delta t) = \Phi \left(- \sum_{j \neq i, |\vec{x}_j - \vec{x}_i| < \epsilon^*} \vec{N}(\vec{x}_j(t) - \vec{x}_i(t)) \right), \quad (52)$$

where $\Phi(\vec{r})$ gives the angle ϑ between its argument vector and a predefined direction (for example the x axis), and $\vec{N} = \vec{u}/|\vec{u}|$. Simulations with low noise and high density show correlated rotational motion (see Fig. 46), in which the direction of the vortices can be either clockwise or anti-clockwise, as it is selected by spontaneous symmetry breaking.

The above constraint (reflective circular wall) is an externally imposed coercion to the bacterium colony. At the same time, in real colonies vortices often can be observed far from the boundaries as well, thus the confinement of the bacteria must be the resultant of some kind of interactions among the cells. Accordingly, the model can be further elaborated by adding “chemoattractants” to the system, which are interpreted in a broad sense: they can be reactions on “passive” physical forces as well (like surface tension, efficiency of the flagella-motors) which depend on the deposited extracellular slime. Cells

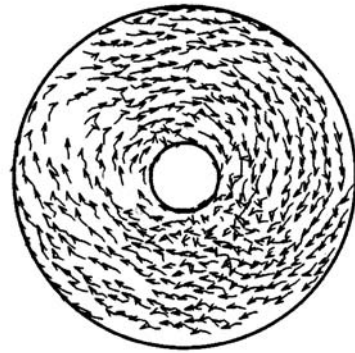


FIG. 46 A stationary state of the system characterized by short-range repulsion among the cells (defined by Eq. (52)) using reflective circular walls. From Czirók *et al.* (1996).

slightly alter their propulsion forces according to the local concentration of the attractant, which results in a torque acting on the colony. To simulate the system that includes the above introduced attractants, the concentration field, c_A (describing the concentration level of the secreted chemoattractants in each point of the field) is discretized by a hexagonal lattice (see Fig. 47). Supposing that a group of bacteria, a “raft”, is held together by intercellular bonds, it can be treated as a rigid body of size d . In this case, the velocity difference Δv at the opposite sides of the raft, in a linear approximation, is proportional to that component of ∇c_A which is orthogonal the velocity \vec{v} :

$$\Delta v \sim \frac{d}{v} |\vec{v} \times \vec{\nabla} c_A|. \quad (53)$$

By neglecting the convective transport caused by the motion of bacteria, the chemoattractant field’s time evolution can be written as

$$\frac{\partial c_A}{\partial t} = D_A \nabla^2 c_A + \Gamma_A \rho - \lambda_A c_A, \quad (54)$$

λ_A is the constant rate of the decay, ρ denotes the local density (number of particles in a unit area) and Γ_A is the rate by which bacteria produce the chemoattractant material. The first term represents the diffusion.

Figure 48 depicts a typical snapshot of the simulations. The secretion of chemoattractants is a process with positive feedback effect, which breaks down the originally homogeneous particle distribution and results denser clusters in sparser regions.

According to the experiments (Dombrowski *et al.*, 2004; Mendelson *et al.*, 1999), dense colonies of *Bacillus subtilis* exhibit surprising behavior as well: in regions of high bacterium concentration (having at least 10^9 cells per cm^3) transient jet-like patterns and vortices appear, which latter ones persist for timescales of $\approx 1s$. The

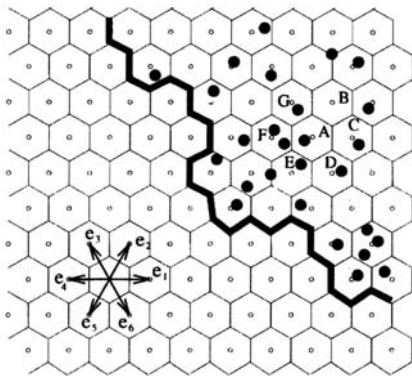


FIG. 47 The discretized concentration field: a hexagonal lattice defined by the lattice vectors $\vec{e}_1, \vec{e}_2, \dots, \vec{e}_6$. The open circles in the middle of the hexagons are those points where the concentration level of the diffusing chemoattractants are calculated at each time-step. The thick line shows the boundary of the system, which reflects the particles (filled dots) which can move off-lattice. To define the average direction $\langle \vec{v} \rangle_{i,\epsilon}$ for the bacterium i in lattice-cell A , the averaging involves all the particles in cells $A - G$. From Cziráok *et al.* (1996).

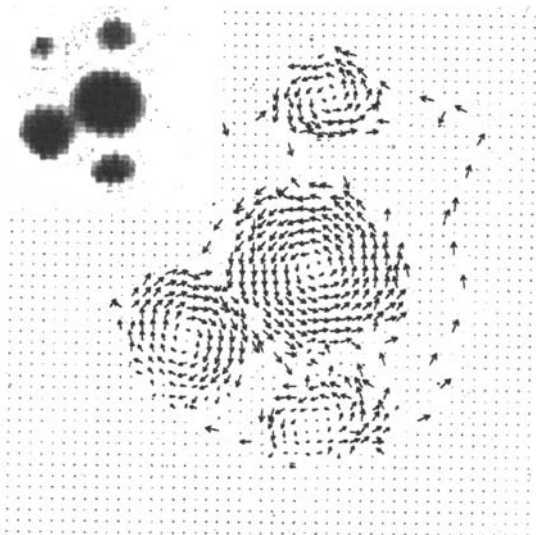


FIG. 48 Typical vortices formed by the model involving chemoattractants. The originally homogeneous particle distribution is destroyed by the positive feedback effect of the attractants. Arrows show the coarse grained velocity of the bacteria, while the corresponding distribution of the chemoattractant concentration is depicted in the upper left corner. From Cziráok *et al.* (1996).

speed of the observed jets are typically larger than that of the individual bacteria. To elucidate these observations, Wolgemuth (2008) developed a two-phase model in which the fluid and the bacteria were modeled by two independent, but interpenetrating continuum phases. Since their propulsive motors (the flagella) do not act on the center of mass, the rod-shaped bacteria exert a dipole force on the fluid. For reasonable parameter-values, the model (a

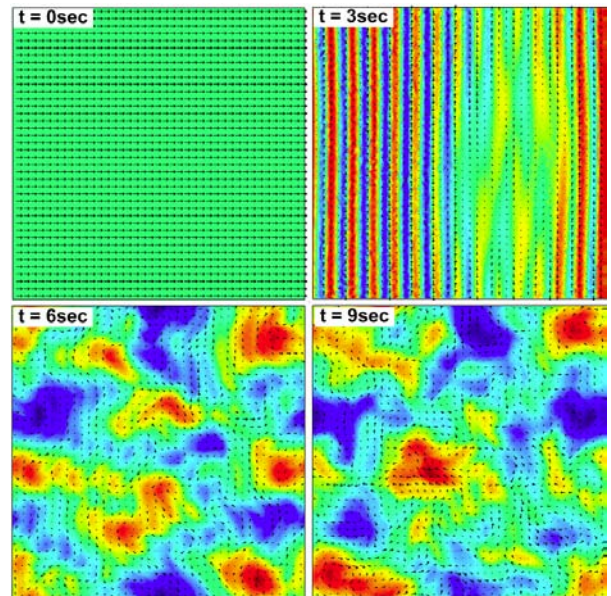


FIG. 49 (Color online) Four snapshots of the model reproducing the onset of the experimentally observed jets and vortices. The color map indicates the bacterial volume fraction, and the little arrows denote the fluid velocity field. According to the initial conditions ($t = 0$), the bacteria are distributed uniformly and the fluid velocity field is directed (with a small random perturbation) along the x axis. From Wolgemuth (2008).

system of partial differential equations) reproduces the observed behavior accurately. Figure 49 represents the onset of the observed turbulent behavior with the jets and vortices.

The interaction between these organisms under similar circumstances (namely, closely packed populations of *Bacillus subtilis*) with one other and with the boundaries (walls) is in the focus of Cisneros *et al.* (2007). Their model swimmer consist of a sphere (which is the “body” of the cell) and a cylinder representing the rotating bundle of helical flagella (see Fig. 50). The occurrence of the turbulent states at small Reynolds numbers (at $Re \ll 1$) is explained by the energy that the bacteria insert into the fluid as they swim in it.

Cziráok *et al.* (2001) used coupled differential equations to describe experimentally observed patterns of bacterial colonies. With such a method, they captured the periodic growth of *Proteus mirabilis* colonies (see Fig. 12 in Sec. II.B). Volfson *et al.* (2008) emphasized the role of bio-mechanical interactions arising from the growth and division of the cells (see also Fig. 13 in Sec. II.B), and developed a continuum model based on equations for local cell density, velocity and the tensor order parameter.

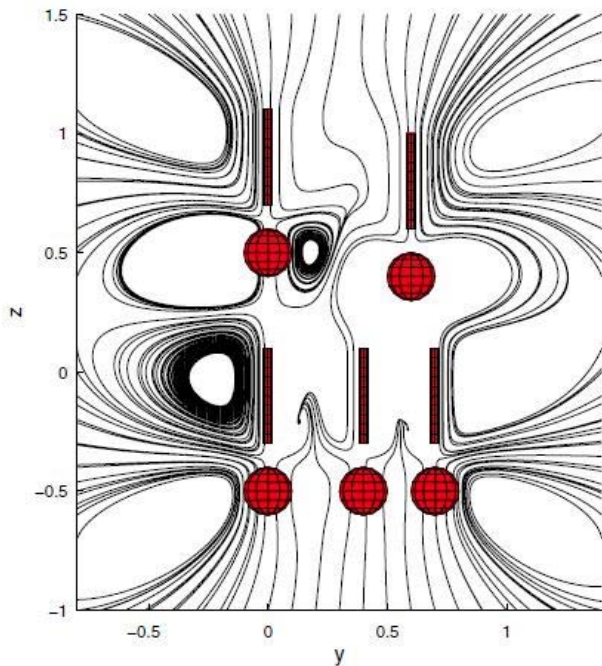


FIG. 50 (Color online) Streamlines of the fluid velocity field surrounding a group of five bacterium near to the walls. As it can be seen, there is little front-to-end penetration of the fluid into the group. Remarkably – as the authors point it out – this circumstance can lead to the split-up of a group because, as it follows, the oxygen supply for the organisms within a phalanx consisting of many bacteria will be insufficient, thus the inner cells will alter their velocity according to the gradient of oxygen concentration. From Cisneros *et al.* (2007).

B. Models with segregating units

Cell sorting denotes a special type of collective motion during which an originally heterogeneous mixture of cells segregate into two (or more) homogeneous cell-clusters without any kind of external field. This can be observed, for example, during the development of organs in an embryo or during regeneration after tissue dissociation. To simulate this phenomena, Belmonte *et al.* (2008) considered two kinds of cells, differing in their interaction intensities. According to the model, N particles move in a two-dimensional space with constant v_0 velocity. The velocity and the angle of the orientation of particle n at time t is denoted by \vec{v}_n^t and θ_n^t , respectively. The new orientation θ_n^{t+1} of particle n is

$$\theta_n^{t+1} = \arg \left[\sum_m \left(\alpha_{nm} \frac{\vec{v}_m^t}{v_0} + \beta_{nm} f_{nm}^t \vec{e}_{nm}^t \right) + \vec{u}_n^t \right], \quad (55)$$

where the summation refers to those particles (m) which are within a radius r_0 . These ‘cells’ exert a force $f_{nm}^t \vec{e}_{nm}^t$ on n , along the direction \vec{e}_{nm}^t . The noise is taken into account by \vec{u}_n^t , which is a random unit vector with uniformly distributed orientation. α_{nm} and β_{nm} are the

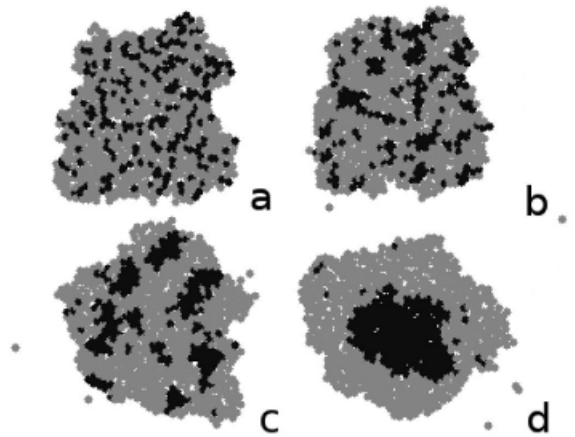


FIG. 51 Cell sorting of 800 cells. The endodermic cells are represented by black, and the ectodermic ones by gray circles. (a) The initial cluster with mixed cell types. (b) the cluster after 3000 time step, and (c) is taken at $t = 3 \times 10^5$. Clusters of endodermic cells form and grow as time passes by. (d) $t = 2 \times 10^6$. A single endodermic cluster is formed, but some isolated cells remain within the ectoderm tissue, in agreement with the experiments of Rieu *et al.* (1998). From Belmonte *et al.* (2008)

control parameters: α controls the relative weights of the alignment interaction, and β shows the strength of the radial two-body forces f_{nm} , which is defined as

$$f_{nm} = \begin{cases} \infty & \text{if } r_{nm} < r_c, \\ 1 - \frac{r_{nm}}{r_e} & \text{if } r_c < r_{nm} < r_0, \\ 0 & \text{if } r_{nm} > r_0, \end{cases} \quad (56)$$

that is, for distances smaller than a core radius r_c , it is a strong repulsive force, around the equilibrium radius r_e it is a harmonic-like interaction, and for distances bigger than the interaction range r_0 it is set to zero. For modeling the observations regarding *Hydra* cells (Rieu *et al.*, 2000), the authors defined two kinds of particles, ‘‘endodermic’’ and ‘‘ectodermic’’, denoted by 1 and 2, respectively. Accordingly, β_{11} and β_{22} stand for the cell cohesion *within* the two cell-types, while β_{12} and β_{21} account for the *inter-cell*-type interactions. These latter ones are assumed to be symmetric, that is, $\beta_{12} = \beta_{21}$. For the sake of simplicity, all the cells have the same α value. Figure 51 shows how a group of 800 cells evolve in time. The proportion is 1:3 of endodermic (black) to ectodermic (gray) cells, and $\alpha=0.01$.

Segregation occurs in various 3D systems as well, such as in flocks of birds or schools of fish. Mostly, models assume *identical* particles to simulate collective motion. At the same time, those simulations which suppose diverse particles, exhibit sorting (Couzin and Krause, 2003; Romey, 1996). This means that behavioral and/or motivational differences among animals effect the structure of the group, since individuals change their positions relative to the others according to their actual inner state.

This involves that if the individual variations are persistent then the group will reassemble to its' original state after perturbations (Couzin *et al.*, 2002). The sorting phenomenon depends primarily on the *relative* differences among the units.

In a similar spirit, Vabø and Skaret (2008) showed that differences in the *motivational level* can cause segregation within a school of spawning herrings. They used an individual based model in which the parameters describing the states of the individuals were varied and they measured a range of parameters at system level. The motion of each individual was determined by the combination of five behavioral rules: (1) avoid boundaries, (2) social attraction, (3) social repulsion, (4) move towards the bottom to spawn and (5) avoid predation. The motivational level was controlled by a parameter. To capture how the system as a whole reacts on changes in the individual level, various metrics were recorded, like the size and age of the school, its' vertical and horizontal extension, etc. By varying the size of the population and the level of the motivational synchronization, different systems emerged regarding its morphology and dynamics. Similar motivational levels resulted in an integrated school, whereas diverse inner states produced a system with frequent split-offs. More complex structure appeared by an intermediate degree of synchronization characterized by layers connected with vertical cylindrical shaped schools (see Fig. 52) allowing ovulating and spent herring to move across the layers, in agreement with the observations (Axelsen *et al.*, 2000). These findings suggest that the level of motivational synchronization among fish determines the unity of the school. Furthermore, this study also demonstrates that larger populations can exhibit such emergent behaviors that smaller ones can not (for example the cylindrical bridges mentioned above).

More general simulations also support these results. You *et al.* (2009) investigated the behavior of two-component swarms, consisting of two different kinds of particles, varying in their parameters, such as mass, self-propelling strength or preferences for shelters. The units – having different parameter-set – were observed to segregated from each other.

Other experiments focus on the emergent patterns of particles having different kinetic parameter settings (preferred speed, the range of perception in which a particle perceives the velocity vectors of other particles, etc.). The study of Sayama *et al.* (2009) was prompted by an in-class experiment aiming to test a new version of a software called “Swarm Chemistry”,³ which is an interactive evolutionary algorithm.

The software assumes that the particles move in an infinite two-dimensional space according to kinetic rules re-

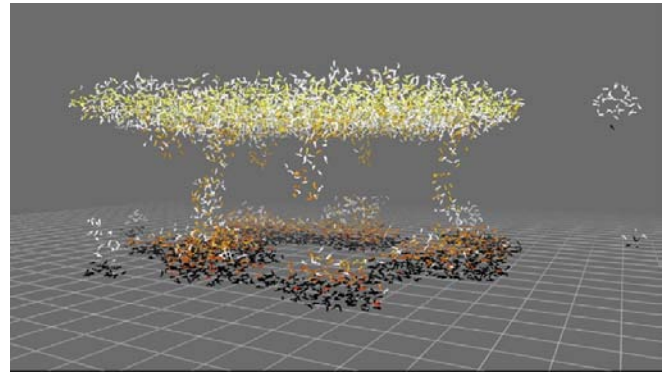


FIG. 52 (Color online) Simulational results, in which the motivational level of the individuals are taken into account. Large herring populations with small motivational synchronization tend to form multi-layered schools in which the layers are connected by cylindrical shaped “bridges”. The motivational level depends primarily on the age of the fish: mature herrings are denoted with yellow color (online), ovulating ones are orange to red, spawning individuals are black and white color registers spent herring. Adapted from Vabø and Skaret (2008).

sembling to the ones introduced by Reynolds (1987) (see Sec. IV.A). The strength of these kinetic rules, as well as the preferred speed and the local perception range, *differ* from particle to particle. Those units that (accidentally) share the same parameter-set, are considered to be of the same type. Some snapshots of the emergent dynamic patterns that these particles produce with their various parameter-sets, can be seen on Fig. 53.

According to the simulations, these mixtures of multiple type units usually spontaneously undergo to some kind of segregation process, often accompanied by the appearance of multilayer structures. Furthermore, the formed clusters may exhibit various dynamic macroscopic behaviors, such as oscillation, rotation or linear motion.

Interestingly, simulations of *hunting* showed segregation as well (Kamimura and Ohira, 2010). Here the two kinds of particles were the chasers (or predators) and the targets (or preys) which differed in their behavior.

C. Models inspired by animal behavioral patterns

1. Insects

Insects are one of the most diverse animal groups on Earth including more than a million described species which makes them represent more than half of all known living organisms (Chapman, 2009). Insects typically move on the ground or fly, or occasionally sink and swim in the water. Some of their species (like water striders) are even able to walk on the surface of water. Most of them live solitary life, but some insects (such as certain ants, bees or termites) are social and are famous of their

³ it can be downloaded from the author's website, <http://bingweb.binghamton.edu/~sayama/SwarmChemistry/>

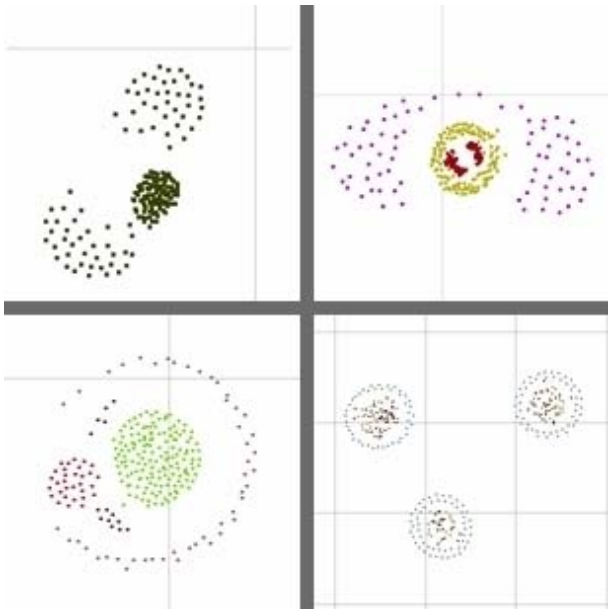


FIG. 53 (Color online) Some snapshots of the emergent patterns that particles with different parameter-set (preferred speed, range of perception and strength of the kinetic rules) can produce. From <http://bingweb.binghamton.edu/~sayama/SwarmChemistry/#recipes>.

large and well-organized colonies. The scope of this review does not cover the models aiming to describe the intricate behavior of insect societies, here we discuss only two models which are more closely related to collective motion. As mentioned in Sec. II.D, Mormon crickets and Desert locusts tend to exhibit cannibalistic behavior in case of the depletion of nutritional resources (Bazazi *et al.*, 2008; Simpson *et al.*, 2006).

Motivated by these observations, it can be shown that individuals with *escape* and *pursuit* behavior-patterns (which special kind of repulsive and attractive behaviors can be correlated with cannibalism) exhibit collective motion. (Romanczuk *et al.*, 2009). The escape reaction is triggered in an individual if it is approached from behind by another one; in this case the escaping animal increases its velocity in order to prevent being attacked from behind. In contrast, if the insect perceives one of its mates moving away, it increases its velocity in the direction of the escaping one; this is the pursuit behavior. Other cases do not trigger any response. According to the simulations, at moderate noise intensity and high particle density, these interactions (pursuit and escape) lead to global collective motion, irrespective of the detailed model parameters (see Fig. 54). Both interaction-types lead to collective motion, but with an opposite effect on the density distribution. Whereas pursuit leads to density-inhomogeneities (that is, to the appearance of clusters, as it can be seen on the first column on Fig. 54), escape calls to forth homogenization. Thus, the collec-

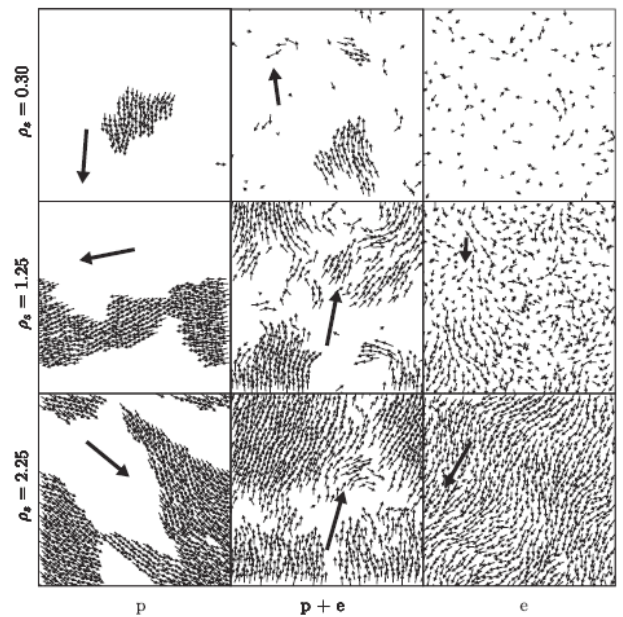


FIG. 54 The global collective motion emerging from escape and pursuit behaviors. ρ_s is the *rescaled density*, which is defined as $\rho_s = Nl_s^2/L^2$, where N is the total number of the individuals, l_s is their interaction range and L is the size of the simulation field. The simulations were carried out by using periodic boundary conditions. The column denoted by p shows the typical spatial configurations for the pursuit-only case, e for the escape-only case, and $p + e$ when both interactions are present. The large arrows indicate the direction and speed of the mean migration. As it can be seen on the top row, at low rescaled densities the emergent patterns strongly vary according to the strength of the escape and pursuit interactions. From Romanczuk *et al.* (2009).

tive dynamic in which both behavior-types are present, is a competition between the two opposite effects.

Another often observed phenomena regarding collective locust motion, is their sudden, coherent switches in the direction of motion. Yates *et al.* (2009) suggested to use Fokker-Plank equations in order to describe these observations. They found a seemingly counterintuitive result, namely that the individual locusts *increased their motional randomness* as a reaction for a *loss* of alignment in the group. This reaction thought to facilitate the group to find a highly aligned state again. They also found that the mean switching time increased exponentially with the number of individuals.

2. Moving in three dimensions – fish and birds

The main goal of the first system-specific models aiming to simulate the motion of animals moving in 3 dimensions (primarily birds and fish) was to produce realistically looking collective motion (Reynolds, 1987), to give system-specific models taking into account many pa-

rameters (McFarland and Okubo, 1997), or to create systems in which some characteristics (for example nearest neighbor distance or density) resembles to an actual biological system (Huth and Wissel, 1994). Later various other aspects and features were also studied, such as the function and mechanism of line versus cluster formation in bird flocks (Bajec and Heppner, 2009), how the fish size and kinship correlates with the spatial characteristics (e.g., animal density) of fish schools (Hemelrijk and Kunz, 2005), the cohort departure of bird flocks (Heppner, 1997), the collective behavior in an ecological context (in which not only the external stimuli, but the internal state of the individuals are also taken into account) (Vabø and Skaret, 2008), or the effect of perceived threat (Bode *et al.*, 2010). This latter circumstance was taken into account by relating it to higher updating frequency, and it resulted a more synchronized group regarding its speed and nearest neighbour distribution. The book of Parrish and Hamner (1997) provides an excellent review on this topic.

Models proposed by biologists tend to take into account many of the biological details of the modeled animals. A good example for this kind of approach is the very interesting work of Heppner and Grenander (1990), who proposed a system of stochastic differential equations with 15 parameters. Huth and Wissel (1992) used a similar approach for schools of fish. Some other models included a more realistic representation of body size and shape (Kunz and Hemelrijk, 2003).

Regarding the methodology of most of the simulations, the *agent-based* (or *individual-based*) approach proved to be very popular (although there are alternative approaches as well, e.g., Hayakawa (2010)). The reason behind this is that this approach provides a link between the behavior of the individuals and the emergent properties of the swarm as a whole, thus appropriate to investigate how the properties of the system depend on the actual behavior of the individuals. The most common rules applied in these models are (i) short-range repulsive force aiming to avoid collision with mates and with the borders (ii) adjusting the velocity vector according to the direction of the neighboring units (iii) a force avoiding being alone, e.g., moving towards the center of the swarm's mass (iv) noise (v) some kind of drag force if the medium is considered in which the individuals move (– which is usually *not* taken into account, in case of birds and fish). Then, the concrete models differ in the rules they apply (usually most of the above ones), in their concrete form and in the system parameters.

Some biologically more realistic, yet still simple individual-based models were also suggested (Couzin *et al.*, 2002; Hemelrijk and Hildenbrandt, 2008). By using such a model, Couzin *et al.* (2002) categorized the emergent collective motions as the function of the system parameters. In this framework, the individuals obey to the following basic rules: (i) they continually attempt

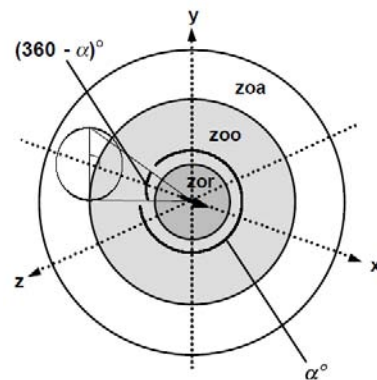


FIG. 55 The interaction zones, centered around each individual. The inner-most sphere with radius R_r is the *zone of repulsion* (“zor”). If others enter this zone, the individual will response by moving away from them to the opposite direction, that is, it will head towards $-\sum_{j \neq i}^{n_r} (\vec{r}_j - \vec{r}_i) / |\vec{r}_j - \vec{r}_i|$, where n_r is the number of individuals being in the zor. The interpretation of this zone is to maintain a personal space and to ensure the avoidance of collisions. The second annulus, “zoo”, represents the *zone of orientation*. If no mates are in the ‘zor’, the individual aligns itself with neighbors within this ‘zoo’ region. The outermost annulus, “zoa”, is the *zone of attraction*. The interpretation of this region is that group-living individuals continually attempt to join a group and to avoid being alone or in the periphery. From Couzin *et al.* (2002).

to maintain a certain distance among themselves and their mates, (ii) if they are not performing an avoidance manoeuvre (described by rule i), then they are attracted towards their mates, and (iii) they align their direction to their neighbors. Their perception zone (in which they interact with the others) is divided into three non-overlapping regions, as illustrated in Fig. 55. The radius of these spheres (zone of repulsion, zone of orientation and zone of attraction) are R_r , R_o and R_a , respectively. Thus, the width of the two outer annulus are $\Delta R_o = R_o - R_r$ and $\Delta R_a = R_a - R_o$. α denotes the field of perception, thus, the “blind volume” is behind the individual, with interior angle $(360 - \alpha)$.

In order to explore the global system behavior, the authors analyzed the consequences of varying certain system parameters, like the number of individuals, preferred speed, turning rate, width of the zones, etc. For every case, the following two global properties were calculated:

$$\varphi(t) = \frac{1}{N} \left| \sum_{i=1}^N \vec{v}_i^u(t) \right|, \quad (57)$$

where N is the number of individuals within the group, ($i = 1, 2, \dots, N$), and $\vec{v}_i^u(t)$ is the unit direction vector of the i th animal at time t . (Since $\vec{v}_i^u(t)$ is a *unit* vector, the expression defined by Eq. (57) is equivalent with the order parameter defined by Eq. (1).)

The other measure, *group angular momentum*, is the sum of the angular momenta of the group-members about the center of the group, \vec{r}_{Gr} . This expression measures the degree of rotation of the group about its center

$$m_{Gr}(t) = \frac{1}{N} \left| \sum_{i=1}^N \vec{r}_{i-Gr}(t) \times \vec{v}_i^u(t) \right|, \quad (58)$$

where $\vec{r}_{i-Gr} = \vec{r}_i - \vec{r}_{Gr}$, is the vectorial difference of the position of individual i , \vec{r}_i , and the position of the group-center, \vec{r}_{Gr} .

$$r_{Gr}(t) = \frac{1}{N} \sum_{i=1}^N r_i^2(t) \quad (59)$$

Figure 56 summarizes the four “basic types” of collective motions emerged according to the various parameter setups.

“*Swarm*.” Both the order parameter (φ) and the angular momentum (m_{Gr}) are small, which means little or no parallel orientation. (Fig. 56, (a) sub-picture)

“*Torus*” or “milling”: Individuals rotate around an empty core with a randomly chosen direction. The order parameter (φ) is small, but the angular momentum (m_{Gr}) is big. This occurs when Δr_a is big, but Δr_o is small. (Fig. 56, (b) sub-picture)

“*Dynamic parallel group*.” Occurs at intermediate or high values of Δr_a and intermediate values of Δr_o . This formation is much more mobile than either of the previous ones. The order parameter (φ) is high but the angular momentum (m_{Gr}) is small. (Fig. 56, (c) sub-picture)

“*Highly parallel group*.” By increasing Δr_o , a highly aligned formation emerges characterized by very high order parameter (φ) and low angular momentum (m_{Gr}). (Fig. 56, (d) sub-picture)

However, the approach of individual (or agent) based modeling has its own limitations or “traps” – as pointed out by Eriksson *et al.* (2009). Namely, that different combinations of rules and parameters may provide the same (or very similar) patterns and collective behaviors. Accordingly, in order to prove that the emergent behavior of a certain biological system obeys given principles, it is not enough to provide a rule and a parameter set (modeling these principles) and demonstrate that they reproduce the observed behavior. (On the other hand, Couzin *et al.* (2002) demonstrated that – vice versa – the same rule and parameter set may result in different collective behavior in the very same system, depending on its recent past, “history”.) Furthermore, the weak predictive power (for example, regarding the rate at which groups change their direction) of these models has to be considered when their relevance is judged (Yates *et al.*, 2009).

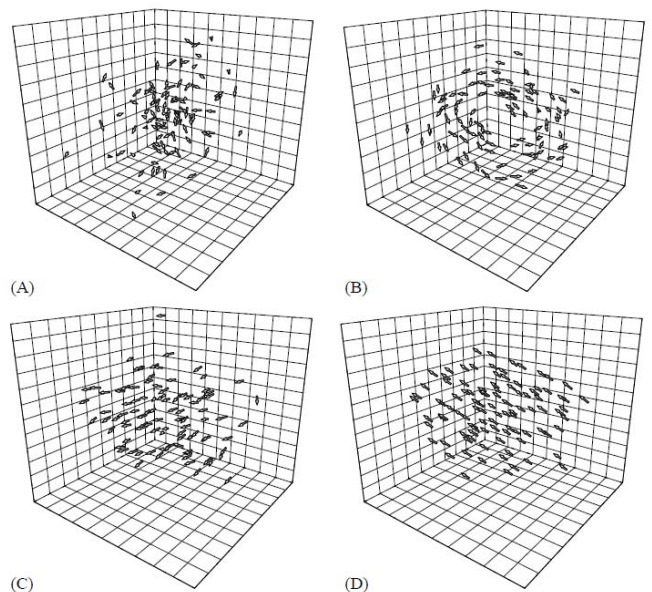


FIG. 56 The “basic types” of collective motions exhibited by the model, according to the various parameter setups. The denominations are (a) swarm (b) torus (c) dynamic parallel group (d) highly parallel group. Adapted from Couzin *et al.* (2002).

D. The role of leadership in consensus finding

Animals traveling together have to develop a method to make collective decisions regarding the places of foraging, resting and nesting sites, route of migration, etc. By slightly modifying (typically extending) models (such as the one described in Sec. V.C.2), a group of individuals can get hold of such abilities. Accordingly, Couzin *et al.* (2005) suggested a simple model in which individuals were not required to know how many and which individuals had information, they did not need to have a signaling mechanism and no individual recognition was required from the group members. The model looks as follows:

N individuals compose the group. The position of the i th particle is described by the vector \vec{r}_i , and it is moving in the direction \vec{v}_i . The group members endeavor to continually maintain a minimum distance, α , among themselves, by turning away from the neighbors j which are within this range towards the opposite direction, described by the desired direction \vec{d}_i

$$\vec{d}_i(t + \Delta t) = - \sum_{j \neq i} \frac{\vec{r}_j(t) - \vec{r}_i(t)}{|\vec{r}_j(t) - \vec{r}_i(t)|} \quad (60)$$

This rule has the highest priority. If there are no mates within this range, than the individual will attempt to align with those neighbors j , which are within the interaction range ρ . If so, the desired direction is defined as

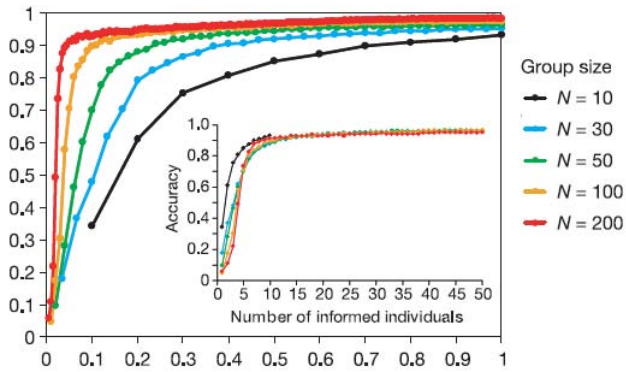


FIG. 57 (Color online) SPPs following simple rules can compose systems in which a few informed individual is capable to guide the entire group towards a preferred direction. The accuracy of the group (following the rules given by Eqs. 60, 61 and 62) increases asymptotically as the portion of the informed individuals increases. Adapted from Couzin *et al.* (2005).

$$\vec{d}_i(t + \Delta t) = \sum_{j \neq i} \frac{\vec{r}_j(t) - \vec{r}_i(t)}{|\vec{r}_j(t) - \vec{r}_i(t)|} + \sum_{j \neq i} \frac{\vec{v}_j(t)}{|\vec{v}_j(t)|}. \quad (61)$$

We will use the corresponding unit vector, $\hat{d}_i(t) = \vec{d}_i(t)/|\vec{d}_i(t)|$.

Until this point the algorithm is very similar to the one described in Sec. V.C.2. In order to study the influence of informed individuals, a portion of the group, p , is given information about a preferred direction, described by the unit vector \vec{g} . The rest of the group is naive, without any preferred direction. Informed individuals balance their social alignment and their preferred direction with the weighting factor ω

$$\vec{d}_i(t + \Delta t) = \frac{\hat{d}_i(t + \Delta t) + \omega \vec{g}_i}{|\hat{d}_i(t + \Delta t) + \omega \vec{g}_i|}. \quad (62)$$

(ω can exceed 1; in this case the individual is influenced more heavily by its own preferences than by its mates.) The *accuracy of the group* (describing the quality of information transfer) is characterized by the normalized angular deviation of the group direction around the preferred direction \vec{g} , similarly to the term given in Eq. 58.

The authors found that for fixed group size, the accuracy increases asymptotically as the portion p of the informed members increased, see Fig. 57. This means, that the larger the group, the smaller the portion of informed members is needed, in order to guide the group towards a preferred direction.

However, informed individuals might also differ in their preferred direction. If the number of individuals preferring one or another direction is equal, than the group direction will depend on the degree to which these preferred

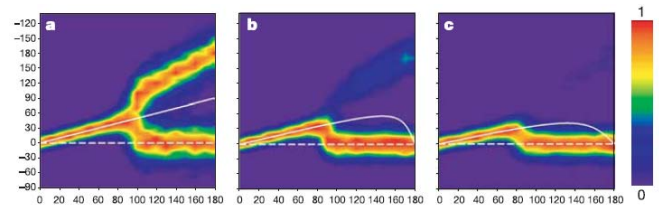


FIG. 58 (Color online) Collective group direction when two groups of informed individuals differ in their preferences. The vertical axis shows the degree of the most probable group motion. The first group (consisting of n_1 informed individuals) prefers the direction characterized by 0 degrees (dashed line), while the second group (consisting of n_2 informed individuals) prefers a direction between 0 – 180 degrees (horizontal axis). The group consists of 100 individuals altogether, of which the numbers of informed individuals are (a) $n_1 = n_2 = 5$, (b) $n_1 = 6$ and $n_2 = 5$ (c) $n_1 = 6$ and $n_2 = 4$. Adapted from Couzin *et al.* (2005).

directions differ from each other: if these preferences are similar, than the group will go in the average preferred direction of all informed individuals. As the differences among the preferred directions increase, individuals start to select randomly one or the another preferred direction. If the number of informed individuals preferring a given direction increases, the entire group will go into the direction preferred by the majority even if that majority is small (see Fig. 58).

Freeman and Biro (2009) extended this model by including a “social importance factor”, h , describing the *strength of the effect* of a given individual on the group movement. That is, h varies with each agent, and the higher this value is, the bigger influence the given unit exerts on the group. Equation 61 is modified accordingly

$$\vec{d}_i(t + \Delta t) = \sum_{j \neq i} h_j \frac{\vec{r}_j(t) - \vec{r}_i(t)}{|\vec{r}_j(t) - \vec{r}_i(t)|} + \sum_{j \neq i} h_j \frac{\vec{v}_j(t)}{|\vec{v}_j(t)|} \quad (63)$$

Importantly, these models show that leadership might emerge from the information differences among group members, that is, leadership can be transient and transferable. Other studies also support these results. (Quera *et al.*, 2010) used an other kind of rule-set by which they agents moved, and observed the same: certain agents did become leaders without anything in the rule-set or in the initial conditions that would have prompted or predicted it.

In addition, even more simple models can lead to consensus decisions. For example, the severe quorum rule (in which the probability that an individual follows a given option, sharply increases when the number of other group members making that very decision reaches a threshold) resulted accurate group decisions as well (Sumpter *et al.*, 2008).

Despite of the many attempts, the research of “human decision making” is still in its infancy. Castellano *et al.*

(2009) give a nice review of the state of the art regarding the physical and mathematical models which have been proposed throughout the years, on this field.

VI. SUMMARY AND CONCLUSIONS

From the quickly growing number of exciting new publications on flocking we are tempted to conclude that collective motion can be regarded as an emerging field on the borderline of several scientific disciplines. Thus, it is a multidisciplinary area with many applications, involving statistical physics, technology and branches of life sciences. Because of the nature of the problem (treating many similar entities) studies in this field make quantitative comparison with observations possible even for living systems and there is a considerable potential for constructing theoretical approaches.

The results we have presented support a deep analogy with equilibrium statistical physics. The essential deviation from equilibrium is manifested in the “collision rule”: since the absolute velocity of the particles is preserved and in most cases an alignment of the direction of motion after interaction is preferred, the total momentum increases both during individual collisions and, as a result, gradually in the whole system of particles as well.

The observations we have discussed can be successfully interpreted in terms of simple simulational models. Using models based on simplified units (also called particles) to simulate the collective behaviour of large ensembles has a history in science, especially in statistical physics, where originally particles represented atoms or molecules. With the rapid increase of computing power and a growing appreciation for ‘understanding through simulations’, models based on a plethora of complex interacting units, nowadays widely called agents, have started to emerge. Agents – even those that follow simple rules – are more complex entities than particles because they have a goal they intend to achieve in an optimal way (for example, using as little amount of resources as possible).

As a rule, models of increasing complexity are bound to be born in order to account for the interesting variants of a fundamental process. However, there is a catch. A really good model must both reproduce truly life-like behaviour and be as simple as possible. If the model has dozens of equations and rules, and correspondingly large numbers of parameters, it is bound to be too specific and rather like an ‘imitation’ than a model that captures the few essential features of the process under study.

Thus, if a model is very simple, it is likely to be applicable to other phenomena for which the outcome is dominated by the same few rules. On the other hand, simplification comes with a price, and some of the exciting details that distinguish different phenomena may be lost. But anyone who is an enthusiastic viewer of natural life movies knows that actual collective behav-

ior in nature typically involves sophisticated, occasionally amazing techniques aimed at coordinating the actions of the organisms to maximize success. The art of designing models of reality is rooted in the best compromise between oversimplification and including too many details (eventually preventing the location of the essential features).

On the basis of the numerous observations and models/simulations we have discussed above, the following conclusions can be made concerning the general features of systems exhibiting collective motion

- Most patterns of collective motion are universal (the same patterns occur in very different systems)
- Simple models can reproduce this behavior
- A simple noise term can account for numerous complex deterministic factors
- Global ordering is due to non-conservation of the momentum during individual collisions/interactions of pairs of units

The universally occurring patterns can be divided into a few classes of motion patterns

- disordered (particles moving in random directions)
- fully ordered (particles moving in the same direction)
- rotational (within a rectangular or circular area)
- critical (flocks of all sizes moving coherently in different directions. The whole system is very sensitive to perturbations)
- quasi-long range velocity correlations and ripples
- Jamming

A few further, less widely occurring patterns are also possible, for example in systems made of two or more distinctively different types of units.

The following types of transitions between the above collective motion classes are possible

- Continuous (second order, accompanied with large fluctuations and algebraic scaling)
- Discontinuous (first order)
- No singularity in the level of directedness
- Jamming (transition to a state in which mobility is highly restricted)

The above transitions usually take place as i) a function of density or ii) the changing magnitude of perturbations the units are subject to. The role of noise is essential; all systems are prone to be strongly influenced by

perturbations. In some cases noise can have a paradoxical effect and, e.g., facilitate ordering. This could be understood, for example, as a result of perturbations driving the system out from an inefficient deterministic regime (particles moving along trajectories systematically (deterministically) avoiding each other) into a more efficient one, characterized by an increased number of interactions.

After reviewing the state of the art regarding collective motion we think that some of the most exciting challenges in this still emerging field can be summarized as: i) Additional, even more precise data about the positions and velocities of the collectively moving units should be obtained for establishing a well defined, quantitative set of interaction rules typical for most of the flocks. ii) the role of leadership in collective decision making should be further explored. Is it hierarchical? Can a leadership-driven decision-making mechanism be scaled up to huge group sizes? iii) The problem of a coherently moving, self-organized flock of unmanned aerial vehicles is still unsolved in spite of its very important potential applications, iv) and last, but far from being the least, the question about the existence of some simple underlying laws of nature (such as, e.g., the principles of thermodynamics) that produce the whole variety of the observed phenomena we discussed is still to be uncovered.

We have seen that using methods common in statistical physics has been very useful for the quantitative description of collective motion. Theories based on approaches borrowed from fluid dynamics, data evaluation techniques making use of correlations functions and many particle simulations all have led to a deeper insight into flocking phenomena. This is all in the spirit of going from a qualitative to a more quantitative interpretation of the observations: a widely preferred direction in life sciences these days.

A quantitative frame for describing the behavior of a system enables important, highly desirable features of treating actual situations. For example, prediction of the global displacement of huge schools of fish may have direct economical advantages. Understanding the collective reaction of people to situations including panic may lead to saving lives. Using computer models to simulate migration of birds or mammals can assist in preserving biodiversity. The list of potential applications is long, and is likely to get longer, especially if we take into account the swiftly increasing interest in collective robotics.

ACKNOWLEDGMENTS

T.V. thanks collaboration and numerous helpful exchanges of ideas with a long list (to long to reproduce here, but cited in the text) of outstanding colleagues over the past 15 years. Writing this review was made possible

in part by a grant from EU ERC No. 227878-COLLMOT. A.Z. is very grateful to Elias Zafiris for his help during the preparation of the manuscript.

REFERENCES

- Ákos, Z., M. Nagy, and T. Vicsek (2008), Proceeding of the National Academy of Sciences of the United States of America **105**, 4139.
- Albert, R., and A.-L. Barabási (2002), Reviews of Modern Physics **74**, 47.
- Aldana, M., V. Dossetti, C. Huepe, V. M. Kenkre, and H. Larralde (2007), Physical Review Letters **98**, 095702.
- Aldana, M., H. Larralde, and B. Vazquez (2009), International Journal of Modern Physics B **23**, 3661.
- Alt, W., A. Deutsch, and G. Dunn, Eds. (1997), *Dynamics of Cell and Tissue Motion* (Birkhuser Basel).
- Arboleda-Estudillo, Y., M. Krieg, J. Stuhmer, N. A. Licata, D. J. Muller, and C. Heisenberg (2010), Current Biology **20**, 161.
- Axelsen, B. E., L. Nøttestad, A. Fern, A. Johannessen, and O. A. Misund (2000), Marine Ecology Progress Series **205**, 259.
- Baglietto, G., and E. V. Albano (2008), Physical Review E **78**, 021125.
- Baglietto, G., and E. V. Albano (2009a), Computer Physics Communications **180**, 527.
- Baglietto, G., and E. V. Albano (2009b), Physical Review E **80**, 050103.
- Bajec, I. L., and F. H. Heppner (2009), Animal Behaviour **78**, 777.
- Ballerini, M., N. Cabibbo, R. Candelier, A. Cavagna, E. Cisbani, I. Giardina, V. Lecomte, A. Orlandi, G. Parisi, A. Procaccini, M. Viale, and V. Zdravkovic (2008), Proceeding of the National Academy of Sciences of the United States of America **105**, 1232.
- Baskaran, A., and M. C. Marchetti (2008), Physical Review Letters **101**, 268101.
- Baskaran, A., and M. C. Marchetti (2009), PNAS **106** (37), 15567.
- Batchelor, G. K. (1970), The Journal of Fluid Mechanics **44**, 419.
- Bazazi, S., J. Buhl, J. J. Hale, M. L. Anstey, G. A. Sword, S. J. Simpson, and I. D. Couzin (2008), Current Biology **18**, 735.
- Beauchamp, G. (2003), Behav. Processes **63**, 111.
- Becco, C., N. Vandewalle, J. Delcourt, and P. Poncin (2006), Physica A **367**, 487.
- Beekman, M., D. J. T. Sumpter, and F. L. W. Ratnieks (2001), Proceeding of the National Academy of Sciences of the United States of America **98**, 9703.
- Belmonte, J. M., G. L. Thomas, K. G. Brunnet, R. M. C. de Almeida, and H. Chate (2008), Physical Review Letters **100**, 248702.
- Ben-Asher, Y., S. Feldman, P. Gurfil, and M. Feldman (2008), AIAA Journal of Aerospace Computing, Information, and Communication **5**, 234.
- Ben-Jacob, E., O. Shochet, A. Tenenbaum, I. Cohen, A. Czirok, and T. Vicsek (1994), Nature **368**, 46.
- Benoit-Bird, K. J., and W. W. L. Au (2003), Behav. Ecol. Sociobiol **53**, 364.

- Bertin, E., M. Droz, and G. Grégoire (2006), *Physical Review E* **74**, 022101.
- Bertin, E., M. Droz, and G. Grégoire (2009), *Journal of Physics A: Mathematical and Theoretical* **42**, 445001.
- Bhattacharya, K., and T. Vicsek (2010), communicated.
- Biro, D., D. J. T. Sumpter, J. Meade, and T. Guilford (2006), *Current Biology* **16**, 2123.
- Blair, D. L., T. Neicu, and A. Kudrolli (2003), *Physical Review E* **67**, 031303.
- Blake, J. R. (1971), *Journal of Fluid Mechanics* **46**, 199.
- Blondel, V. D., J. M. Hendrickx, A. Olshevsky, and J. N. Tsitsiklis (2005), *Proceedings of the 44th IEEE Conference on Decision and Control, and the European Control Conference*, 2996.
- Bode, N. W. F., J. J. Faria, D. W. Franks, J. Krause, and A. J. Wood (2010), *Proceedings of the Royal Society B: Biological Sciences*.
- Boyd, S. P., A. Ghosh, B. Prabhakar, and D. Shah (2005), *Proceedings IEEE Infocomm* **3**, 1653.
- Brady, J. F., and G. Bossis (1988), *Annual Review of Fluid Mechanics* **20**, 111.
- Brady, J. F., R. J. Phillips, J. C. Lester, and G. Bossis (1988), *Journal of Fluid Mechanics* **195**, 257.
- Brankov, I., D. M. Danchev, N. S. Tonchev, and J. G. Brankov (2000), *Theory of critical phenomena in finite-size systems: scaling and quantum effects* (World Scientific Publishing Company).
- Breder, C. M. (1954), *Ecology* **35**, 361.
- Bronsted, H. V. (1936), *Acta Zoologica (Stockholm)* **17**, 75.
- Buhl, J., D. J. T. Sumpter, I. D. Couzin, J. J. Hale, E. Despland, E. R. Miller, and S. J. Simpson (2006), *Science* **312**, 1402.
- Butt, T., T. Mufti, A. Humayun, P. B. Rosenthal, S. Khan, S. Khan, and J. E. Molloy (2010), *The Journal of Biological Chemistry* **285**, 4964.
- Camazine, S., J.-L. Deneubourg, N. R. Franks, J. Sneyd, G. Theraulaz, and E. Bonabeau (2001), *Self-organization in Biological Systems* (Princeton University Press).
- Cardy, J. (1996), *Scaling and Renormalization in Statistical Physics* (Cambridge University Press).
- Carrillo, J. A., M. Fornasier, J. Rosado, and G. Toscani (2010), To appear in *SIAM Journal on Mathematical Analysis*.
- Castellano, C., S. Fortunato, and V. Loreto (2009), *Reviews of Modern Physics* **81**, 591.
- Cavagna, A., A. Cimarelli, I. Giardina, G. Parisi, R. Santagati, F. Stefanini, and M. Viale (2010), *Proceeding of the National Academy of Sciences of the United States of America* **107**, 11865.
- Celikkanat, H., and E. Sahin (2010), *Neural Computing & Applications*.
- Chapman, A. D. (2009), *Numbers of Living Species in Australia and the World*, 2nd ed. (Report for the Australian Biological Resources Study, Canberra).
- Chaté, H., F. Ginelli, G. Grégoire, F. Peruani, and F. Raynaud (2008a), *Eur. Phys. J. B* **64**, 451.
- Chaté, H., F. Ginelli, G. Grégoire, and F. Raynaud (2008b), *Physical Review E* **77**, 046113.
- Chaté, H., F. Ginelli, and R. Montagne (2006), *Physical Review Letters* **96**, 180602.
- Cisneros, L. H., R. Cortez, C. Dombrowski, R. E. Goldstein, and J. O. Kessler (2007), *Experiments in Fluids* **43**, 737.
- Conradt, L., and C. List (2009), *Philosophical Transactions of the Royal Society B – Biological Sciences* **364**, 719.
- Conradt, L., and T. J. Roper (2003), *Nature* **421**, 155.
- Conradt, L., and T. J. Roper (2005), *Trends in Ecology & Evolution* **20**, 449.
- Conradt, L., and T. J. Roper (2010), *Behavioural Processes* **84**, 675.
- Couzin, I. D., and N. R. Franks (2003), *Proceedings of the Royal Society of London, Series B* **270**, 139.
- Couzin, I. D., and J. Krause (2003), *Advances in the Study of Behavior* **32**, 1.
- Couzin, I. D., J. Krause, N. R. Franks, and S. A. Levin (2005), *Nature* **433**, 513.
- Couzin, I. D., J. Krause, R. James, G. D. Ruxton, and N. R. Franks (2002), *Journal of Theoretical Biology* **218**, 1.
- Cox, R. G. (1970), *The Journal of Fluid Mechanics* **44**, 791.
- Csahók, Z., and A. Czirók (1997), *Physica A* **243**, 304.
- Cucker, F., and J.-G. Dong (2010), *IEEE Transactions on Automatic Control* **55**, 1238.
- Cucker, F., and C. Huepe (2008), *Mathematics in Action* **1**, 1.
- Cucker, F., and E. Mordecki (2008), *Journal de Mathématiques Pures et Appliquées* **89**, 278.
- Cucker, F., and S. Smale (2007a), *IEEE Transactions on Automatic Control* **52**, 852.
- Cucker, F., and S. Smale (2007b), *Japanese Journal of Mathematics* **2**, 197.
- Cui, X., C. T. Hardin, R. K. Ragade, and A. S. Elmaghraby (2004), in *Proceedings of the 16th IEEE International Conference on Tools with Artificial Intelligence*, pp. 424–430.
- Cullen, J. M., E. Shaw, and H. A. Baldwin (1965), *Animal Behavior* **13**, 534.
- Czirók, A., A.-L. Barabási, and T. Vicsek (1999), *Physical Review Letters* **82**, 209.
- Czirók, A., E. Ben-Jacob, I. Cohen, and T. Vicsek (1996), *Physical Review E* **54** (2), 1791.
- Czirók, A., M. Matsushita, and T. Vicsek (2001), *Physical Review E* **63** (3), 031915.
- Czirók, A., K. Schlett, E. Madarász, and T. Vicsek (1998), *Physical Review Letters* **81** (14), 3038.
- Czirók, A., H. E. Stanley, and T. Vicsek (1997), *Journal of Physics A: Mathematical and General* **30**, 1375.
- Czirók, A., E. A. Zamir, A. Szabo, and C. D. Little (2008), *Current Topics in Developmental Biology* **81**, 269.
- Dalmao, F., and E. Mordecki (2009), arXiv:0912.4535.
- Deisboeck, T. S., and I. D. Couzin (2009), *BioEssays* **31**, 190.
- Dell’Ariccia, G., G. Dell’Omo, D. P. Wolfer, and H. P. Lipp (2008), *Animal Behaviour* **76**, 1165.
- Derzsi, A., G. Szóllósi, and T. Vicsek (2009), “Most minimal spp model.”
- Deseigne, J., O. Dauchot, and H. Chate (2010), .
- Dombrowski, C., L. Cisneros, S. Chatkaew, R. E. Goldstein, and J. O. Kessler (2004), *Physical Review Letters* **93**, 098103.
- Dorigo, M., G. D. Caro, and L. M. Gambardella (1999), *Artificial Life* **5**, 137.
- Dorigo, M., and L. Gambardella (1997), *BioSystems* **43**, 73.
- Dyer, J. R. G., C. C. Ioannou, L. J. Morrell, D. P. Croft, I. D. Couzin, D. A. Waters, and J. Krause (2008), *Animal Behaviour* **75**, 461.
- Dyer, J. R. G., A. Johansson, D. Helbing, I. D. Couzin, and J. Krause (2009), *Philosophical Transactions of the Royal Society B* **364**, 781.
- Eberhart, R. C., Y. Shi, and J. Kennedy (2001), *Swarm Intelligence* (Morgan Kaufmann).
- Elgar, M. A. (1989), *Biological Reviews of the Cambridge*

- Philosophical Society **64**, 13.
- Erdmann, U., W. Ebeling, and A. S. Mikhailov (2005), *Physical Review E* **71**, 051904.
- Eriksson, A., M. N. Jacobi, J. Nystrom, and K. Tunstrom (2009), arXiv:0905.0917.
- Faria, J. J., J. R. G. Dyer, N. Holt, D. Waters, A. J. W. Ward, R. Clement, J. Goldthorpe, I. D. Couzin, and J. Krause (2010a), *Behavioral Ecology and Sociobiology*.
- Faria, J. J., J. R. G. Dyer, C. R. Tosh, and J. Krause (2010b), *Animal Behaviour* **79** (4), 895.
- Fischhoff, I. R., S. R. Sundaresan, J. Cordingley, H. M. Larkin, M.-J. Sellier, and D. I. Rubenstein (2007), *Animal Behaviour* **73**, 825.
- Forster, D., D. R. Nelson, and M. J. Stephen (1977), *Physical Review A* **16**, 732.
- Franks, N. R., N. Gomez, S. Goss, and J. L. Deneubourg (1991), *Journal of Insect Behavior* **4**, 583.
- Freeman, R., and D. Biro (2009), *The journal of navigation* **62**, 33.
- Friedl, P. (2004), *The International Journal of Developmental Biology* **48**, 441.
- Friedl, P., and D. Gilmour (2009), *Nature Reviews Molecular Cell Biology* **10**, 445.
- Fujikawa, H., and M. Matsushita (1989), *J. Phys. Soc. Japan* **58**, 3875.
- Galanis, J., D. Harries, D. L. Sackett, W. Losert, and R. Nossal (2006), *Physical Review Letters* **96**, 028002.
- Ginelli, F., F. Peruani, M. Bär, and H. Chaté (2010), *Physical Review Letters* **104**, 184502.
- Glazier, J. A., and F. m. c. Graner (1993), *Physical Review E* **47** (3), 2128.
- Gotwald, J. W. H. (1995), *Army ants: the biology of social predation* (Cornell University Press).
- Gov, N. S. (2007), *Proceeding of the National Academy of Sciences of the United States of America* **104**, 15970.
- Graner, F. m. c., and J. A. Glazier (1992), *Physical Review Letters* **69** (13), 2013.
- Grégoire, G., and H. Chaté (2004), *Physical Review Letters* **92**, 025702+.
- Grégoire, G., H. Chaté, and Y. Tu (2003), *Physica D* **181**, 157.
- Grossman, D., I. S. Aranson, and E. B. Jacob (2008), *New Journal of Physics* **10**, 023036.
- Grunbaum, D. (1998), *Evolutionary Ecology* **12**, 503.
- Ha, S. Y., K. Lee, and D. Levy (2009), *Communications in Mathematical Sciences* **7**, 453.
- Ha, S.-Y., and J.-G. Liu (2009), *Communication in Mathematical Sciences* **7**, 297.
- Ha, S.-Y., and E. Tadmor (2008), *Kinetic and Related Models* **1**, 415.
- Halley, J., G. Sempo, G. Caprari, C. Rivault, M. Asadpour, F. Tache, I. Said, V. Durier, S. Canonge, J. M. Ame, C. Detrain, N. Correll, A. Martinoli, F. Mondada, R. Siegwart, and J. L. Deneubourg (2007), *Science* **318**, 1155.
- Hatwalne, Y., S. Ramaswamy, M. Rao, and R. A. Simha (2004), *Physical Review Letters* **92** (11), 118101.
- Hayakawa, Y. (2010), *Europhysics Letters* **89**, 48004.
- Helbing, D., I. Farkas, and T. Vicsek (2000), *Nature* **407**, 487.
- Helbing, D., F. Schweitzer, J. Keltsch, and P. Molnár (1997), *Physical Review E* **56** (3), 2527.
- Helfman, G., B. Collette, and D. Facey (1997), *The Diversity of Fishes* (Wiley-Blackwell).
- Hemelrijk, C. K., and H. Hildenbrandt (2008), *Ethology* **114**, 245.
- Hemelrijk, C. K., and H. Kunz (2005), *Behavioral Ecology* **16** (1), 178.
- Heppner, F. (1997), in *Animal groups in three dimensions*, edited by J. K. Parrish and W. M. Hamner (Cambridge University Press) pp. 68–89.
- Heppner, F., and U. Grenander (1990), in *The ubiquity of chaos*, edited by E. Krasner (AAAS Publications) pp. 233–238.
- Hoare, D. J., I. D. Couzin, J. G. J. Godin, and J. Krause (2004), *Animal Behaviour* **67**, 155.
- Holland, O., J. Woods, R. D. Nardi, and A. Clark (2005), *Proceedings of the IEEE Swarm Intelligence Symposium*, 217.
- Holldobler, B., and E. O. Wilson (2008), *The Superorganism: The Beauty, Elegance, and Strangeness of Insect Societies* (W. W. Norton & Company).
- Huepe, C., and M. Aldana (2004), *Physical Review Letters* **92**, 168701.
- Huepe, C., and M. Aldana (2008), *Physica A* **387**, 2809.
- Hunter, J. R. (1966), *Journal of the Fisheries Research Board of Canada* **23**, 547.
- Huth, A., and C. Wissel (1992), *Journal of Theoretical Biology* **156**, 365.
- Huth, A., and C. Wissel (1994), *Ecological Modelling* **75–76**, 135.
- Ibele, M., T. E. Mallouk, and A. Sen (2009), *Angewandte Chemie International Edition* **48**, 3308.
- Ihle, T. (2010), arXiv:1006.1825v1.
- Ishikawa, T., J. T. Locsei, and T. J. Pedley (2008), *Journal of Fluid Mechanics* **615**, 401.
- Ishikawa, T., and T. J. Pedley (2008), *Physical Review Letters* **100**, 088103.
- Isihara, A. (1971), *Statistical Physics* (Academic Press, New York).
- Jadbabaie, A., J. Lin, and A. S. Morse (2003), *IEEE Transactions on Automatic Control* **48**, 988.
- Kaiser, D. (2003), *Nature Reviews Microbiology* **1**, 45.
- Kamimura, A., and T. Ohira (2010), *New Journal of Physics* **12**, 053013.
- Keller, E., and L. Segel (1971), *J. Theor. Biol.* **30**, 225.
- Kelly, I., and D. Keating (1996), *Proceedings of The Third International Conference on Mechatronics and Machine Vision in Practice* **1**, 14.
- Kessler, D. A., and H. Levine (1993), *Physical Review E* **48**, 4801.
- Keys, G. C., and L. A. Dugatkin (1990), *Condor* **92**, 151.
- King, A. J., C. M. S. Douglas, E. Huchard, N. J. B. Isaac, and G. Cowlshaw (2008), *Current Biology* **18**, 1833.
- Környei, Z., A. Czirók, T. Vicsek, and E. Madarász (2000), *Journal of Neuroscience Research* **61**, 421.
- Krause, J., D. Hoare, S. Krause, C. K. Hemelrijk, and D. I. Rubenstein (2000), *Fish and Fisheries* **1**, 82.
- Krause, J., G. D. Ruxton, and S. Krause (2010), *Trends in Ecology and Evolution* **25**, 28.
- Kudrolli, A. (2010), *Physical Review Letters* **104**, 088001.
- Kudrolli, A., G. Lumay, D. Volfson, and L. S. Tsimring (2008), *Physical Review Letters* **100**, 058001.
- Kulinskii, V. L., and A. A. Chepizhko (2009), *Mathematical and Statistical Physics* **1198**, 25.
- Kunz, H., and C. K. Hemelrijk (2003), *Artificial life* **9**, 237.
- Lauga, E., and T. R. Powers (2009), *Reports on Progress in Physics* **72**, 096601.
- Lighthill, M. J. (1952), *Communications in Pure and Applied*

- Mathematics **5**, 109.
- Lindhe, M., P. Ogren, and K. Johansson (2005), Proceedings of IEEE International Conference on Robotics and Automation, ICRA'05 **2**, 1785.
- Lipperts, S., and B. Kreller (1999), in *Proceedings of the 5th International Conference of Information Systems, Analysis and Synthesis*.
- Lukeman, R., Y.-X. Li, and L. Edelstein-Keshet (2010), Proceeding of the National Academy of Sciences of the United States of America **107**, 12576.
- Major, P. F., and L. M. Dill. (1978), Behavioral Ecology and Sociobiology **4**, 111.
- Makris, N. C., P. Ratilal, S. Jagannathan, Z. Gong, M. Andrews, I. Bertatos, O. R. Godø, R. W. Nero, and J. M. Jech (2009), Science **323**, 1734.
- Makris, N. C., P. Ratilal, D. T. Symonds, S. Jagannathan, S. Lee, and R. W. Nero (2006), Science **311**, 660.
- Maree, A. F. M., and P. Hogeweg (2001), Proceedings of the National Academy of Science (PNAS) **98**, 3879.
- Marshall, M. B. (2005), *A Swarm Intelligence Approach to Distributed Mobile Surveillance*, Master's thesis (Virginia Polytechnic Institute and State University).
- Mataric, M. J. (1994), *Interaction and Intelligent Behavior*, Tech. Rep. (MIT EECS PhD Thesis AITR-1495, MIT AI Lab).
- McFarland, W., and A. Okubo (1997), in *Animal groups in three dimensions*, edited by J. K. Parrish and W. M. Hamner (Cambridge University Press) pp. 301–312.
- Mehandia, V., and P. Nott (2008), Journal of Fluid Mechanics **595**, 239.
- Mendelson, N. H., A. Bourque, K. Wilkening, K. R. Anderson, and J. C. Watkins (1999), Journal of Bacteriology **181**, 600.
- Mishra, S., A. Baskaran, and M. C. Marchetti (2010), Physical Review E **81**, 061916.
- Moscana, A. (1952), Experimental Cell Research **3**, 535.
- Moyle, P. B., and J. J. Cech (2003), *Fishes: An Introduction to Ichthyology*, 5th ed. (Benjamin Cummings).
- Nagano, S. (1998), Physical Review Letters **80** (21), 4826.
- Nagy, M., Z. Ákos, D. Biro, and T. Vicsek (2010), Nature **464**, 890.
- Nagy, M., I. Daruka, and T. Vicsek (2007), Physica A **373**, 445.
- Narayan, V., N. Menon, and S. Ramaswamy (2006), Journal of Statistical Mechanics: Theory and Experiment, 01005.
- Narayan, V., S. Ramaswamy, and N. Menon (2007), Science **317**, 105.
- Nardi, R. D., and O. Holland (2006), in *In Proceedings of the SAB Workshop on Swarm Robotics* (Springer) pp. 116–128.
- Newman, M. E. J. (2004), The European Physical Journal B **38**, 321.
- Newman, M. E. J. (2006), Proceeding of the National Academy of Sciences of the United States of America **103**, 8577.
- Olfati-Saber, R. (2006), IEEE Transactions on Automatic Control **51**, 401.
- Olfati-Saber, R., J. A. Fax, and R. M. Murray (2007), Proceedings of the IEEE **95**, 215.
- Olfati-Saber, R., and R. M. Murray (2004), IEEE Transactions on Automatic Control **49**, 1520.
- Ordemann, A., G. Balazsi, and F. Moss (2003), Physica A **325**, 260.
- Palla, G., A.-L. Barabási, and T. Vicsek (2007), Nature **446**, 664.
- Palla, G., I. Derényi, I. Farkas, and T. Vicsek (2005), Nature **435**, 814.
- Parrish, J. K., and W. H. Hamner, Eds. (1997), *Animal groups in three dimensions* (Cambridge University Press).
- Parrish, J. K., and P. Turchin (1997), in *Animal groups in three dimensions*, edited by J. K. Parrish and W. M. Hamner, 1st ed., Chap. 9 (Cambridge University Press, USA) pp. 126–142.
- Parrish, J. K., S. V. Viscido, and D. Grnbaum (2002), The Biological Bulletin **202**, 296.
- Partridge, B. L., T. J. Pitcher, J. M. Cullen, and J. Wilson (1980), Behavioral Ecology and Sociobiology **6**, 277.
- Pathria, R. K. (1996), *Statistical Mechanics*, 2nd ed. (Butterworth-Heinemann).
- Pedley, T. J., and J. O. Kessler (1992), Annu. Rev. Fluid Mech. **24**, 313.
- Perea, L., P. Elosegui, and G. Gomez (2009), Journal of Guidance, Control, and Dynamics **32**, 526.
- Peruani, F., A. Deutsch, and M. Bär (2006), Physical Review E **74**, 030904(R).
- Peruani, F., A. Deutsch, and M. Bär (2008), European Physical Journal Special Topics **157**, 111.
- Peruani, F., J. Starrus, V. Jakovljevic, L. Sogaard-Andersen, M. Bär, and A. Deutsch (2010), Preprint.
- Petit, O., and R. Bon (2010), Behavioural Processes **84**, 635.
- Pimentel, J. A., M. Aldana, C. Huepe, and H. Larralde (2008), Physical Review E **77**, 061138.
- Pitcher, T. J. (1983), Animal Behaviour **31**, 611.
- Potts, W. K. (1984), Nature **24**, 344.
- Quera, V., F. S. Beltran, and R. Dolado (2010), Journal of Artificial Societies and Social Simulation **13** (2), 8.
- Raffel, M., C. Willert, and J. Kompenhans (2002), *Particle Image Velocimetry: A Practical Guide*, 2nd ed. (Springer-Verlag).
- Rappel, W.-J., A. Nicol, A. Sarkissian, and H. Levine (1999), Physical Review Letters **83**, 1247.
- Reebs, S. G. (2000), Animal Behaviour **59**, 403.
- Ren, W., and R. W. Beard (2005), IEEE Transactions on Automatic Control **50**, 655.
- Reynolds, C. W. (1987), in *Computer Graphics*, pp. 25–34.
- Riedel, I. H., K. Kruse, and J. Howard (2005), Science **309**, 300.
- Rieu, J. P., N. Kataoka, and Y. Sawada (1998), Physical Review E **57**, 924.
- Rieu, J. P., A. Upadhyaya, J. A. Glazier, N. B. Ouchi, and Y. Sawada (2000), Biophysical Journal **79**, 1903.
- Roberts, S., T. Guilford, I. Rezek, and D. Biro (2004), Journal of Theoretical Biology **227**, 39.
- Romanczuk, P., I. D. Couzin, and L. Schimansky-Geier (2009), Physical Review Letters **102**, 010602.
- Romey, W. L. (1996), Ecological Modelling **92**, 65.
- Rorth, P. (2007), TRENDS in Cell Biology **17**, 575.
- Saintillan, D., and M. J. Shelley (2007), Physical Review Letters **99** (5), 058102.
- Sakurai, T., E. Mihaliuk, F. Chirila, and K. Showalter (2002), Science **296**, 2009.
- Sankararaman, S., and S. Ramaswamy (2009), Physical Review Letters **102** (11), 118107.
- Sárová, R., M. Spinka, J. L. A. Panamá, and P. Simecek (2010), Animal Behaviour **79**, 1037.
- Savill, N. J., and P. Hogeweg (1997), Journal of Theoretical Biology **184**, 229.
- Sayama, H., S. Dionne, C. Laramée, and D. S. Wilson (2009), in *IEEE Symposium on Artificial Life, ALife '09*, pp. 85–

- 91.
- Schaller, V., C. Weber, C. Semmrich, E. Frey, and A. R. Bausch (2010), .
- Schoetz, E.-M. (2008), *Dynamics and Mechanics of Zebrafish Embryonic Tissues* (Vdm Verlag).
- Scott, J. (2000), *Social Network Analysis: A Handbook* (Sage Publications, London).
- Shang, Y. (2009), arXiv:0909.3343.
- Shapiro, J. A. (1988), *Scientific American* **256**, 82.
- Shapiro, J. A., and M. Dworkin, Eds. (1997), *Bacteria as Multicellular Organisms* (Oxford University Press, USA).
- Shaw, E. (1978), *American Scientist* **66**, 166.
- Shimoyama, N., K. Sugawara, T. Mizuguchi, Y. Hayakawa, and M. Sano (1996), *Physical Review Letters* **76**, 3870.
- Short, M. B., C. A. Solari, S. Ganguly, T. R. Powers, J. O. Kessler, and R. E. Goldstein (2006), *Proceeding of the National Academy of Sciences of the United States of America* **103**, 8315.
- Simha, R. A., and S. Ramaswamy (2002), *Physical Review Letters* **89** (5), 058101.
- Simpson, S. J., G. A. Sword, P. D. Lorch, and I. D. Couzin (2006), *Proceeding of the National Academy of Sciences of the United States of America* **103**, 4152.
- Sinclair, A. R. E. (1977), *The African buffalo: a study of resource limitation of populations* (University of Chicago Press, Chicago, USA).
- Smith, J. A., and A. M. Martin (2009), "Comparison of hard-core and soft-core potentials for modelling flocking in free space,".
- Sokolov, A., I. S. Aranson, J. O. Kessler, and R. E. Goldstein (2007), *Physical Review Letters* **98**, 158102.
- Sokolov, A., R. E. Goldstein, F. I. Feldchtein, and I. S. Aranson (2009), *Physical Review E* **80**, 031903.
- Steinberg, M. S. (1963), *Science* **141**, 401.
- Suematsu, N. J., S. Nakata, A. Awazu, and H. Nishimori (2010), *Physical Review E* **81** (5), 056210.
- Sueur, C., and O. Petit (2008), *International Journal of Primatology* **29**, 1085.
- Sugawara, K., Y. Hayakawa, T. Mizuguchi, and M. Sano (2007), in *Human Robot Interaction*, edited by N. Sarkar, Chap. 20 (IN-TECH) pp. 357–368.
- Sumpter, D., J. Krause, R. James, I. Couzin, and A. Ward (2008), *Current Biology* **18**, 1773.
- Szabó, B., G. J. Szóllósi, B. Gönci, Z. Jurányi, D. Selmeczi, and T. Vicsek (2006), *Physical Review E* **74**, 061908.
- Szabó, P., M. Nagy, and T. Vicsek (2009), *Physical Review E* **79**, 021908.
- Tanner, H. G., A. Jadbabaie, and G. J. Pappas (2003a), *Proceedings of the 42nd IEEE Conference on Decision and Control* **2**, 2010.
- Tanner, H. G., A. Jadbabaie, and G. J. Pappas (2003b), *Proceedings of the 42nd IEEE Conference on Decision and Control* **2**, 2016.
- Tinsley, M., A. Steele, and K. Showalter (2008), *The European Physics Journal, Special Topics* **165**, 161.
- Tokita, R., T. Katoh, Y. Maeda1, J. Wakita, M. Sano, T. Matsuyama, and M. Matsushita (2009), *Journal of the Physical Society of Japan* **78**, 074005.
- Toner, J., and Y. Tu (1995), *Physical Review Letters* **75**, 4326.
- Toner, J., and Y. Tu (1998), *Physical Review E* **58**, 4828.
- Trepat, X., M. Wasserman, T. E. Angelini, E. Millet, D. A. Weitz, J. P. Butler, and J. J. Fredberg (2009), *Nature Physics* **5**, 426.
- Trinkaus, J. P., and P. W. Groves (1955), *Proceeding of the National Academy of Sciences of the United States of America* **41**, 787.
- Turgut, A. E., H. Celikkanat, F. Gokce, and E. Sahin (2008), *Swarm Intelligence* **2**, 97.
- Underhill, P. T., J. P. Hernandez-Ortiz, and M. D. Graham (2008), *Physical Review Letters* **100**, 248101.
- Vabø, R., and G. Skaret (2008), *Ecological Modelling* **214**, 125.
- Vaughan, R. B., and J. P. Trinkaus (1966), *Journal of Cell Science* **1**, 407.
- Vicsek, T. (2001a), *Fluctuations and Scaling in Biology* (Oxford University Press, USA).
- Vicsek, T. (2001b), *Nature* **411**, 421.
- Vicsek, T., M. Cserző, and V. K. Horváth (1990), *Physica A* **167**, 315.
- Vicsek, T., A. Czirók, E. Ben-Jacob, I. C. I., and O. Shochet (1995), *Physical Review Letters* **75**, 1226.
- Volfson, D., S. Cookson, J. Hasty, and L. S. Tsimring (2008), *Proceeding of the National Academy of Sciences of the United States of America* **105**, 15346.
- Ward, A. J. W., D. T. J. Sumpter, I. D. Couzin, P. J. B. Hart, and J. Krause (2008), *Proceeding of the National Academy of Sciences of the United States of America* **105**, 6948.
- Watts, D. J., and S. H. Strogatz (1998), *Nature* **393**, 440.
- Weiss, P. (1941), *Third Growth Symposium* **5**, 163.
- Weiss, P., and A. C. Taylor (1960), *Proceeding of the National Academy of Sciences of the United States of America* **46**, 1177.
- Welsby, J., C. Melhuish, C. Lane, and B. Qy (2001), in *In Proceedings of Towards Intelligent Mobile Robots. 3rd British Conference on Autonomous Mobile Robotics and Autonomous Systems*.
- Wilson, E. O. (1971), *The Insect Societies* (Belknap Press of Harvard University Press).
- Wilson, E. O. (1975a), *Sociobiology: The New Synthesis* (Harvard University Press, Boston, USA).
- Wilson, H. V. (1907), *The Journal of Experimental Zoology* **5**, 245.
- Wilson, H. V., and J. T. Penney (1930), *The Journal of Experimental Zoology* **56**, 73.
- Wilson, K. G. (1975b), *Reviews of Modern Physics* **47** (4), 773.
- Wolgemuth, C. W. (2008), *Biophysical Journal* **95**, 1564.
- Wu, Y., Y. Jiang, D. Kaiser, and M. Alber (2007), *PLoS Computational Biology* **3**.
- Wu, Y., A. D. Kaiser, Y. Jiang, and M. S. Alber (2009), *Proceeding of the National Academy of Sciences of the United States of America* **106**.
- Xiao, F., and L. Wang (2006), *International Journal of Control* **79**, 1277.
- Yamada, D., T. Hondou, and M. Sano (2003), *Physical Review E* **67**, 040301(R).
- Yamazaki, Y., T. Ikeda, H. Shimada, F. Hiramatsu, N. Kobayashi, J. Wakita, H. Itoh, S. Kurosu, M. Nakatsuchi, T. Matsuyama, and M. Matsushita (2005), *Physica D* **205**, 136.
- Yates, C. A., R. Erban, C. Escudero, I. D. Couzin, J. Buhl, I. G. Kevrekidis, P. K. Maini, and D. J. T. Sumpterh (2009), *Proceeding of the National Academy of Sciences of the United States of America* **106**, 5464.
- You, S. K., D. H. Kwon, Y. I. Park, S. M. Kim, M. H. Chung, and C. K. Kim (2009), *Journal of Theoretical Biology* **261**, 494.

- Zaikin, A. N., and A. M. Zhabotinsky (1970), *Nature* **225**, 535.
- Zamir, E. A., A. Czirók, C. Cui, C. D. Little, and B. J. Rongish (2006), *Proceeding of the National Academy of Sciences of the United States of America* **103**.
- Zhang, H. P., A. Be'er, R. S. Smith, E.-L. Florin, and H. L. Swinney (2009), *Europhysics Letters* **87**, 48011.
- ZhiXin, L., and G. Lei (2008), *Science China Series F: Information Sciences* **51**, 848.